DOKUZ EYLUL UNIVERSITY
GRADUATE SCHOOL OF NATURAL AND APPLIED SCIENCES

INVESTIGATION OF THE UTILIZATION OF SOME FLUORESCENT ORGANIC DYES IN MODIFIED POLYMER OR SOL-GEL MATRICES AS OPTICAL SENSOR AGENTS

by

Gizem DEMİRYAS

September, 2011

İZMİR

INVESTIGATION OF THE UTILIZATION OF SOME FLUORESCENT ORGANIC DYES IN MODIFIED POLYMER OR SOL-GEL MATRICES AS OPTICAL SENSOR AGENTS

A Thesis Submitted to the
Graduate School of Natural and Applied Sciences of
Dokuz Eylul University
In Partial Fulfillment of the Requirements for
the Degree of Master of Science in Chemistry Program

by
Gizem DEMİRYAS

September, 2011
İZMİR

M. Sc. THESIS EXAMINATION RESULT FORM

We have read the thesis entitled **"INVESTIGATION OF THE UTILIZATION OF SOME FLUORESCENT ORGANIC DYES IN MODIFIED POLYMER OR SOL-GEL MATRICES AS OPTICAL SENSOR AGENTS"** completed by **GİZEM DEMİRYAS** under supervision of **ASSOCIATED PROFESSOR DR. ÖZLEM ÖTER** and we certify that in our opinion it is fully adequate, in scope and in quality, as a thesis for the degree of Master of Science.

Associated Professor Dr. Özlem ÖTER

Supervisor

Prof. Dr. Yavuz ERGÜN

(Jury Member)

Assistant Prof. Dr. Özlem KARADENİZ

(Jury Member)

Prof. Dr. Mustafa SABUNCU

Director Graduate School of Natural and Applied Sciences

ACKNOWLEDGMENTS

I would like to express sincere gratitute to my supervisor Associated Professor Dr. Özlem Öter for providing the fascinating subject, for her valuable support during this thesis and for the great working conditions at our laborotory.

I gratefully acknowledge the extensive help of Prof.Dr. Kadriye Ertekin and Prof. Dr. Yavuz Ergun. I also thank to my colleague Müge Çöldür, Ph. D. student Sibel Kaçmaz and Ph. D. student Sibel Aydoğdu during experimental studies.

Finally, I want to thank to my parents for their tolerant attitude to my working effort during the elaboration of this dissertation and for their incessant support during all the years of my studies.

Gizem DEMİRYAS

INVESTIGATION OF THE UTILIZATION OF SOME FLUORESCENT ORGANIC DYES IN MODIFIED POLYMER OR SOL-GEL MATRICES AS OPTICAL SENSOR AGENTS

ABSTRACT

In the first part of this work, three different ionic liquids, 1-butyl-3-methylimidazolium tetrafluoroborate, 1-butyl-3-methylimidazolium thiocyanate and 1-butyl-3-methylimidazolium hexafluorophosphate were employed for the modification of acid- catalyzed tetraethyl orthosilicate (TEOS) based sol-gel matrix. Photophysical characteristics and emission based response of tris (bipyridine) ruthenium (II) dye to gaseous oxygen was investigated in these ionic liquid containing sol–gel matrix by spectrofluorimetric method. Effects of the ionic liquid type, ionic liquid concentration, dye concentration and some sol gel parameters such as acid catalyze concentration; pH, gelation time, TEOS/water molar ratios and drying temperature to the oxygen sensitivity were evaluated.In the second part, the photo physical characterization of synthesized carbazole bearing oxazolones (4-[4-(9H-carbazol-9-yl)benzylidene]-2-(4-nitrophenyl)-1,3-oxazol-5(4H)-one (3), 4-[(9-methyl-9H-carbazol-3-yl)methylene]-2-(4-nitrophenyl)-1,3-oxazol-5(4H)-one (5a) and 4-[(9-hexyl-9H-carbazol-3-yl)methylene]-2-(4-nitrophenyl)-1,3-oxazol-5(4H)-one (5b) were investigated in polymer matrix of polyvinylchloride (PVC) by using absorption and emission spectrometry. The response of the dye doped PVC films were also evaluated in terms of the effect of pH and sensitivity to some metal cations and anions. The immobilized dye, 3 was found to exhibit a selective response for Zn (II) ions in direction of decrease in fluorescence intensity. Besides the selectivity of the dye to Zn (II) ions, high quantum yield value, the response in nanomolar concentrations level and high linear working range makes the dye promising for optical zinc ion sensor designs.

Keywords: optical sensors**,** ionic liquids, polyvinyl chloride, sol-gel, oxygen sensor, zinc ion sensor.

ORGANİK BOYAR MADDELERİN MODİFİYE POLİMER VEYA SOL-JEL MATRİKSLERİNDE OPTİK SENSÖR AJANI OLARAK KULLANILABİLİRLİĞİNİN ARAŞTIRILMASI

ÖZ

Bu çalışmanın birinci kısmında, 1-bütil-3-metilimidazolyumtetrafloraborat,1-bütil-3-metilimidazolyum tiyosiyanatve 1-bütil-3-metilimidazolyum hegzaflorafosfatolmak üzere üç değişik iyonik sıvı asit-katalizli tetraetil ortosilikat (TEOS) temelli sol-jel matrikslerinin modifikasyonu için kullanılmıştır.Fotofiziksel karakteristikler ve tris (bipyridine) ruthenium (II) boyasının bu iyonik sıvıları içeren sol-jel matrikslerinde oksijene emisyon temelli yanıtları spektroflorimetrik metotla tayin edilmiştir.İyonik sıvı çeşidi, iyonik sıvı konsantrasyonu, boya konsantrasyonu, asit kataliz konsantrasyonu, pH, jelleşme süresi, TEOS/su molar oranı ve kurutma sıcaklığı gibi bazı sol-jel parametrelerinin oksijen duyarlılığına etkisi değerlendirilmiştir.İkinci bölümde ise okzazole içeren sentezlenmiş karbazolun (4-[4-(9H-carbazol-9-yl)benzylidene]-2-(4-nitrophenyl)-1,3-oxazol-5(4H)-one (3), 4-[(9-methyl-9H-carbazol-3-yl)methylene]-2-(4-nitrophenyl)-1,3-oxazol-5(4H)-one (5a) and 4-[(9-hexyl-9H-carbazol-3-yl)methylene]-2-(4-nitrophenyl)-1,3-oxazol-5(4H)-one (5b)) fotofiziksel özellikleri polivinil klorür (PVC) polimer matriksinde absorpsiyon ve emisyon spektroskopisi kullanılarak incelenmiştir. Boya katkılı PVC filmlerinin yanıtları pH, bazı metal katyonlarının ve anyonlarının duyarlılık etkisi göz önünde bulundurularak değerlendirildi. İmmobilize haldeki boya(3) Zn (II) iyonları için floresans şiddetinin azalması yönünde seçici bir tepki gösterdi.Boyanın Zn (II) iyonlarına seçici yanıtıtnın yanı sıra, yüksek quantum verimi, nanomolar konsantrasyonlar seviyesindeki yanıtı ve yüksek doğrusal çalışma aralığı boyayı optik çinko iyon sensör tasarımları için umut verici yapar.

Anahtar Kelimeler: optik sensörler, iyonik sıvılar, polivinil klorür, sol-jel, oksijen sensörü, çinko iyon sensörü.

CONTENTS **Page**

M.Sc THESIS EXAMINATION RESULT FORM ii

ACKNOWLEDGEMENTS iii

ABSTRACT iv

ÖZ v

CHAPTER ONE –INTRODUCTION 1

1.1 Chemical Sensors 1

1.1.1 Semiconducting oxide sensors 3

1.1.2 Electrochemical sensors 3

1.1.3 Ion-selective electrodes 3

1.1.4 Solid electrolyte sensors 4

1.1.5 Optical chemical sensors 4

1.1.5.1 Advantages of chemical optical sensors 4

1.1.5.2 Disadvantages of chemical optical sensors 6

1.1.5.3 Fiber optic sensors (FOS) 6

1.2 Sensors for Gases 8

1.2.1 O_2 Sensors 9

1.3 Optical Chemical Sensors for the Determination of Heavy Metal Ions 10

1.3.1 Sensors based on intrinsic optical properties 10

1.3.2 Sensors based on chromophores 11

1.3.3 Sensors based on fluorophores 11

1.3.4 Sensors based on ionophores 12

1.4 Types of Polymers Used in Optical Sensing 13

1.4.1 Lipophilic Polymers and Plasticizers 13

1.4.2 Hydrophilic Polymers 13
1.4.3 Ionic Polymers (polyelectrolytes) 14
1.5 Ionıc Liquids 14
1.6 UV-Vis Spectrophotometric Method 16
1.6.1 Basic Principles of UV-Vis Spectrophotometric Method 16
1.6.2 UV-visible Spectroscophy 19
1.7 Luminescence 21
1.7.1 Stoke's Shift 23
1.7.2 Quantum Yield 23
1.8 The sol-jel process 24
1.8.1 Hydrolysis 27
1.8.1.1 Acid-Catalyzed Mechanism 28
1.8.1.2 H_2O/Si Molar Ratio (R) 29
1.8.2 Condensations 29
1.8.2.1 Acid-Catalyzed Mechanism 30

CHAPTER TWO – EXPERIMENTAL METHOD AND INSTRUMENTATION 31

2.1 Construction of fiber optical system 33
2.2 Schematic illustration of experimental set-up used for O_2 sensing 34
2.3 Mixing of the gases 35
2.4 Sol-gel cocktail preparation 36
2.5 PVC coctail preparation 36
2.6 Quantum Yield Calculations 37
2.7 Buffer Solutions 38

CHAPTER THREE - ENHANCED $O_{2(g)}$ RESPONSE of TRIS(BIPYRIDINE)RUTHENIUM(II) in PRESENCE of DIFFERENT IONIC LIQUIDS IN SOL-JEL MATRIX 40

3.1 Introduction 40

3.2 Experimental 41

3.3 Results and discussion 44

3.3.1 O_2 sensing studies 44

3.3.2 Effect of ionic liquid concentration 50

3.3.3 O_2 sensing studies with cocktails of mol ratio of water/TEOS = 2 (R = 2) and mol ratio of water/TEOS = 4 (R = 4) 56

3.3.4 Absorption, emission and excitation spectra 104

3.3.5 Response and regeneration 107

3.3.6 Dissolved oxygen sensing 110

3.4 Conclusion 113

CHAPTER FOUR - PHOTOCHARACTERIZATION OF DYES AND INVESTIGATION OF THE UTILITY AS AN OPTICAL SENSOR in PVC MATRIX 115

4.1 Introduction 115

4.2 Coctail preparation protocols 115

4.3 Results and discussion 116

4.3.1 UV Spectrum of Dyes 116

4.3.2 Emission and Excitation Spectra of Dyes in PVC 117

4.3.3 Quantum Yield of Dyes 118

4.3.4 Effect of the pH 131

4.3.5 Response of Dyes to Different Metal Ions 123

4.3.6 Response of Dye 3 to Zinc Ions 124

4.4 Conclusion 125

CHAPTER FIVE-CONCLUSIONS 127

REFERENCES 129

CHAPTER ONE

INTRODUCTION

1.1 Chemical Sensors

A chemical sensor is a device that transforms chemical information, ranging from the concentration of aspecific sample component to total composition analysis, into an analytically useful signal. The chemical information, mentioned above, may originate from a chemical reaction of the analyte or from a physical property of the system investigated (Hulanicki, Geab & Ingman, 1991).

Different definitions of sensors are given in the literature and the discussion aboutthe features and the requirements of sensors is still going on. The following definition is given by an IUPAC commission on sensors.

"A chemical sensor is a device that transforms chemical information ranging from the concentration of a spesific sample component to total composition analysis into analytical usefull signal. The chemical information mentioned above may originate from a chemical reaction of the analyte or from a physical property of the system invesitigated. A chemical sensor is an essential component of an analyser. In addition to the sensor, the analyser may contain that perform the following functions: sampling, sample transport, signal processing, data processing" (Wolfbeis, 1991).

Chemical sensors have been widely used in such applications ascritical care, safety, industrial hygiene, process controls, product quality controls, human comfort controls, emissions monitoring, automotive, clinical diagnostics, home safety alarms, and, more recently, homeland security. In these applications, chemical sensors have resulted in both economic and social benefits (Stetter, Penrose & Yao, 2003).

Sensors can be classified in many different ways. They may be classified according to the principle of operation of the transducer in two main groups as “physical” and “chemical” sensors (Oter, 2007).

A physical sensor is a device that provides information about a physical property of the system.

A chemical sensor is an essential component of an analyzer.In addition to the sensor, the analyzer may contain devices that perform the following functions: sampling, sample transport, signal processing, dataprocessing. An analyzer may be an essential part of an automated system. The analyzer workingaccording to a sampling plan as a function of time acts as a monitor.

Chemical sensors contain two basic functional units: a receptor part and a transducer part. Some sensors may include a separator which is, for example, a membrane.

In the receptor part of a sensor the chemical information is transformed into a form of energy which may be measured by the transducer. The transducerpart is a device capable of transforming the energy carrying the chemical information about the sample into a useful analytical signal. The transducer as such does not show selectivity.

The receptor part of chemical sensors may be based upon various principles:
- Physical, where no chemical reaction takes place. Typical examples are those based upon measurement of absorbance, refractive index, conductivity, temperature or mass change.
- Chemical, in which a chemical reaction with participation of the analyte gives rise to the analytical signal.
- Biochemical, in which a biochemical process is the source of the analytical signal.

Sensors can be classified in many different ways. They may be classified according to the principle of operation of the transducer in two main groups as “physical” and “chemical” sensors (Oter, 2007).

A physical sensor is a device that provides information about a physical property of the system.

A chemical sensor is an essential component of an analyzer.In addition to the sensor, the analyzer may contain devices that perform the following functions: sampling, sample transport, signal processing, dataprocessing. An analyzer may be an essential part of an automated system. The analyzer workingaccording to a sampling plan as a function of time acts as a monitor.

Chemical sensors contain two basic functional units: a receptor part and a transducer part. Some sensors may include a separator which is, for example, a membrane.

In the receptor part of a sensor the chemical information is transformed into a form of energy which may be measured by the transducer. The transducerpart is a device capable of transforming the energy carrying the chemical information about the sample into a useful analytical signal. The transducer as such does not show selectivity.

The receptor part of chemical sensors may be based upon various principles:
- Physical, where no chemical reaction takes place. Typical examples are those based upon measurement of absorbance, refractive index, conductivity, temperature or mass change.
- Chemical, in which a chemical reaction with participation of the analyte gives rise to the analytical signal.
- Biochemical, in which a biochemical process is the source of the analytical signal.

Optical examples are microbial potentiometric sensors or immunosensors. They may beregarded as asubgroup of the chemical ones. Such sensors are called biosensors (Hulanicki, Geab & Ingman, 1991).

Sensors also can be divided into sub groups as optical, electrochemical, electrical, mass sensitive, magnetic and thermometric devices. Sensors can also be classified as direct and indirect sensors or as reversible or non-reversible ones and respect of their applications or sizes (Oter, 2007).

1.1.1 Semiconducting Oxide Sensors

The heated metal oxide sensor is probably the most investigated and widelyproduced chemical sensor. The working principle of this type of sensor is that the resistance of the metal oxide semiconductor changes when it is exposed to the target gas because the target gas reacts with the metal oxide surface and changes its electronic properties. New materials such as the rare earth oxides or gallium oxide are being used as the active sensor elements. Recent reviews include many examples of this type of gas sensors (Göpel &Schierbaum, 1995; Shimizu &Egashira, 1999).

1.1.2 Electrochemical Sensors

There are two major sensor classes that use liquid electrolytes: amperometric and potentiometric sensors. The earliest example of an amperometric gas sensor, the Clark oxygen sensor used for the measurement of oxygen in the blood is more than 40 years old. The amperometric sensor produces current signal, which is related to the concentration of the analyte by Faraday's law and the laws of mass transport (Cao, Shakin &Sun, 1992).

1.1.3 Ion-selective Electrodes

Ion-selective electrodes (ISEs) belong to potentiometric chemical sensor group and are most often based on the measurement of the interfacial potential at an

electrode surface caused by a selective ion exchange reaction. The wellknown glass pH electrode is a typical ISE (Galster, 1991).

1.1.4 Solid Electrolyte Sensors

Using a solid electrolyte to replace the liquid electrolyte in an electrochemical sensor, one can construct a solid electrolyte electrochemical sensor. Solid electrolyte sensors are typically designed to operate at high temperature and can operate in either a potentiometric or amperometric mode. Over the past ten years, two potentiometric designs have evolved: surface-modified solid electrolyte gas sensors and mixed potential gas sensors (Göpel, Reinhardt & Rösch, 2000; Mukundan, Brosha, Brown &Garzon, 1999; Yamazoe &Miura, 1996).

1.1.5 Optical Chemical Sensors

Optical chemical sensors or optods have become an important area of research since their introduction two decades ago. Optical sensors are compact and ideally suited to miniaturization while at the same time they are resisting to electrical interference and utilize the simplicity of photometric measurements. Many optical chemical sensors utilize colorcomplexing or redox reagents immobilized in suitable polymeric membrane (Ensafi&Bakhshi, 2003).

Optical chemical sensors can be classified in three groups: Probes, fiber-optic chemical sensors and non fiber optic chemical sensors. Sensors which produce an irreversible response to the presence of analytes are referred to as ‘probes’. If the signal is reversible and continuous then it is called as sensor. Fiber optic sensors are based on optical spectroscopy performed on sites inaccessible to conventional spectroscopy, over large distances, or even on several spots along the fiber (Oter, 2007).

1.1.5.1 Advantages of Chemical Optical Sensors

There are numerous advantages of chemical optical sensors described below.

- Optical sensors do not require a reference signal as in potentiometry which increases the cost and causes perturbations.
- The ease of miniaturization allows the development of very small, light and flexible sensors much smaller than any electrochemical sensor especially for sensing in clinical chemistry and medicine.
- Low loss optical fibers allow transmittance of optical signals over wide distances. Remote sensing makes it possible to perform analyses when samples are hard to reach, dangereous, too hot or too cold, in harsh environments or radioactive.
- They are not influenced from electrical interferences, strong magnetic fields and surface potentials. On the other hand fibers do not present a risk for health since they do not disperse any electrical signal.
- Analyses can be performed in almost real time without any need of sampling.
- Since several fiber sensors placed in different sites can be coupled to one fluorimeter, the method allows multiple analyses with a single control instrument.
- Coupling of small sensors for different analytes to produce a sensor bundle of small size allows simultaneous monitoring of various analytes without any interference.
- Extremely small sample volume is not a disadvantage as in polarographic electrodes.
- Fiber optical sensing is a non-destructive analytical method.
- Fibers are manufactured from nonrusting materials, so that they have excellent stability. They are also resistant to radiation.
- In practice, a single fiber may be used to assay several analytes at the same time.
- Especially sensors based on dynamic fluorescence quenching have a useful dynamic range often larger than that of electrochemical sensors.
- Most fiber sensors can be employed over a wider temperature range than electrodes (Wolfbeis, 1991).

1.1.5.2 Disadvantages of Chemical Optical Sensors

Besides these advantages optical sensors also have some disadvantages:

- Ambient light can interphere so optical isolation is nesessary.
- They have limited long term stability because of photobleaching and wash out. The signal drifts due to these reasons can be compensated by using ratiometric method or time resolved measurements.
- The fiber optics used at present have impurities that can give background absorption, fluorescence and Raman Scatter. Low-priced (plastic) fibers are confined to visible range, whereas UV light is transmitted by rather expensive quartz fibers only. Because of this sensing dyes that can be excited at visible range are preferred in sensor designs.
- More selective indicators have to be found for various important analytes and the immobilization techniques have to be improved(Wolfbeis, 1991).

1.1.5.3 Fiber Optic Sensors(FOS)

Fiber optic sensors are a class of sensors that use optical fibers to detect anaytes. Fiber-optic cable consists of a plastic or glass core surrounded by alayer of cladding material.

Principle of optical fibre is total internal reflection of light through the core of the fiber. Light is generated by a light source and is sent through an optical fiber. Total internal reflection is the complete transmission of light through fiber optics, which states that all the light striking a boundary between two media will be totally reflected. That is, no light energy will ever be lost across the boundary. The light then returns through the optical fiber and is captured by a photo detector.

Some optical fiber sensors use a single optical fiber while others use separate optical fibers for the light source and for the detector.

Optical fiber can be made of either glass or plastic. There are three general classes of fiber optic sensors (Figure 1.1). The first type is completely passive. A spectroscopic method can be used to detect individual types of analytes. This method involves sending a light source directly through the optical fiber and analyzing the light that is reflected or emitted by the anayte. The refractive index of the material at the tip of the optical fiber can be used to determine what phases (vapor, water, or NAPL) are present.

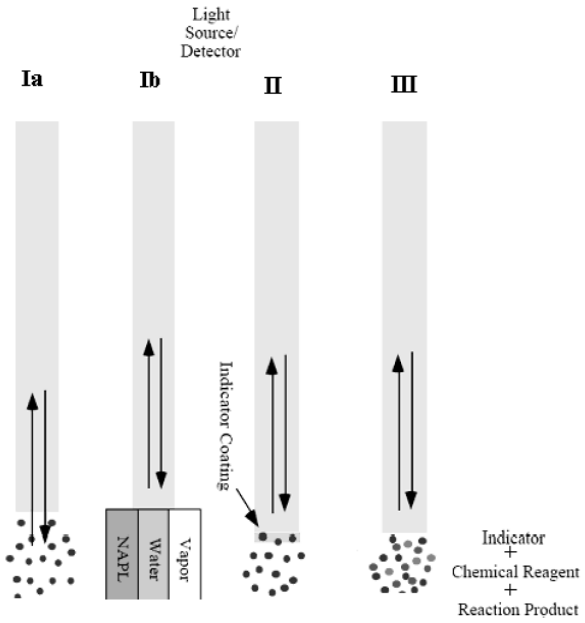

Figure 1.1 Three types of fiber optic sensors Ia: spectroscopic Measurement of fluorescent or phosphorescent anayte; Ib: refractive index changesdue to vapor, water and NAPL; II: indicator is coated at the tip ofthe opticfiber and change color due to the binding with analyte; III: a chemical reaction is considered between the addedreagent and the analyte. Reaction product ismeasure

A second class of fiber optic sensors consists of a fiber optic sensor with a chemically interacting thin film attached to the tip. This film is formulated to bind with certain types of chemicals. Analyte concentration can be found by measuring the color of the thin film, the change in refractive index, or by measuring the flourescing of the film.

The third type of fiber optic sensors involves injecting a reagent near the sensor. This reagent reacts either chemically or biologically with the anayte. The reaction products are detected to give an estimate of the analyte concentration(Oter, 2007).

1.2 Sensors for Gases

There are a variety of gas sensors so far developed. In the two decades since, extensive efforts have been compiled not only for advancing these sensors but also for developing various new gas sensors, which have been in great demand to make sure safety, health, amenity, environmental reservation, energy saving and so on (Yamazoe, 2005).

Current investigations include the detection of traces of toxic gases such as NH_3,H_2S, Cl_2, SO_2, HCHO, HCl, etc. and also other gases such as O_2using chemicallysensitive matrices that can be interfaced to the optical fibres to produce devices that will have probe configurations and employ reflectance or fluorescence detection techniques at the chemical transducer. Recent works include the investigation of organic and organometallic optical thin films for gas sensors (Oter, 2007).

1.2.1 O_2 Sensors

The determination of oxygen concentration in both gaseous and aqueous media is of major importance inmany industrial, medical and environmental applications. Optical oxygen sensors are more attractive than conventional amperometric devices because, in general, they have a fast response, do not consume oxygen and are not easily poisoned (Mcevoy, Macdonagh &Maccraith, 1998).

Luminescent transition metal complexes currently show great promise as sensor materials in fiber optic sensors. In particular, oxygen sensors based on luminescence quenching are attractive. Aswith other luminescent sensors, these systems frequently display microheterogeneity with nonlinear Stern-Volmer quenching curves and

complex luminescence decay kinetics that can be characterized assumes of several exponentials or as distribution functions of exponentials (Sacksteder, Demas & DeGraff, 1993).

In these sensors, different types of organic dyes (pyrene and its derivatives, quinoline and phenanthrene), transition metal complexes of ruthenium and osmium, rhenium polypyridine complexes and metalloporphyrins were dispersed in oxygen permeable polymers or sol–gel matrices (Oter, Ertekin &Derinkuyu, 2009).

The instrument evaluates the oxygen dependent change of the luminescence lifetime of an oxygen indicator using a phase modulation technique. Optical oxygen sensors generally are based on the fluorescence of a ruthenium complex in a polymer matrix to measure the partial pressure of oxygen. This kind of sensors generally uses the below working mechanism:

1. The pulsed LED lamp sends light to an optical fiber.
2. The optical fiber carries the light to the probe. The distal end of the probe tipconsists of a thin layer of a hydrophobic polymer material. A rutheniumcomplex is trapped in the matrix, effectively immobilized and protected fromwater.
3. The light from the LED excites the ruthenium complex at the probe tip.
4. The excited ruthenium complex fluoresces, emitting energy.
5. If the excited ruthenium complex encounters an oxygen molecule, the excessenergy is transferred to the oxygen molecule in a non-radiative transfer,decreasing or quenching the fluorescence signal. The degree of quenchingcorrelates to the level of oxygen concentration or to oxygen partial pressurein the film, which is in dynamic equilibrium with oxygen in the sample.
6. The energy is collected by the probe and carried through the optical fiber tothe spectrometer. The analog data will be converted to digital data that the PCcan understand (Oter, 2007).

1.3 Optical Chemical Sensors for the Determination of Heavy Metal Ions

Recent years, chemical sensors for heavy metal ions have seen an increasing interest. A ‘metal sensor’ is described as a device which is capable of responding to the presence of a heavy metal ion in a reversible and continuous manner. Sensors which produce an irreversible response to the presence of heavy metal ions are referred to as ‘metal probes’. The optical properties of a material may be measured by the conventional methods of absorbance, fluorescence and reflectance spectroscopy, and in various formats such as test strips and disposable tips, while employing optical waveguides such as optical fibres, integrated optics and capillarytype devices (Oehme &Wolfbeis, 1997).

1.3.1 Sensors Based on Intrinsic Optical Properties

So far, the optical sensors discussed have been based on an immobilised reagent which acts as a chemical transducer for the desired analyte. However, there are sensors which rely on the intrinsic optical properties of heavy metal ions. In this case, quantification is achieved via the measurement of the absorbance (UV-visible) or luminescence of the sample solution. Suitable analytes for this mode of measurement include the transition metal ions Fe (II), Co (II), Cu (II), Cr (III), Ni (II) (Andrew &Worsfold, 1994), the lanthanide ions europium and terbium, and the radionuclides uranium and plutonium. Such sensors lack specificity since they are subject to interference from any species absorbing at the same wavelength as the analyte, and sample turbidity and changes in refractive index will also have a significant effect. Absorbance based analysis is applicable only at relatively high concentrations of heavy metal ions because their molar absorptivities are low, typically 10-100 mol^{-1} dm^3 cm^{-1}.

1.3.2 Sensors Based on Chromophores

The majority of heavy metal ion sensors are based on the use of an indicator dye which undergoes a binding reaction with the ions. This reaction is accompanied by a change in the absorbance or fluorescence of such chelators. In other words, anindicator acts as a transducer for the chemical species that cannot be determined directly by optical means. This has an important implication in that it is the concentration of the indicator species that is quantified rather than the analyte itself. Many indicators cannot be used in optical sensors because of unfavourable analytical wavelengths, poor photostability, low molar absorptivity or the need for additional reagents. Most of them bind with the metal ion irreversibly or only at low or high pH so they can not be used for continuous sensing at near neutral pH. Upon binding with the metal ion, most indicators undergo a change in colour, with one band appearing as the other disappears, rather than an intensity change of one single band (Oter,2007).

1.3.3 Sensors Based on Fluorophores

In contrast to chromogenic reagents, fluorescent indicators are of the yes/no type in that only one of the species (the complexed or the noncomplexed) is fluorescent. Fluorescent indicators frequently provide improved sensitivity (which is important in miniature sensors) and also selectivity because it is unlikely that an interfering species would have the same absorbance and emission as the analyte complex. Fluorimetry (and luminescence spectrometry in a wider sense) also offers a broad variety of spectroscopic techniques including the measurement of lifetime, polarisation and energy transfer. An important group of indicators is based on the quenching of luminescence by heavy metals and transition metals. In the case of static quenching, the quencher interacts with the fluorophore in its ground state. In dynamic (collisional) quenching, the interaction between the metal ion (quencher) and the fluorophore occurs in the excited state only and leads to a reduction in both the emission intensity and the decay time. The photophysical process of dynamic quenching is fully reversible, that is, the indicator is not consumed. Hence,

quenchable fluorophores comprise an important class of indicators for reversible sensors. Most heavy metals quench by virtue of the heavy atom effect, and the quenching efficiency of many transition metals, in particular Fe (III), Co (II) and Ni (II) is thought to be due to their numerous unpaired spins (Oter,2007).

1.3.4 Sensors Based on Ionophores

Due to limitations of conventional reagents (mainly caused by their high stability constants) there has been an increase in the use of ionophores in optical chemical sensors. Ionophores are non-coloured ion-complexing organic molecules, or lipophilic ion carriers, which are capable of reversibly binding to ions and transporting them across organic membranes by carrier translocation. Their mostwidespread application so far is in ion-selective membranes for alkali and alkaline earth metal ions, the best example being valinomycin, a highly specific neutral carrier for potassium ions (Hisamoto et al., 1995; Wolfbeis &Schaffar, 1987). Several sensing schemes are used in which ionophore selectivity is combined with an optical readout, namely (a) the introduction of chromogenic or fluorogenic moieties into ionophores to obtain so-called chromoionophores or fluoroionophores, (b) the combination of ionophores with potentially sensitive indicators, (c) the extraction of ions into membranes using neutral ion carriers (ion exchange), and (d) the extraction of an ion along with a counterion into a membrane phase (coextraction). Recognition of heavy metals is accomplished by neutral ionophores capable of binding the metal ion, while the optical signal is provided by a proton selective chromoionophore. On extraction of a heavy metal ion (of charge n) into the membrane, n protons are released by the chromoionophore, resulting in a change in its colour or fluorescence. The interesting feature of this approach is that it is only the carrier for a specific heavy metal ion that needs to be varied, while the chromoionophore can remain the same.

1.4 Types of Polymers Used in Optical Sensing

1.4.1 Lipophilic Polymers and Plasticizers

Polymers that have a high glass transition temperature (Tg) are brittle (Figure 1.2). They require plasticizers to make them flexible. Furthermore, the high density/rigidity of the polymer chains (without plasticizers) hinders diffusion of ions and gases in the polymer matrix. Therefore, plasticizer to polymer ratios of up to 2:1 is required. While polyvinylchloride (PVC) is soluble in tetrahydrofuran and cyclopentanone, polymers such as methacrylate, polystyrene and polyvinyl acetate are also soluble in ethyl acetate, ethylmethyl ketone, dichloromethane, etc.

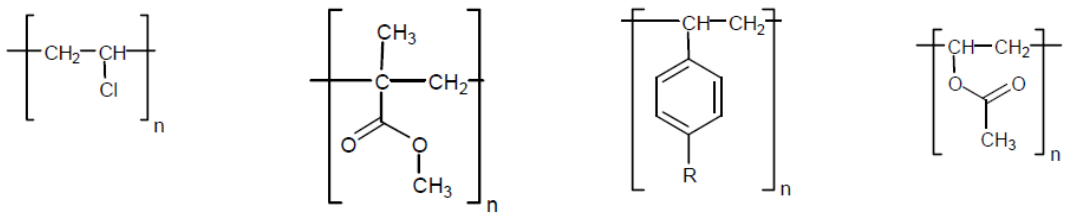

Figure 1.2 Lipophilic Polymers and Plasticizers that have a high glass transition temperature.

1.4.2 Hydrophilic Polymers

Hydrophilic polymers provide a matrix which corresponds to an aqueous environment (Figure 1.3). Ions can diffuse quite freely, but the possible water uptake (10-1000%) can cause significant swelling of the polymer. Swelling of the matrix affects the optical properties of the sensors and, consequently, the signal changes.

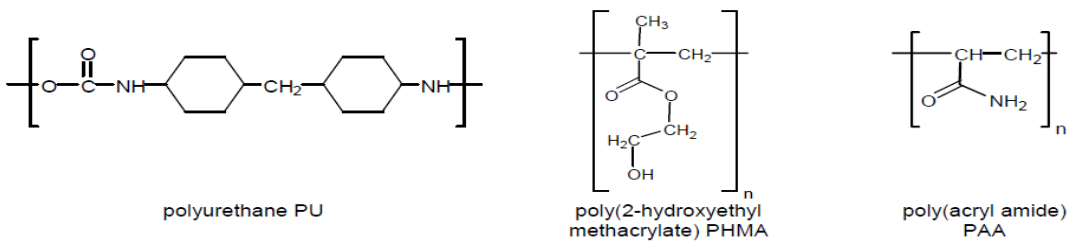

Figure 1.3 Hydrophilic polymers.

1.4.3 Ionic Polymers (polyelectrolytes)

Polyelectrolytes exhibit a large amount of dissociable groups. These compounds are often used for ion exchange chromatography. They can also be used to exchange their counterions with indicator ions (Figure 1.4).

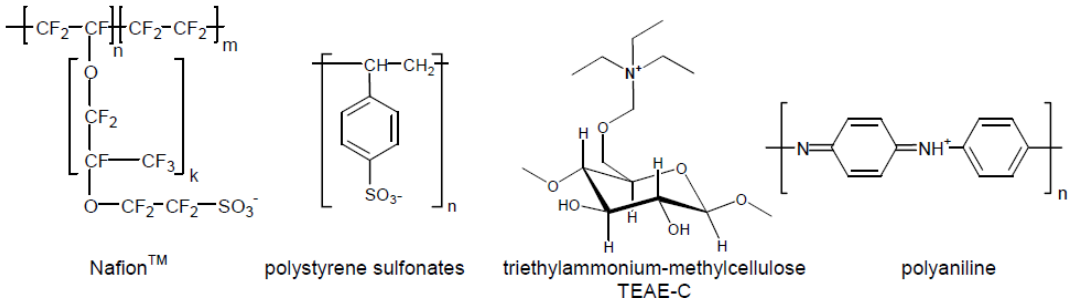

Figure1.4 Ionic Polymers.

1.5 Ionic Liquids

Ionic liquids (ILs) are liquids composed entirely of ions. For a salt to be classified as an IL, itmust have a melting point of ≤100°C. Ionic liquids are termed room-temperature ionic liquids(RTILs) if they are composed of a salt that is liquid at room temperature. ILs almost always contain an organic ion as either the cation or the anion. Typical cations are based on the imidazolium, pyridinium, ammonium, or phosphonium group. Anions are more likely to be inorganic (such as halides, BF_4, PF_6) than are the cations, but organic anions are also common [examples include trifluoromethanesulfonate (triflate) and bis[(trifluoromethyl)sulfonyl]amide (NTF_2)] (Soukup-Hein, Warnke & Armstrong, 2009).

Room temperature ionic liquids (RTILs) have a lot of advantages, such as high viscosity, high ionic conductivity, low volatility, wide electrochemical windows, and high chemical and thermal stability, which have been applied to modify the electrodes and have shown excellent electrochemical behaviors (Khani, Rofouei, Arab, Gupta & Vafaei, 2010).

One of the most special properties for ionic liquids is their high polarity (Rantwijk, Lau&Sheldon, 2003). The polarity values of ionic liquids are sometimes sensitive to the temperature and the presence of water (Baker, S.N., Baker G.A. &Bright, 2002). Because of the high polarity, ionic liquids present an ideal reaction melieu for chemical and biochemical reactions due to their ability to dissolve a wide range of different substances including polar and nonpolar organic, inorganic, and polymeric compounds (Oter,2007).

Despite of their high polarity, most of ionic liquids are hydrophobic and can dissolve up to 1% of water, and the presence of water may affect the physical properties of the ionic liquids (Seddon, Stark &Torres, 2000). However, the solubility of water in ionic liquids varies unpredictably (Rantwijk et al., 2003). For example, although 1-butyl-3-methylimidazolium tetrafluoroborate ([BMIM][BF_4]) and 1-butyl-3-methylimidazolium thiocyanate ([BMIM][SCN]**)** are completely water-miscible 1-butyl-3-methylimidazolium hexafluorophosphate ([BMIM][PF_6]) is slightly soluble in water (Oter, 2007).

Although there have been numerous details concerning their properties, probably the most important one is that room-temperature ionic liquids have been utilized as “clean solvents” and “catalysts” for green chemistry.Additionally, their gas sorption–desorption dynamic is very fast and desorption by vacuuming is completely reversible. These characteristics make the RTILs exceptionally promising for gas sensors (Oter, Ertekin & Derinkuyu, 2009).

1.6 UV-Vis Spectrophotometric Method

Ultraviolet and visible spectrometers have been in general use for the last 35 years and over this period have become the most important analytical instrument in the modern day laboratory. In many applications, other techniques could be employed but UV-Visible spectrometry has been the most intensively used one due to its simplicity, versatility, speed, accuracy and cost-effectiveness (Ultraviolet theory, 2011, www.molecularinfo.com)

UV/Vis spectroscopy is routinely used in analytical chemistry for the quantitative determination of different analytes, such as transition metal ions, highly conjugatedorganic compounds, and biological macromolecules(Ultraviolet–visible spectroscopy, 2011, www.en.wikipedia.org).

1.6.1 Basic Principles of UV-Vis Spectrophotometric Method

The electromagnetic spectrum is the range of all possible frequencies of electromagnetic radiation(Figure 1.5). The "electromagnetic spectrum" of an object is the characteristic distribution of electromagnetic radiation emitted or absorbed by that particular object (Electromagnetic spectrum, 2011, www.en.wikipedia.org).

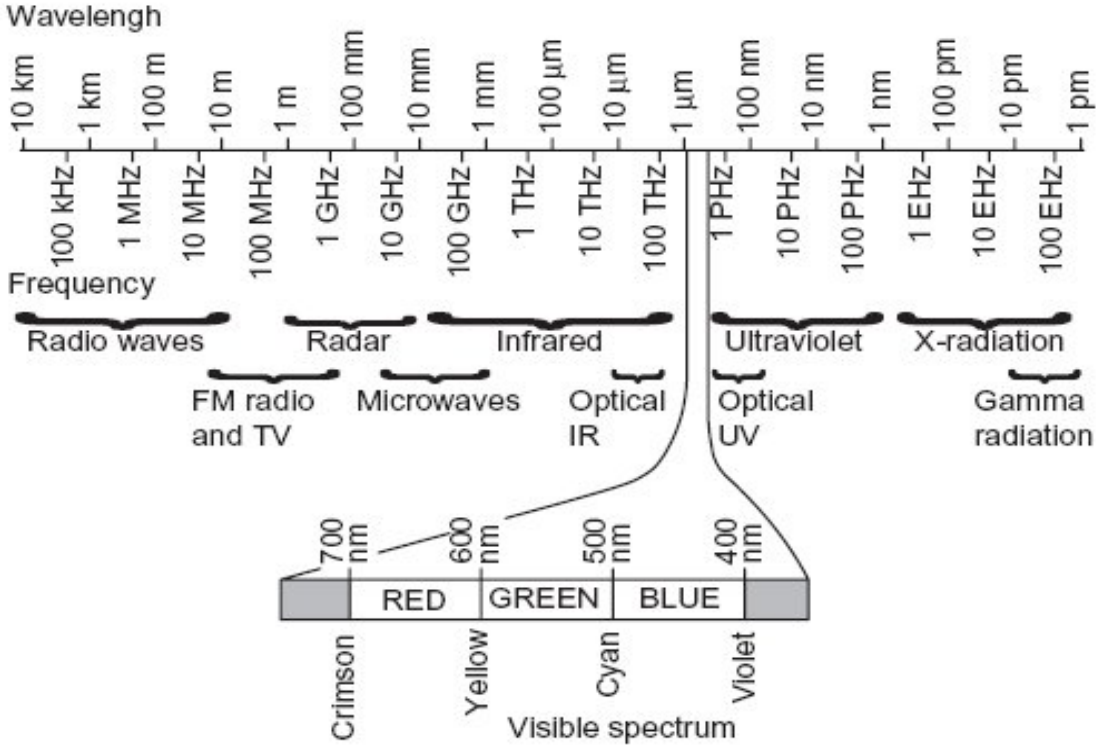

Figure 1.5The electromagnetic spectrum.

The energy associated with electromagnetic radiation is defined by the following equation:

$$E = \mathrm{h}.\ \nu$$

Where E is energy (in joules), h is Planck's constant (6.62×10^{-34} Js), and ν is frequency (in seconds) (Owen, 2000).

The wavelength of a sinusoidal wave is the spatial period of the wave – the distance over which the wave's shape repeats. It is usually determined by considering the distance between consecutive corresponding points of the same phase, such as crests, troughs, or zero crossings, and is a characteristic of both traveling waves and standing waves, as well as other spatial wave patterns. Wavelength is commonly designated by the Greekletterlambda (λ) (Figure 1.6),(Wavelength, 2011, www.en.wikipedia.org).

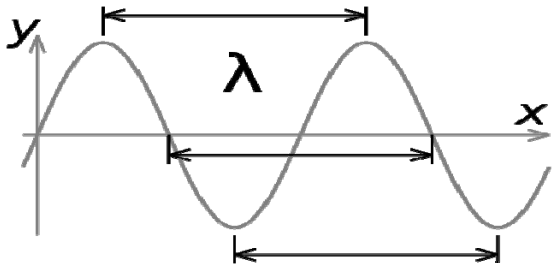

Figure 1.6 Wavelength of a sine wave.

Frequency in oscillation is the number of cycles per second, and in wave motion, it is the number of waves that pass through a given point per second (Frequency, 2011,www.answers.com).

Frequency has an inverse relationship to the concept of wavelength; simply, frequency is inversely proportional to wavelength λ (lambda). The frequency f is equal to the phase velocity$v$ of the wavedivided by the wavelength λ of the wave:

$$f = \nu / \lambda$$

In the special case of electromagnetic waves moving through a vacuum, then $v = c$, where$c$ is the speed of light in a vacuum, and this expression becomes(Frequency, 2011, www.en.wikipedia.org)

$$f = c / \lambda$$

In UV-visible spectroscopy, wavelength usually is expressed in nanometers (1 nm= 10^{-9} m). It follows from the above equations that radiation with shorter wavelength has higher energy. In UV visible spectroscopy, the low-wavelength UV light has the highest energy (Owen,2000).

When light passes through or is reflected from a sample, the amount of lightabsorbed is the difference between the incident radiation (I_o) and the transmitted radiation (I). The amount of light absorbed is expressed as either transmittance or absorbance. Transmittance usually is given in terms of a fraction of 1 or as a percentage and is defined as follows:

$$T= I / I_o \text{ or } \%T= (I / I_o) \times 100$$

Absorbance is defined as follows:

$$A= – \log T$$

For most applications, absorbance values are used since the relationship between absorbance and both concentration and path length normally is linear (Owen, 2000).

1.6.2 UV-visible Spectroscopy

A diagram of the components of a typical spectrometer is shown in Figure 1.7. The functioning of this instrument is relatively straightforward. A beam of light from a visible and/or UV light source (colored red) is separated into its component wavelengths by a prism or diffraction grating. Each monochromatic (single wavelength) beam in turn is split into two equal intensity beams by a half-mirrored device.

One beam, the sample beam (colored magenta), passes through a small transparent container (cuvette) containing a solution of the compound being studied in a transparent solvent. The other beam, the reference (colored blue), passes through an identical cuvette containing only the solvent. The intensities of these light beams

are then measured by electronic detectors and compared. The intensity of the reference beam, which should have suffered little or no light absorption, is defined as I_0. The intensity of the sample beam is defined as I. Over a short period of time, the spectrometer automatically scans all the component wavelengths in the manner described. The ultraviolet (UV) region scanned is normally from 200 to 400 nm, and the visible portion is from 400 to 800 nm.

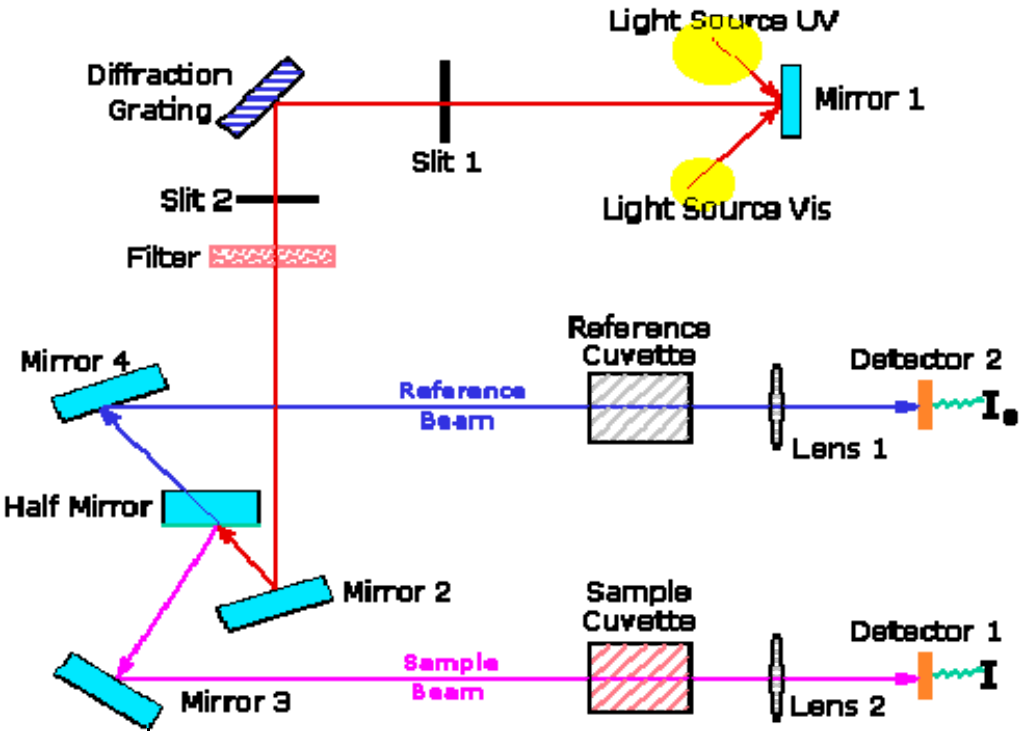

Figure 1.7 A diagram of the components of a typical spectrometer.

Different compounds may have very different absorption maxima and absorbances. Intensely absorbing compounds must be examined in dilute solution, so that significant light energy is received by the detector, and this requires the use of completely transparent (non-absorbing) solvents. The most commonly used solvents are water, ethanol, hexane and cyclohexane. Solvents having double or triple bonds, or heavy atoms (e.g. S, Br & I) are generally avoided. Because the absorbance of a sample will be proportional to its molar concentration in the sample cuvette, a corrected absorption value known as the molar absorptivity(ε)is used when comparing the spectra of different compounds. This is defined as:

$$\varepsilon = A/ (l.c)$$

Where *A*= absorbance, c = sample concentration in moles/liter &l= length of light path through the cuvette in cm (UV-Visible Spectroscopy, 2011, www2.chemistry.msu.edu).

The principles of UV centre on the fact that molecules have the ability to absorb ultraviolet or visible light. When a molecule absorbs energy an electron is promoted from the Highest Occupied Molecular Orbital (HOMO) to the Lowest Unoccupied Molecular Orbital (LUMO).It must be noted that occupied molecular orbital with the lowest energy are the σ orbitals, then at a slightly higher energy are the π orbitals and nonbonding orbitals (those with unshared pair of electrons) at still a higher energy(Figure 1.8). The highest energy orbitals belong to π*, σ*,i.e. the unoccupied or as otherwise as known as, the antibonding orbitals(UV-VIS Spectroscopy, 2011, www.updetd.up.ac.za).

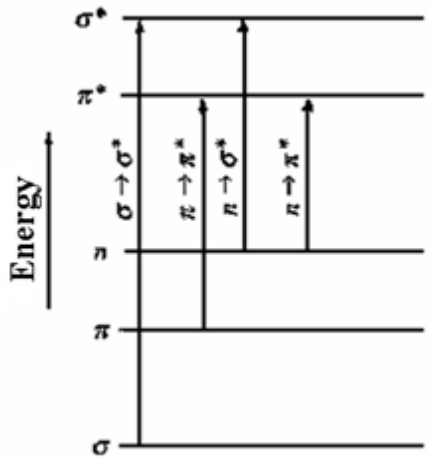

Figure1.8Electronic energy levels and transitions.

1.7 Luminescence

Luminescence means emission of light by electronically excited atoms or molecules. Electronic excitation requires the supply of energy. Various kinds of

luminescence, such as electroluminescence, chemiluminescence, thermoluminescence and photoluminescence, are known and called by the source from which energy is derived. In the case of photoluminescence (fluorescence andphosphorescence), the energy is provided by the absorption of infrared, visible or ultra-violet light.

The absorption and emission of light is illustrated by Jablonski level diagram, shown in Figure 1.9. According to the Boltzmann distribution, at room temperature the valance electrons are in the lowest vibration level (ν=0) of the ground electronic state. A transition ofthese electrons from the ground state (level 0 of S_0) to higher energy levels takes place on absorption (a) of light. The Franck-Condon principle states that there is approximately no change in nuclear position and spin orientation, because absorption of light occurs in about 10^{-15}s. Therefore, the electronic transition is represented by a vertical line.

Molecules excited to an upper vibrational level of any excited state rapidly lose their excess of vibrational energy by collision with solvent molecules, and falls to the lowest vibrational level. Molecules in the upper excited states (S_2, S_3, ...) relax by internal conversion (IC), radiationless to the lowest excited singlet state (S_1) within 10^{-12} s. Transition from this level to the vibration levels of the ground state can take place by emitting photons (f). A portion of the excited molecules may return to the ground state by other mechanisms, such as electron transfer, collision, intersystem crossing (ICS), internal conversion or chemical reaction.

Fluorescence emission occurs spontaneously, again in accordance with the Franck-Condon principle, if the radiationless transition lifetime is sufficiently long. The radiative lifetime of fluorescence lies between 10^{-9} s for spin allowed transitions ($\pi * \pi$) to 10^{-6} for less probable transitions ($\pi * n$). Molecules in the lowest excited state (S_1) can also undergo conversion to the first triplet state (T_1) by intersystem crossing (ISC).

This process requires a time of the same order of magnitude as fluorescence radiation lifetime and therefore competes with fluorescence. Although radiative

transitions between states of different multiplicity are spin forbidden, these transitions do take place with low probability compared with singlet-singlet, or triplet-triplet transitions. Emission from the first triplet state (T_1) to the ground state is termed phosphorescence, and usually shifted to higher wavelengths than fluorescence. The radiation lifetime for this transition is about 10^{-2} to 10^{+2}s (Lakowicz, 1993; Parker, 1968; Schmidt, 1994).

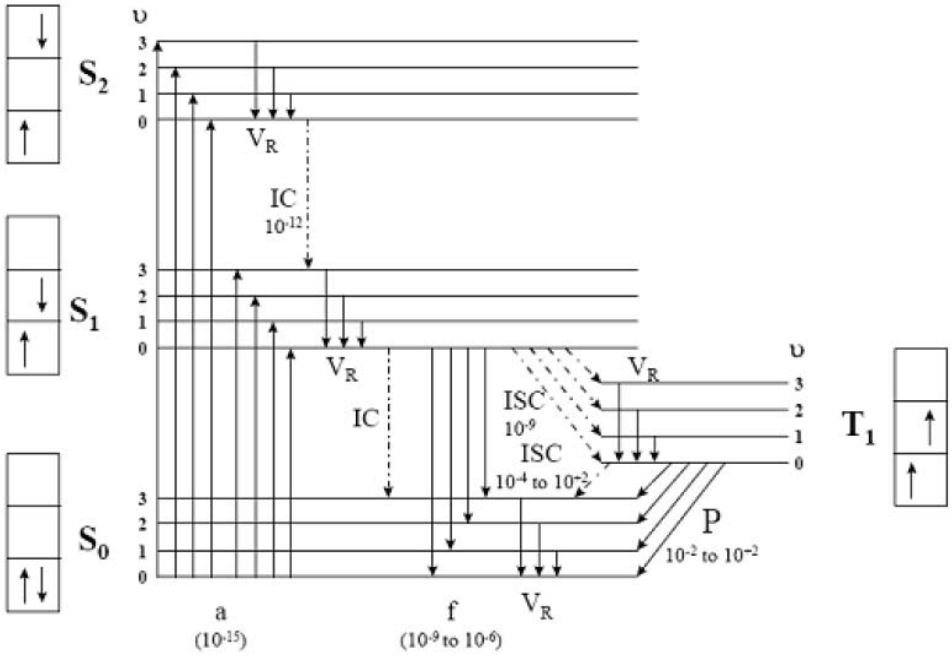

Figure1.9Jablonski diagram with the reciprocal rates of transition in [s].

1.7.1 Stokes Shift

When a system (be it a molecule or atom) absorbs a photon, it gains energy and enters an excited state. One way for the system to relax is to emit a photon, thus losing its energy (another method would be the loss of heat energy). When the emitted photon has less energy than the absorbed photon, this energy difference is the Stokes shift (Kitai, 2008).

1.7.2 Quantum Yield

A molecule in the relaxed state S_1 (the lowest excited state) can return to the ground state, radiationless or by the emission of fluorescence. The fluorescence quantum yield is the ratio of the number of photons emitted to the number absorbed expressed by the rate constants Γand k, respectively. Hence, the quantum yield can be written as:

$$\varphi = \frac{\tau}{\tau + k}$$

The quantum yield can be close to unity if the radiationless rate of deactivation (k) is much smaller than the rate of radiative emission ($k << \tau$) (Lakowicz, 1993; Parker, 1968; Schmidt, 1994).

1.8 The sol-jel process

The sol-gel process, also known as chemical solution deposition, is a wet-chemical technique widely used in the fields of materials science and ceramic engineering. Such methods are used primarily for the fabrication of materials (typically a metal oxide) starting from a chemical solution (or *sol*) that acts as the precursor for an integrated network (or *gel*) of either discrete particles or network polymers. Typical precursors are metalalkoxides and metal chlorides, which undergo various forms of hydrolysis and polycondensation reactions (Sol-gel, 2011, www.wikipedia.org).

The sol-gel process allows the preparation of glass films where indicator chemistry can be incorporated. Theproduction of ceramic materials and glassy networks is based on the polymerisation of suitable precursors at low temperature. The increasing popularity of sol-gels in sensor applications results from the processing versatility.

There are a number of variables which affect the hydrolysis and condensation rates and hence the microstructure of the sol-gel glass. The detailed microstructure of sol-gel glasses depends on parameters such as nature and concentration of the catalyst, water sol-gel precursor ratio (R), and precursor type, nature of the solvent, ageing time, ageing temperature, drying time and drying temperature. The process can be adapted for formation of thin sensor layers. At the sol stage, thin glass films can be formed by dip-coating or spin-coating. These films are porous and are used for sensor applications(Materials and Polymers in Optical Sensing, 2011, www.personal.uni-jena.de).

Components of the sol-gel cocktail are the sol-gel precursor, water, a catalyst, the indicator and a solvent such as ethanol. The sol-gel precursors are mostly low molecular weight alkoxysilanes such as tetramethoxysilanes (TMOS) and tetraethoxysilanes (TEOS) which are not miscible with water. Mixing these components causes hydrolysis of the ester, silanol-ester condensation, and silanol-silanol condensation of the precursors. In this process, the alkoxy groups hydrolyze and the hydroxy groups condense. This general reaction scheme can be seen in equations:

- $Si(OR)_4 + H_2O \rightarrow Si(OR)_3OH + ROH$ (hydrolysis) (1)
- $Si(OR)_3OH + Si(OR)_4 \rightarrow Si(OR)_3$ -O- $Si(OR)_3 + ROH$ (condensation) (2)
- R-Si-OH + HO-Si-R → R-Si-O-Si-R + H_2O (condensation) (3)

The first phase in the process is the formation of the “sol”. A sol is a colloidal suspension of solidparticles in a liquid. Colloids are solid particles with diameters of 1-100 nm. After a certain period, the colloidal particles and condensed silica species link to form a “gel” - an interconnected, rigid network with pores of submicrometer dimensions and polymeric chains whose average length is greater than micrometer. After the sol-gel transition, the solvent phase is removed from the interconnected pore network. If removed by conventional drying such as evaporation, so-called “xerogels” are obtained, if removed via supercritical evacuation; the product is an “aerogel”.

“Ageing” is the process that takes place after mixing precursor, water, solvent and catalyst to form a sol, but before coating, in the case of coating sols. Ageing or pre-polymerisation of the sol causes aggregation due to hydrolysis and condensation reactions, and consequently an increase in viscosity. During this step, the sol is allowed to stand either at room temperature or at a higher temperature for a period of time during which hydrolysis and condensation reactions cause aggregation and cross-linking.

The “gel point” is defined as the point at which the entire solid mass becomes interconnected. The physical characteristics of the gel network depend upon the size of particles and extent of cross-linking prior to gelation.

Sol-gel glass is ion-permeable due to residual hydroxy groups and its porosity, and can be used to optically measure pH by entrapping (caging) conventional pH indicator dyes in the material. Often, water soluble indicator dyes do not have to be chemically modified for immobilisation because due to their size they are retained in the pores of the sol-gel glass and do not wash out (Lobnik, 1998).

Ormosils (organically modified siloxanes) represent hybrid systems in whichseveral precursor types such as organotrialkoxysilanes or diorganodialkoxysilane precursors ($R'Si(OR)_3$or $R'_2Si(OR)_2$, respectively) are combined in which R’ represents a non-hydrolyzable organic substituent (e.g. methyl or phenyl). The substituent R’ can also be a reactive aminopropyl group which allows subsequent covalent binding of indicators. Ormosils are not as hydrophilic and brittle as conventional sol-gel glass. If the content of alkyl chains R’ increases, then thematerial turns hydrophobic and ion-impermeable. Nevertheless, due to its gas permeability, it can be used for sensing acidic or basic gases which permeate the material and react with indicator dyes (e.g. by protonation/deprotonation of pH indicators) (Materials and Polymers in Optical Sensing, 2011, www.personal.uni-jena.de).

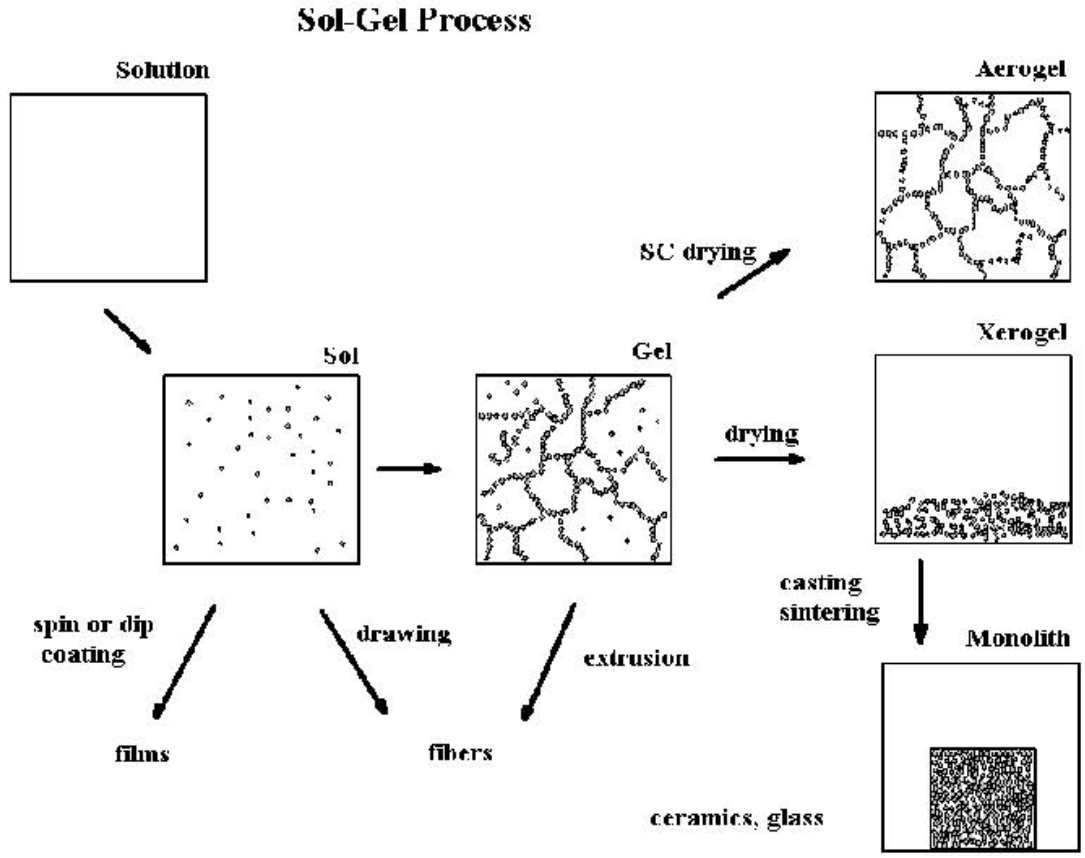

Figure 1.10 Sol-Gel Process.

1.8.1 Hydrolysis

Although hydrolysis can occur without addition of an external catalyst, it is most rapid and complete when they are employed. Mineral acids (HCl) and ammonia are mostlly used; however, other catalysts are acetic acid, KOH, amines, KF, and HF (Brinker &Scherer, 1990).

With weaker bases such as, ammonium hydroxide and pyridine, measurable speeds of reaction were produced only if large concentrations were present. Therefore, compared to acidic conditions, base hydrolysis kinetics is more strongly affected by the nature of the solvent (Aelion, Loebel &Eirich, 1950).

pH, substituents, solvent and water are the effects on hydrolysis rate.

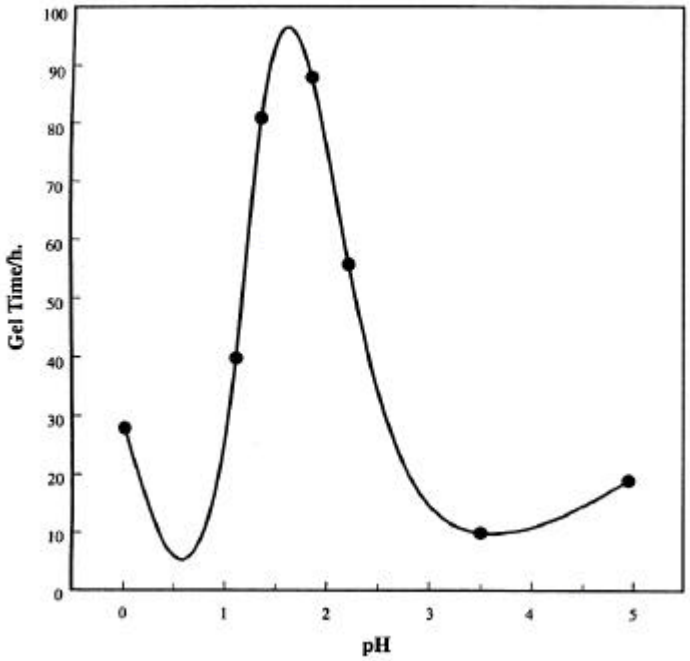

Figure 1.11Rate of H+ catalyzed TEOS hydrolysis (gel time) as a function of pH.

1.8.1.1 Acid-Catalyzed Mechanism

Under acidic conditions, it is likely that an alkoxide group is protonated in a rapid first step. Electron density is withdrawn from the silicon atom, making it more electrophilic and thus more susceptible to attack from water. This results in the formation of a penta-coordinate transition state with significant SN2-type character (Brinker &Scherer, 1990). The transition state decays by displacement of an alcohol and inversion of the silicon tetrahedron, as seen in Figure 1.12.

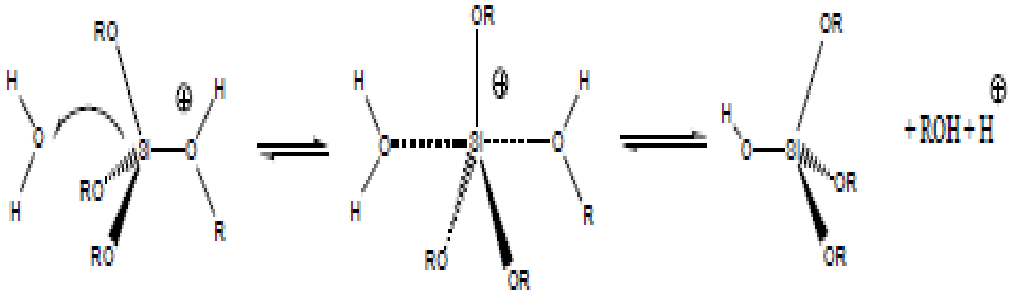

Figure 1.12Acid catalysed hydrolysis.

1.8.1.2 H_2O/Si Molar Ratio (R)

From hydrolysis equation, an increased value of R is expected to promote the hydrolysis reaction. The most obvious effect of the increased value of R is the acceleration of the hydrolysis reaction. Additionally, higher values of R caused more complete hydrolysis of monomers before significant condensation occurs. Differing extents of monomer hydrolysis should affect the relative rates of the alcohol- or waterproducing condensation reactions. Generally, with understoichiometric additions of water (R << 2), the alcohol producing-condensation mechanism is favored, whereas, the water-forming condensation reaction is favored when R ≥2 (Assink &Kay, 1998).

Although increased values of R generally promote hydrolysis, when R is increased while maintaining a constant solvent silicate ratio, the silicate concentration is reduced. This in turn reduces the hydrolysis and condensation rates, resulting in longer gel times.

1.8.2 Condensation

Polymerization to form siloxane bonds occurs by either an alcohol-producing or a water-producing condensation reaction. It has been shown by Engelhardt, Altenburg, Hoebbel &Wieker (1977) that a typical sequence of condensation products is monomer, dimer, linear trimer, cyclic trimer, cyclic tetramer, and higher order rings.

As with hydrolysis, condensation can proceed without catalyst, however, their use in organosiloxanes is highly helpful. It has been shown that condensation reactions are acid and base specific (Pohl &Osterholtz, 1985). In addition, Iler (1979) has shown that under more basic conditions, gel times are observed to increase. Condensation reactions continue to proceed, however, gelation does not occur.

1.8.2.1 Acid-Catalyzed Mechanism

It is generally believed that the acid-catalyzed condensation mechanism involvesa protonated silanol species. Protonation of the silanol makes the silicon moreelectrophilic and thus susceptible to nucleophilic attack. The most basic silanolspecies (silanols contained in monomers or weakly branched oligomers) are the mostlikely to be protonated. Therefore, condensation reactions may occur preferentiallybetween neutral species and protonated silanols situated on monomers, end groups ofchains, etc. (Brinker &Scherer, 1990).

CHAPTER TWO

EXPERIMENTAL METHODS AND INSTRUMENTATION

The absorption spectra were recorded using a Shimadzu 1601 UV–Visible spectrophotometer. Steady state fluorescence emission and excitation spectra were measured using the spectrofluorometer of Varian Cary Eclipse. To measure the pH values of the sol–gel composites we have used pH strips (Merck).

The sol-gel precursor tetraethyl orthosilicate (TEOS) was obtained from Merck (98 % purity, for synthesis). The additive Triton X-100 was obtained from Merck (98 % purity, GR). The O_2 sensitive fluorescent dye, tris (2, 2'-bipyridyl) ruthenium (II) chloride ($Ru(bipy)_3^{2+}$) was supplied from Aldrich (99.5% purity). The commercial ionic liquids 1-butyl-3-methylimidazolium tetrafluoroborate ([BMIM][BF_4]), 1-butyl-3-methylimidazolium thiocyanate ([BMIM][SCN]) and 1-butyl-3-methylimidazolium hexafluorophosphate ([BMIM][PF_6]) were supplied from Fluka. Structures of the ionic liquids and the ruthenium dye were given in Figure 2.1and Figure 2.2.

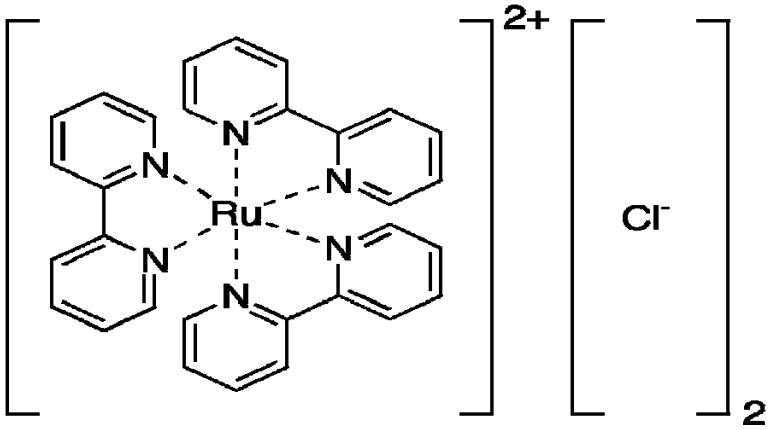

Figure 2.1 Structure of the ruthenium dye, ($Ru(bipy)_3^{2+}$) tris (2, 2'-bipyridyl) ruthenium (II) chloride.

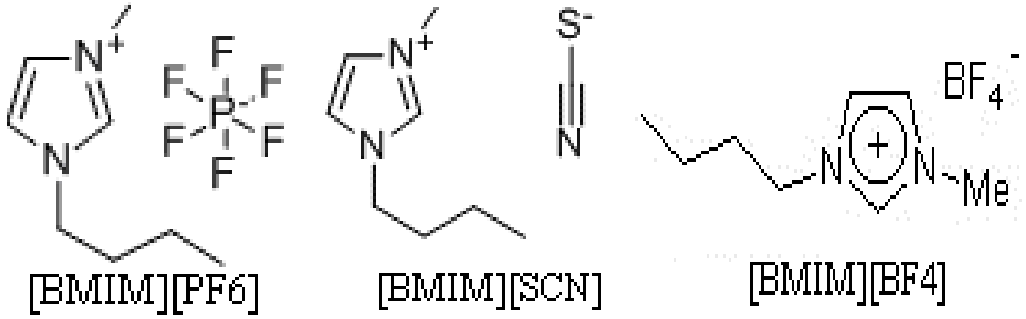

Figure 2.2 Structure of the ionic liquids.

The fiber optic components were obtained from Varian and explained in detail in Section 2.1. Schematic illustration of experimental set-up used for O_2 sensing was shown in Section 2.2. The gas mixtures were prepared with a Sonimix 7000 Gas Diluter instrument and were explained in detail in Section 2.3.

The polymer polyvinyl chloride (PVC) was high molecular weight and obtained from Fluka. The plasticiser, dioctylphtalate (DOP) was 99 % from Aldrich. The additive potassium tetrakis (4-chlorophenyl) borate was selectophore, 98 % from Fluka and metal solutions were 1000 $mg.L^{-}$ atomic absorption spectroscopy (AAS) standard solutions. 4-[4-(9H-carbazol-9-yl)benzylidene]-2-(4-nitrophenyl)-1,3-oxazol-5(4H)-one (3), 4-[(9-methyl-9H-carbazol-3-yl)methylene]-2-(4-nitrophenyl)-1,3-oxazol-5(4H)-one (5a) and 4-[(9-hexyl-9H-carbazol-3-yl)methylene]-2-(4-nitrophenyl)-1,3-oxazol-5(4H)-one (5b) were synthesized in the laborotories of University of Dokuz Eylül by the organic chemistry group. The structures of dyes were given in Figure 2.3and PVC coctail preparation was explained inSection2.5.

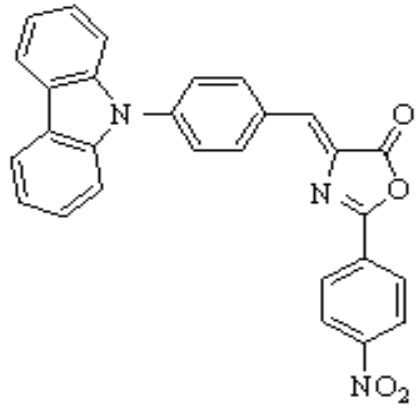

(3)

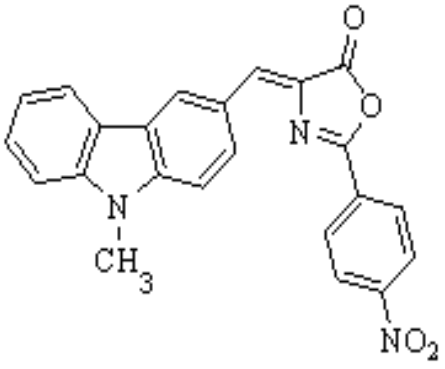

(5a)

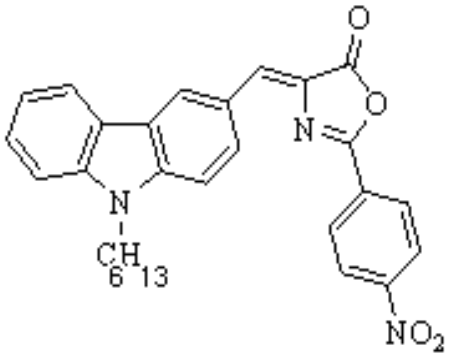

(5b)

Figure 2.3 Structures of dyes.

2.1 Construction of fiber optical system

The fiber optical sensor was constructed with the commercial accessories ofVarian Cary Eclipse Spectrofluoremeter (Figure 2.4) : Eclipse Fibre optic coupler, Fluorescence remote read probe (2 metres), Probe tip for solid measurements and Probe tips for liquid measurements (10 mm and 20 mm length tips). This method also allows the examination of samples remote from the instrument. The installation steps are:

The fibre optic coupleris an accessory that enables the use of a fiber optic probe with Carry Eclipse spectrofluoremeter. After the removal of the sample compartment

of the Carry Eclipse, the fibreoptic coupler was stabilized to the same position by the help of the screws.

•The fiber optic probewas connected to the coupler accessory by inserting the two connector ends into the two key holds.

•The probe tipswere screwed onto the end of the probe. Due to the phase of the sample (solid or liquid), either a solid sample probe tip or a liquid sample probe tip were used.

•To ensure that the fibre optic system will operate at maximum performance, it is nesessary to optimize the efficiency with which light passes through the coupling device before experimentation begins. The allignment was done by using the software of the instrument (Oter, 2007).

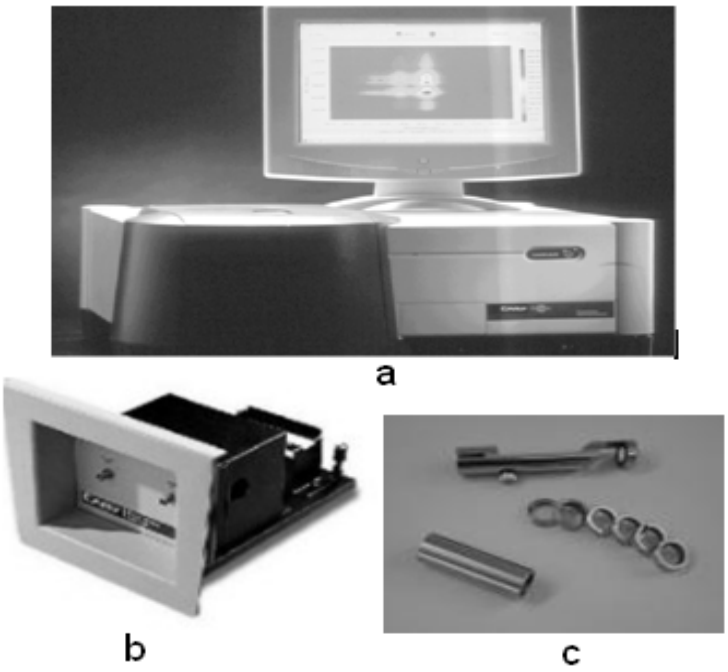

Figure 2.4 Varian Cary Eclipse Spectrofluoremeter (a) and fiber optical system accessories: Fiber optic coupler(b) and probe tips(c).

2.2 Schematic illustration of experimental set-up used for O_2sensing

Gas phase measurementswere carried out with fiber optic probe (2mlong) and solid sample tip accessories constructed on the spectrofluorometer. The tip of the

bifurcated fiber optic probe was interfaced with the sensing slide in a sealed small beaker (Figure2.5) (Oter, Ertekin & Derinkuyu, 2009).

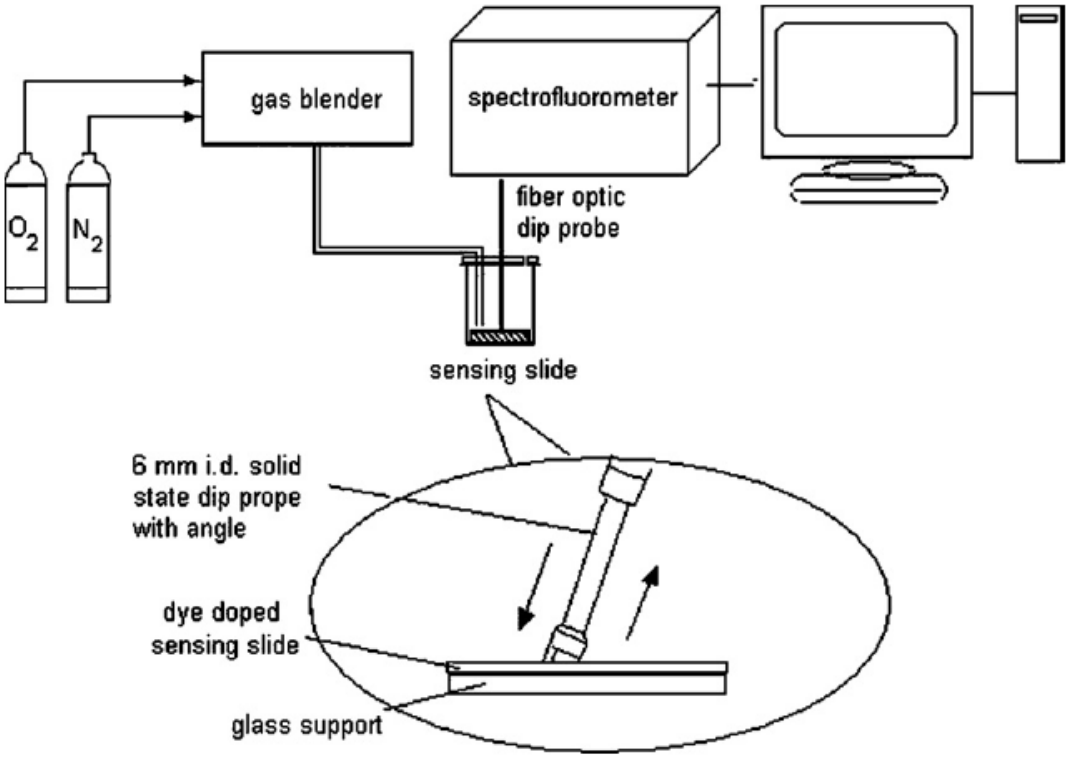

Figure 2.5 Schematic illustration of experimental set-up used for O_2sensing (Oter, Ertekin & Derinkuyu, 2009).

2.3 Mixing of the gases

Gaseous oxygen (99.99%) and nitrogen (99.99%) were mixed at different concentrations by the Sonimix 7000A gas mixing system (Figure 2.6). The output flow rate of the gas mixture was maintained at 5000 mL min^{-1}.

Figure 2.6Sonimix 7000 Gas Diluter

2.4 Sol-gel cocktail preparation

The sols were prepared by the acid catalyzed method from a solution containing TEOS, HCl-acidified water, ethanol (EtOH), ethanolic solution of $Ru(bipy)_3^{2+}$ complex, Triton X-100 and ionic liquids. The detailed preparation procedur was told in Section 3.3.

2.5 PVC cocktail preparation

The membranes were prepared to contain the dye, 33% PVC (High molecularweight), 66% plasticizer (Dioctyl phthalate, DOP) by weight and the additivepotassium tetrakis-(4-chlorophenil) borate (PTCPB). The chemical structures of PVC, DOP and PTCPB were shown in Figure 2.7. The mixture was dissolved in the solvent of tetrahydrofuran (THF) and mixed by several hours by the help of a magnetic stirrer.

The resulting cocktail was spread on a 125 μm polyester support (Mylar from Du Pont) which was optically fully transparent, ion impermeable and exhibited good adhesion to PVC.

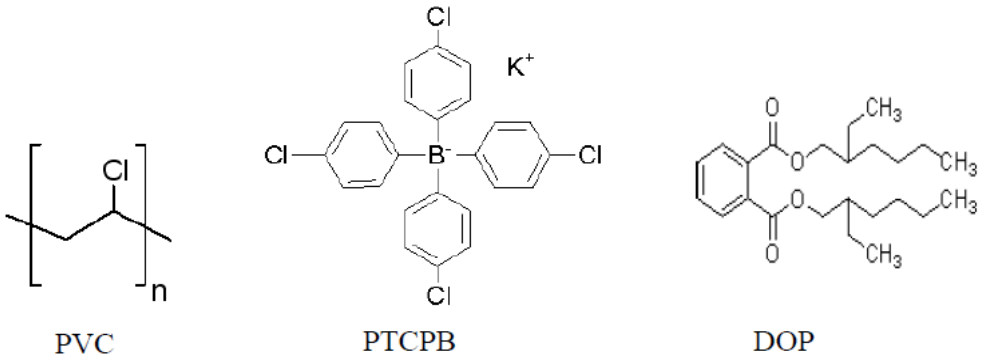

Figure 2.7 Structures of PVC, PTCPB and DOP

For absorbance and steady state fluorescence measurements each sensing film was cut to 1.2 cm width and 2.5 cm length and fixed diagonally into the sample cuvette (Figure 2.8) and the absorption or emission spectra were recorded.

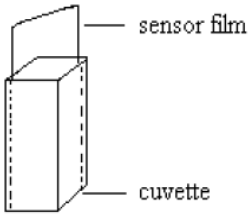

Figure 2.8 The placement of the
sensor film in the sample cuvette.

2.6 Quantum yield calculations

Fluorescence quantum yield values (Φ_F) of the employed dyes were calculated by using the comparative William's method (Williams, Winfield &Miller, 1983). This is a reliable method for recording Φ_F and involves the use of well characterised standard samples with known Φ_F values. Essentially, solutions of the standard and test samples with identical absorbance at the same excitation wavelength can be assumed to be absorbing the same number of photons. Hence, a simple ratio of the integrated fluorescence intensities of the two solutions (recorded under identical conditions) will yield the ratio of the quantum yield values. Since Φ_F for the standard sample is known, it is trivial to calculate the Φ_F for the test sample.

According to this method, the standard samples should be chosen to ensure they absorb at the excitation wavelength of choice for the test sample, and, if possible, emit in a similar region to the test sample. In order to minimise re-absorption effects (Dhami et al., 1995) absorbances in the 10 mm fluorescence cuvette should never exceed 0.1 at and above the excitation wavelength. Above this level, non-linear effects may be observed due to inner filter effects, and the resulting quantum yield values may be perturbed. This maximum allowable value of the recorded absorbance must be adjusted depending upon the path length of the absorption cuvette being used (for example, 10 mm = 0.1 maximum, 20 mm = 0.2 maximum etc). In this study, standard 10 mm path length fluorescence and absorption cuvettes were used for running the fluorescence and absorbance measurements. The UV-vis absorption (absorbance$\leq$0.10 at the excitation wavelength) and corrected fluorescence emission

spectra were recorded for three or more solutions with increasing concentrations of the sample and the standard. The integrated fluorescence intensities (that is, the area of the fluorescence spectrum) were calculated from the fully corrected fluorescence spectrum. Graphs of integrated fluorescence intensity *vs* absorbance were plotted. The gradient of the plots were later used in the quantum yield calculations according to the following equation:

$$\theta_x = \theta_{st}\left(\frac{Grad_x}{Grad_{st}}\right)\left(\frac{n_x^2}{n_{st}^2}\right)$$

Where the subscripts *ST* and *X* denote standard and test respectively, Φ is the fluorescence quantum yield, *Grad* the gradient from the plot of integrated fluorescence intensity *vs* absorbance and n is the refractive index of the solvent (Oter, 2007).

2.7 Buffer Solutions

The pH of the solutions were monitored by use of a digital pH-meter (ORION) calibrated with standard buffers of pH 12.00, 7.00 and 4.00 at 25±1 °C.

In all of the studies ultra pure water of Millipore was used. Deionised water, generated by a Milli-Q deionised water unit, which had a resistance better than 18.2 M cm, was used for the preparation of all the solutions.

Preparation of 0.005 M acetic acid / acetate buffer:0.286 mL of acetic acid (d=1.05 and 17.48 Molar) were dissolved in 950 mL ultra pure water. The solution was titrated to pH 5.0 at the lab temperature of 20^{o}C either with 0.1 M HNO_3 or 0.1 M NaOH as needed. The resulting solution was made up to 1000 ml with ultra pure water in a volumetric flask. The buffer solutions in the range of pH 4.0-6.0 were prepared by the same way by adjusting to the desired pH.

Preparation of 0.005 M NaH_2PO_4 / Na_2HPO_4 buffer:0.78 g of $NaH_2PO_4.2H_2O$ (MA=156.01) and 1.79 g of $Na_2HPO_4.12H_2O$ (MA=358.14) were dissolved in 950 mL ultra pure water. The solution was titrated to pH 7.0 at the lab temperature of 20 ^oC either with 0.1 M HNO_3 or 0.1 M NaOH as needed. The resulting solution was made up to 1000 ml with ultra pure water in a volumetric flask. The buffer solutions in the range of pH 7.0-9.0 and 10-12 were prepared by the same way by adjusting to the desired pH.

CHAPTER THREE

ENHANCED O2(g) RESPONSE OF TRIS(BIPYRIDINE)RUTHENIUM(II) IN PRESENCE OF DIFFERENT IONIC LIQUIDS IN SOL-JEL MATRIX METHODS

3.1 Introduction

Optical oxygen sensors have many advantages such as zero oxygen destruction, no interference from exterior electromagnetic field and no need for a reference electrode (Choi &Xiao, 1999; Xu, McDonough, Langsdorf, Demas &DeGraff, 1994). Sol gel films are widely used as chemical optic sensor matrix materials because they have many advantages such as being chemically inert, optically transparent, photochemically and thermally stable and mechanically strong.

However, some further investigations are still expected to improve the performances of O_2 sensing sol-gel films. For this purpose, there are some investigations icluding the modification of sol-gel membranes by changing the sensitive dye, parameters of sol-gel process (the sol-gel precursor type, the molar ratio of water:precursor (R), pH, catalyst type, catalyst concentration, ageing time, ageing temperature, drying time, drying temperature) or by the addition of some chemicals into the sol coctail.

The $Ru(bpy)_3^{2+}$ complex was selected in this study as the photosensitizer dye because of its attractive characteristics such as strong visible absorption, high photochemical stability, relatively high luminescence and long lifetime of metal-toligand charge transfer (MLCT) excited states.

In this work three different ionic liquids, 1-butyl-3-methylimidazolium tetrafluoroborate ($[BMIM^+][BF_4^-]$), 1-butyl-3-methylimidazolium thiocyanate

([BMIM][SCN]**)** and 1-butyl-3-methylimidazolium hexafluorophosphate ([BMIM][PF_6]) were employed for the modification of acid- catalyzed tetraethyl orthosilicate (TEOS) based sol-gel matrix. Photophysical characteristics and emission based response of (Ru $(bipy)_3^{2+}$) to gaseous oxygen was investigated in these ionic liquid containing sol–gel matrix by spectrofluorimetric method. Effects of the ionic liquid type, ionic liquid concentration, dye concentration and some sol gel parameters such as acid catalyze concentration; pH, gelation time, TEOS/water molar ratios and drying temperature to the oxygen sensitivity were evaluated.

3.2 Experimental

The O_2 sensitive fluorescent dye, tris (2, 2'-bipyridyl) ruthenium (II) chloride($Ru(bipy)_3^{2+}$) was supplied from Aldrich (99,5% purity). The ionic liquids,1-butyl-3-methylimidazolium hexafluorophosphate ([BMIM][PF_6]), (RTIL-I); 1-butyl-3-methylimidazolium thiocyanate ([BMIM][SCN]**),** (RTIL-II) and 1-butyl-3-methylimidazolium tetrafluoroborate ([$BMIM^+$][BF_4^-]),(RTIL-III)were supplied from Fluka. The structures of the ionic liquids and the ruthenium dye were given in Figure 2.1 and Figure 2.2 in Chapter 2.

The sols were prepared by the acid catalyzed method from a solution containing TEOS, HCl-acidified water, ethanol (EtOH), ethanolic solution of $Ru(bipy)_3^{2+}$ complex, Triton X-100 and ionic liquids. Equal volumes of TEOS and EtOH (0.5 ml) were added into a clean glass vial and stirred for 10 min. Then the HCl-acidified water and EtOH solution of $Ru(bipy)_3^{2+}$ dye were added into the vial respectively and the mixture was stirred continually to promote the hydrolysis and condensation reactions.

Triton X-100 was added in order to improve the homogeneity of the silica sol-gel and to give a crack-free monolith. The sol gel was also prepared by the addition of different ionic liquids with the same method.

In all cases the solutions were aged at room temperature in open glass vials. After the manuel coating of the sol-gel to glass slides, the slides were left to dry at room temperature or at 70 °C in oven. Glass slides were used as solid support onto which the sol-gel was cast by manual dip-coating technique. Prior to casting, the glass surface was activated by treatment with concentrated HNO_3 for 24 h, washed with distilled water, and then ethanol.

The molar ratios of TEOS, ethanol and water were either 1:1:4 (R=4) or 1:1:2 (R=2).The concentration of $Ru(bipy)_3^{2+}$ dyewas 10^{-5} M in the sol. The exact compositions of the solswere given in Table 3.1.In all cases the solutions were aged at room temperature in open glass vials. After the manuel coating of the sol-gel to glass slides, the slides were left to dry at room temperature or at 70 °C in oven. Glass slides were used as solid support onto which the sol-gel was cast by manual dip-coating technique. Prior to casting, the glass surface was activated by treatment with concentrated $HNO_3$for 24 h, washed with distilled water, and then ethanol.

Table 3.1 Compositions of the cocktails used as O_2-sensing agents.

Coctail Name	Acidified Water (µl)	Triton-x 100 (µl)	RTIL-I (µl)	RTIL-II (µl)	RTIL-III (µl)	dye solution (µl)	Gelation time (min)	Coctail pH	Drying Temperature (^{0}C)	I_0/I
Sol-1	193[a]	60	-	-	-	25	25	2	25	1.30
Sol-2	193[a]	60	60	-	-	25	17	2	25	1.70
Sol-3	193[a]	60	-	60	-	25	17	3	25	1.20
Sol-4	193[a]	60	-	-	60	25	16	2	25	1.03
Sol-5	193[a]	60	60	-	-	50	19	2	25	1.40
Sol-6a	193[a]	60	120	-	-	50	19	2	25	1.88
Sol-6b	193[a]	60	120	-	-	50	10	2	25	1.13
Sol-6c	193[a]	60	120	-	-	50	30	2	25	1.52
Sol-6d	193[a]	60	120	-	-	50	60	2	25	1.40
Sol-6e	193[a]	60	120	-	-	50	180	2	25	1.16
Sol-7	193[a]	60	120	-	-	25	10	2	25	1.49
Sol-8a	193[b]	60	-	-	-	50	10	4	25	1.34
Sol-8b	193[b]	60	-	-	-	50	10	4	70	1.12
Sol-8c	193[b]	60	-	-	-	50	20	4	25	1.09
Sol-8d	193[b]	60	-	-	-	50	20	4	70	1.17
Sol-8e	193[b]	60	-	-	-	50	30	4	25	1.39
Sol-8f	193[b]	60	-	-	-	50	30	4	70	1.13
Sol-9a	193[b]	60	120	-	-	50	10	5	25	1.15
Sol-9b	193[b]	60	120	-	-	50	20	5	25	1.25
Sol-9c	193[b]	60	120	-	-	50	20	5	70	1.64
Sol-9d	193[b]	60	120	-	-	50	30	5	25	2.20
Sol-9e	193[b]	60	120	-	-	50	30	5	70	2.10
Sol-9f	193[b]	60	120	-	-	50	60	5	25	1.21
Sol-9g	193[b]	60	120	-	-	50	60	5	70	1.10
Sol-10a	96.5[c]	60	-	-	-	50	48h	6	25	1.08
Sol-10b	96.5[c]	60	-	-	-	50	48h	6	25	1.04
Sol-11a	96.5[c]	60	120	-	-	50	48h	7	25	1.11
Sol-11b	96.5[c]	60	120	-	-	50	48h	7	25	1.22

[a] 193 refers to 169 μl water 24 μl concentrated HCl (R=4).

[b] 193 refers to 169 μl water 24 μl 0.1M HCl (R=4).

[c] 96.5 refers to 84.5 μl water 12 μl 0.1M HCl (R=2).

3.3 Results and discussion

The sol–gel matrix provides many advantages for spectroscopic studies. It is chemically and mechanically stable, acts as a diluted and optically transparent medium like a solution, and also provides a rigid microenvironment for doped molecules. It is also a valuable matrix for bio-technological and clinical applications. In our previous investigations we have improved the oxygen response of sol–gel composites and we have obtained a crackless free sol gel surface by the addition of ionic liquids. However, our sol gel composites could not capture the ruthenium dye inside because of the water solubility of the appliedd ionic liquids. So, in this study, we aimed to improve the oxygen response of the $Ru(bipy)_3^{2+}$ dye in sol gel by the addition of other ionic liquids which of two are hydrophilic ([BMIM][SCN] and $[BMIM^+][BF_4^-]$) and one is hydrophobic ($[BMIM][PF_6]$). By the addition of hydrophobic ($[BMIM][PF_6]$), we also aimed to prevent the leakage of the ruthenium dye from the sol gel matrix. We also examined the oxygen response in case of the ionic liquid type, ionic liquid concentration, dye concentration and some sol gel parameters such as acid catalyze concentration; pH, gelation time, TEOS/water molar ratios and drying temperature.

3.3.1 O_2 sensing studies

Oxygen as a triplet molecule is able to quench efficiently the fluorescence of ruthenium complex via collision with the fluorophore in its excited state leading to a non-radiative transfer of energy. This effect is called “dynamic fluorescence quenching”. The degree of fluorescence quenching relates to the frequency of collisions, and therefore to the concentration, pressure, temperature and the sensor matrix material. The employed oxygen sensitive cocktail compositions yield emission peaks between λ_{max} = 590–600 nm which respond to O_2 by a decrease in

emission intensity that can be used as the analytical signal.The fluorescence intensity can be expressed in terms of theStern–Volmer equation where the fluorescence is related quantitativelyto the partial pressure of oxygen: $I_0/I = K_{SV}pO_2 + 1$. I_0 is the intensity of fluorescence at zero pressure of oxygen, I is the intensity of fluorescence at a pressure p of oxygen and K_{SV} is the Stern–Volmer constant. For a given media, and at a constant total pressure and temperature, the partial pressure of oxygen is proportional to oxygen mole fraction. The oxygen sensitivity is proportional to K_{SV}, which in turn, is proportional to the oxygen permeability and diffusion coefficient of the sol–gel film.

The diffusion efficiency of oxygen is related to the microstructure of the sol–gel membrane where the microstructure of the porous sol–gel glass is dependent to molar water:silisium ratio (R), pH, precursor type, nature of catalyst, aging time, aging temperature, drying time and drying temperature, ionic liquid type and ionic liquid concentration. In this study, the employed precursor was TEOS, the R value was 2 or 4, and the process was acid catalyzed with the mineral acid of HCl. The employed ionic liquids were hydrophilic [BMIM][SCN] and [$BMIM^+$][BF_4^-] and hydrophobic [BMIM][PF_6]. The I_0/I values were found to be 1.30 in the absence of ionic liquid and 1.20, 1.03 and 1.70 for sol-1–4, respectively. The response of the dye were 22 %, 18%, 3 % and 42 % (sol-2), respectively(Figure 3.1-3.4, Table 3.2-3.9).The further studies were performed with the [BMIM][PF_6] becuse of the higher I_0/I value and to prevent the leakage of the ruthenium dye from the sol gel matrix with its hydrophobic character.In order to optimize the coctail compositions, different coctails, which have different amounts of $Ru(bipy)_3^{2+}$ and [BMIM][PF_6] were prepared.The response of the dye was investigated for the ruthenium concentrations of 5.0×10^{-6} M and 10^{-5} M. The best response was observed for the 10^{-5} M concentrations of the dye and the further studies were performed with the concerning films. The aging time was dependent on the cocktail composition and was between 16–180 min(R=4, concentrated HCl), between 10–60 min (R=4, 0.1 M HCl) and between 10–2910 min (R=2, 0.1 M HCl). The films were left todry for 18 h at roomtemperature and at 70 °C prior to the gasphase measurements. Different amounts of ionic liquid were usedtogether with Triton X-100 in the preparation of

the sol–gel monolithsin order to reduce the risk of fracture and increase the sensorstability and response as we have observed in our previous study (Oter, Ertekin & Derinkuyu, 2009). The employed sol gel monolits and the applied conditions with the I_0/I values were given in detail in Table 3.1. Room-temperature ionic liquids were shown that they couldbe either used to modify in a controlled fashion the properties ofthe conventional micelles or just themselves as micelles (Wasserscheid & Welton, 2003; Welton, 2004; Vanyur, Biczok and Miskolczy, 2007).Also surfactant behavior and possibility of surfactant self-assemblywithin ILs have been investigated by research groups (Matos et al., 2006). Theusage of surfactants in the sol–gel process reduces the interfacialenergy and thereby decreases the capillary stress. Anotheradvantage of addition of ionic liquids into the sol–gel glass is theirco-immobilization with sensing agent in silica which can increasethe stability of the sensor.

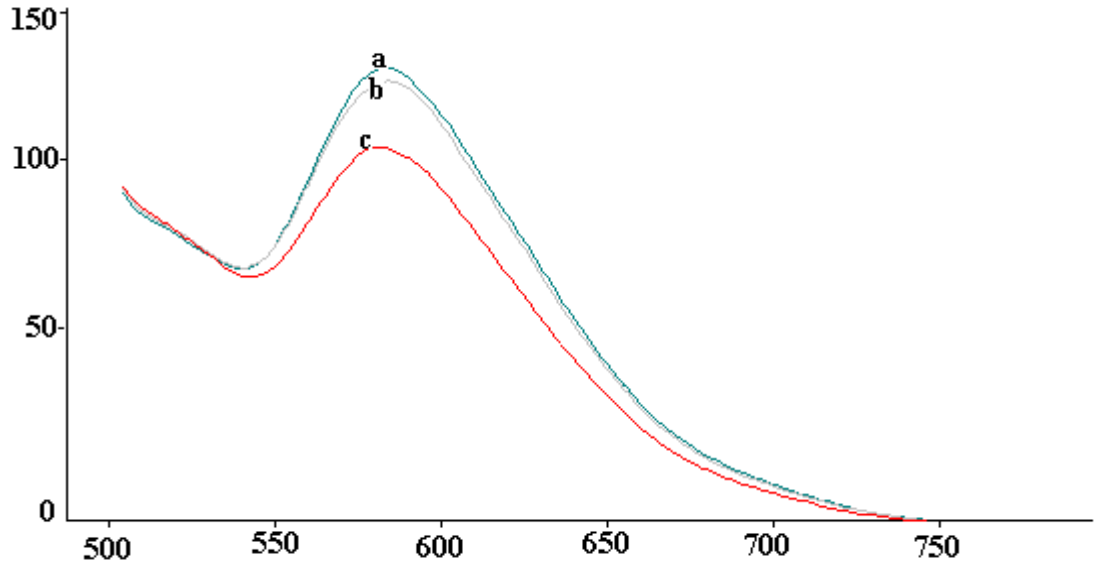

Figure 3.1 Response of sol-1 to $O_{2(g)}$ (a) 0% (b) 20% (c) 100% O_2 (relative signal change is 22%).

Table 3.2 Fluorescence intensity of sol-1

% O_2	I_{em}	I_0/I
0	135	1.3
20	130	
100	105	

Table 3.3 Composition of the sol-1

Coctail Name	Acidified Water (µl)	Triton-x 100 (µl)	RTIL-I (µl)	RTIL-II (µl)	RTIL-III (µl)	dye solution (µl)	Gelation time (min)	Coctail pH	Drying Temperature (^{0}C)	I_0/I
Sol-1	193[a]	60	-	-	-	25	25	2	25	1.30

[a] 193 refers to 169 ul water 24 µl concentrated HCl

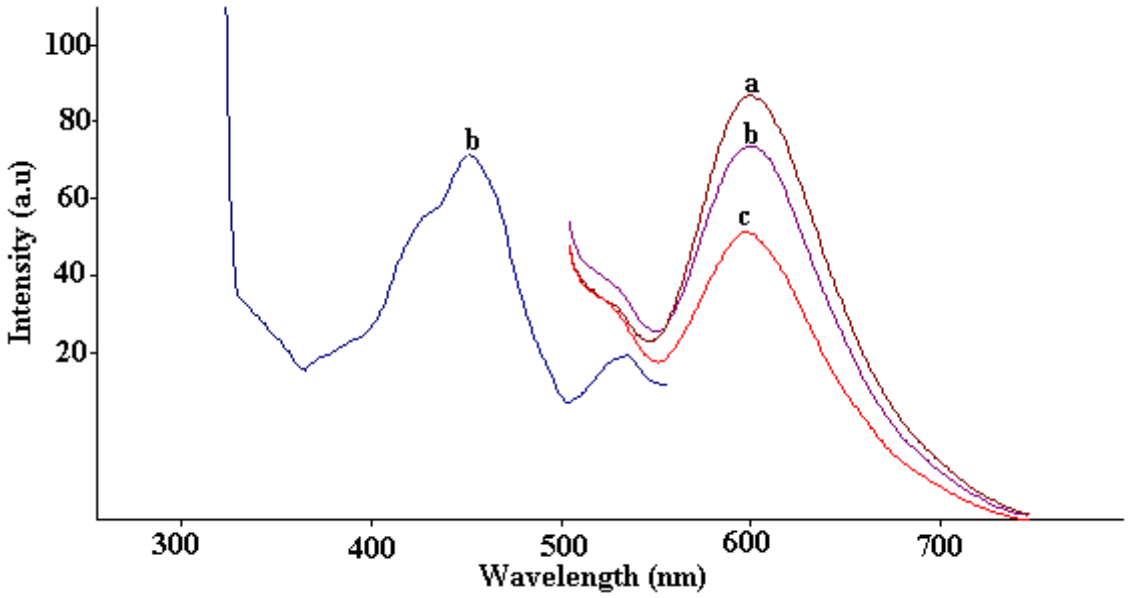

Figure 3.2 Response of sol-2 to $O_{2(g)}$ (a) 0% (b) 20% (c) 100% O_2 (relative signal change is 42%).

Table 3.4 Fluorescence intensity of sol-2

% O_2	I_{em}	I_0/I
0	85	1.7
20	70	
100	49	

Table 3.5 Composition of the sol-2

Coctail Name	Acidified Water (µl)	Triton-x 100 (µl)	RTIL-I (µl)	RTIL-II (µl)	RTIL-III (µl)	dye solution (µl)	Gelation time (min)	Coctail pH	Drying Temperature (^{0}C)	I_0/I
Sol-2	193[a]	60	60	-	-	25	17	2	25	1.70

[a]193 refers to 169 ul water 24 µl concentrated HCl

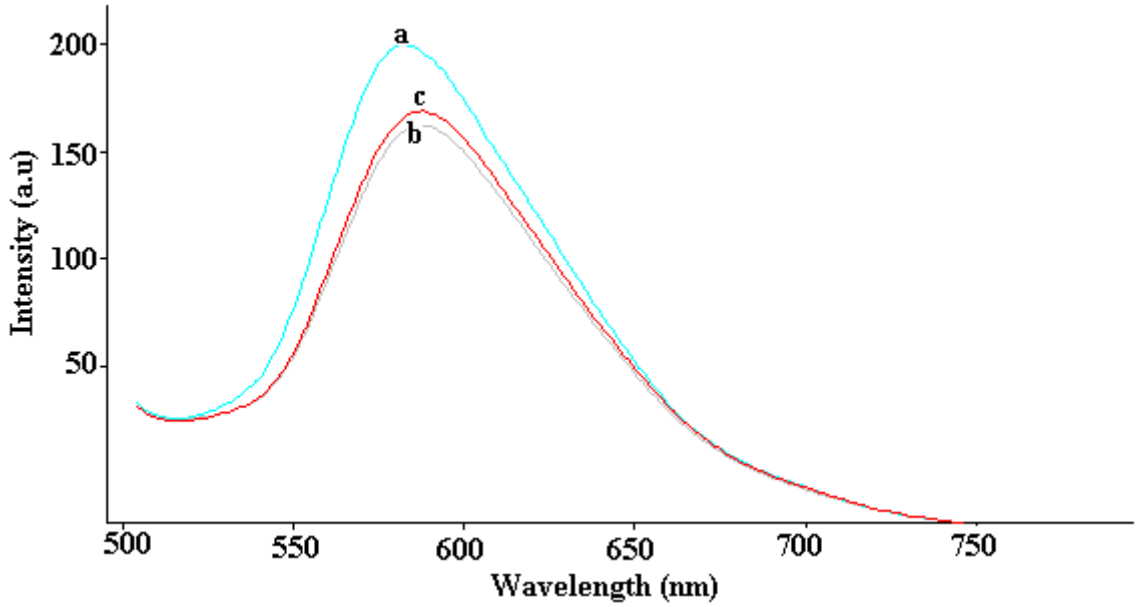

Figure 3.3 Response of sol-3 to $O_{2(g)}$ (a) 0% (b) 20% (c) 100% O_2 (relative signal change is 18%)

Table 3.6Fluorescence intensity of sol-3

% O_2	I_{em}	I_0/I
0	195	1.2
20	155	
100	160	

Table 3.7 Composition of the sol-3

Coctail Name	Acidified Water (µl)	Triton-x 100 (µl)	RTIL-I (µl)	RTIL-II (µl)	RTIL-III (µl)	dye solution (µl)	Gelation time (min)	Coctail pH	Drying Temperature (^{0}C)	I_0/I
Sol-3	193[a]	60	-	60	-	25	17	3	25	1.20

[a] 193 refers to 169 ul water 24 µl concentrated HCl

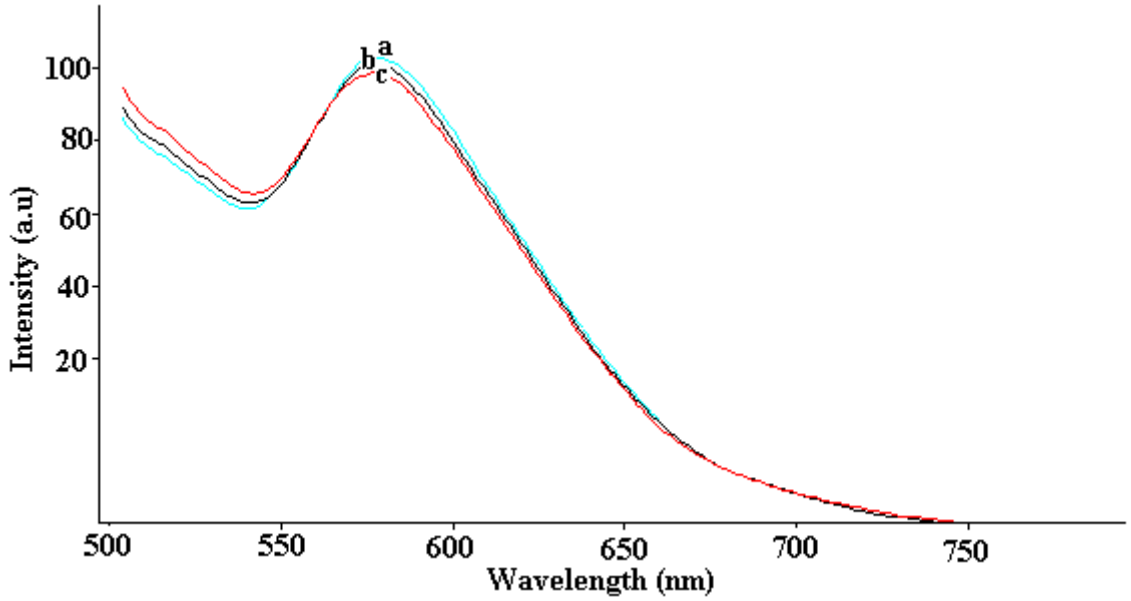

Figure 3.4 Response of sol-4 to $O_{2(g)}$ (a) 0% (b) 20% (c) 100% O_2 (relative signal change is 3%)

Table 3.8 Fluorescence intensity of sol-4

% O_2	I_{em}	I_0/I
0	100	1.03
20	99	
100	97	

Table 3.9 Composition of the sol-4

Coctail Name	Acidified Water (µl)	Triton-x 100 (µl)	RTIL-I (µl)	RTIL-II (µl)	RTIL-III (µl)	dye solution (µl)	Gelation time (min)	Coctail pH	Drying Temperature (^{0}C)	I_0/I
Sol-4	193[a]	60	-	-	60	25	16	2	25	1.03

[a] 193 refers to 169 ul water 24 µl concentrated HCl

3.3.2 Effect of ionic liquid concentration

Figures 3.5-3.10 shows the spectrofluorimetric oxygen response of the sol–gel monolithsprepared from two different amounts of ionic liquid [BMIM][PF_6] containing sols (sol 5, 6a, 7, Table 3.1, Table 3.10-3.15) and the Stern–Volmer plots.In the case of sol-5, upon exposureto 100% of O_2, therelative signal change was 29 % and the I_0/I value was found as 1.40. In the case of sol-6a (the ionic liquid concentration was twice the sol 5), the relative signal change was enhanced to 47 % and the I_0/I value was found as 1.88. Thus, the sol 6a exhibited better responsewhen compared with that of IL-free TEOS based sol–gelfilms and 120 µL ionic liquid is optimum for the preparation of concerned ionic liquid modified sol–gel cocktails. This behavior is related to the microstructural differences between the two different composites. The addition of excess amount of ionic liquid did not result with significant increase in the oxygen sensitivity. The Stern–Volmer plot of sol-6a exhibited a good linearity for the gaseous oxygen in the partial pressure rangeof 0.0–100% pO_2 and can be described with the equations of y = 0.0078x+1.0552; R^2 =

0.9659. TheStern–Volmer constants (KSV) were found to be 0.003 and 0.0078 for sol-5 and sol-6a, respectively.We attribute the good linearity of Stern–Volmer plots to theuniform distribution of luminophore in the network of the ionicliquid-doped silicate matrix. The high linearity of the plots revealsthat, only one type of quenching; dynamic quenching occursthroughout the oxygen measurements.

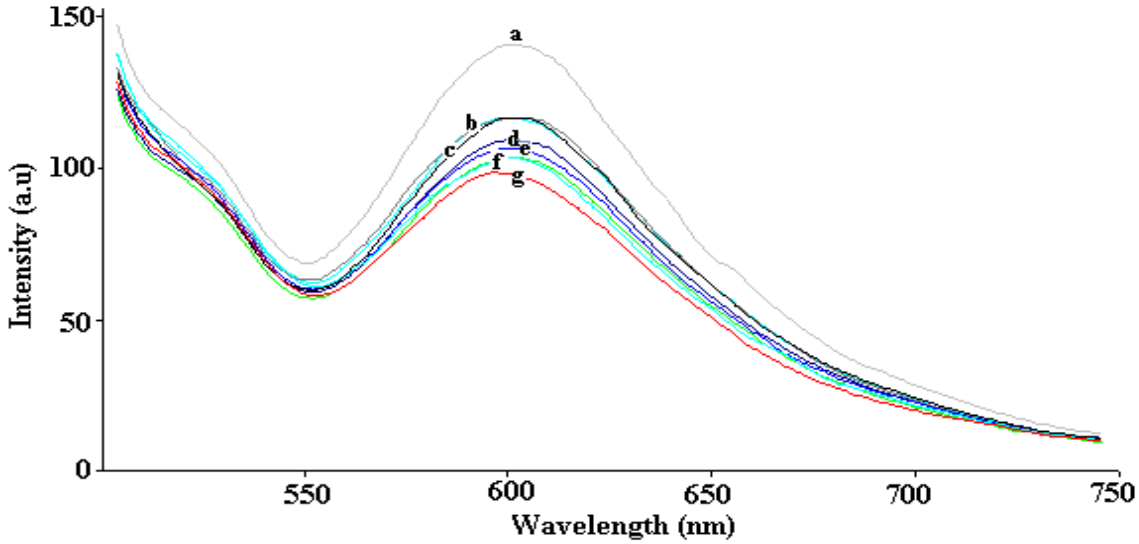

Figure 3.5Response of sol-5 to $O_{2(g)}$ (a) 0% (b) 10%, (c) air(d) 20% O_2 (e) 40% O_2 (f) 60%, 80% O_2(g) 100% O_2 (relative signal change is 29%).

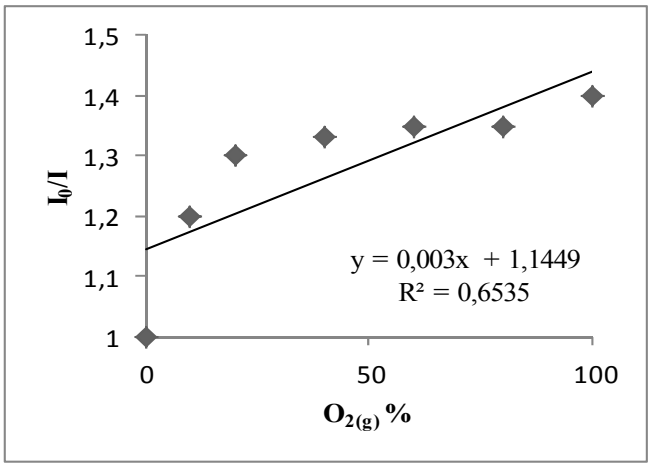

Figure 3.6 Stern–Volmer plot for sol-5.

Table 3.10 Fluorescence intensity of sol-5

% O_2	**I_{em}**	**I_o/I**
0	138	1
10	115	1.2
air	115	1.2
20	106	1.3
40	104	1.33
60	102	1.35
80	102	1.35
100	98	1.4

Table 3.11 Composition of the sol-5

Coctail Name	**Acidified Water (µl)**	**Triton-x 100 (µl)**	**RTIL-I (µl)**	**RTIL-II (µl)**	**RTIL-III (µl)**	**dye solution (µl)**	**Gelation time (min)**	**Coctail pH**	**Drying Temperature (^{0}C)**	**I_0/I**
Sol-5	193[a]	60	60	-	-	50	19	2	25	1.40

[a] 193 refers to 169 ul water 24 µl concentrated HCl

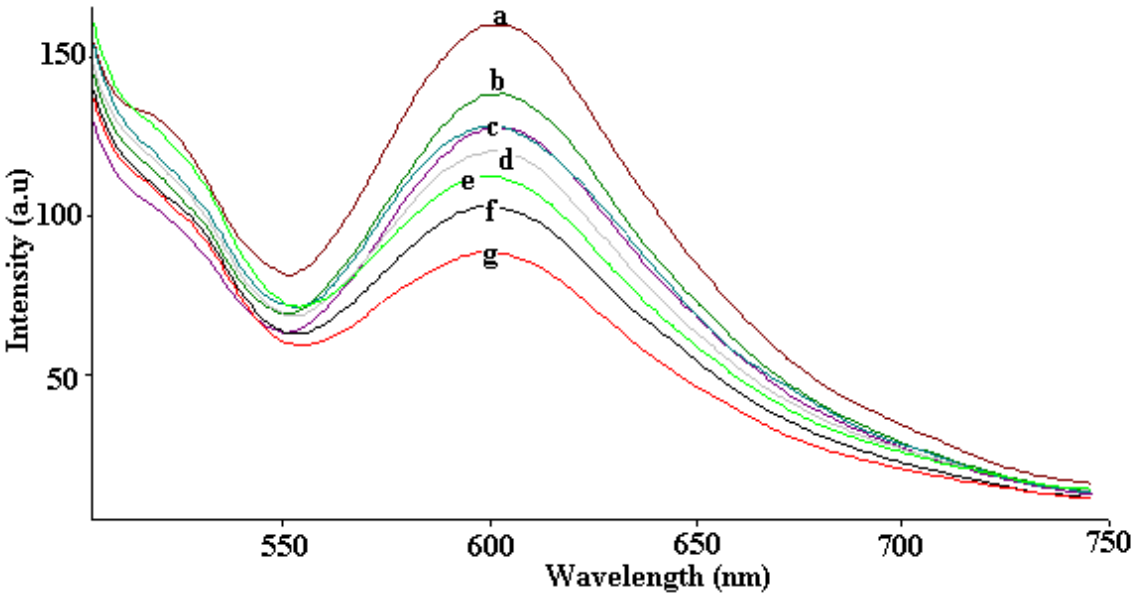

Figure 3.7Response of sol-6a to $O_{2(g)}$ (a) 0% (b) 10%, (c) 20% O_2,air(d) 40% O_2 (e) 60% O_2 (f) 80% O_2 (g) 100% O_2 (relative signal change is 47%).

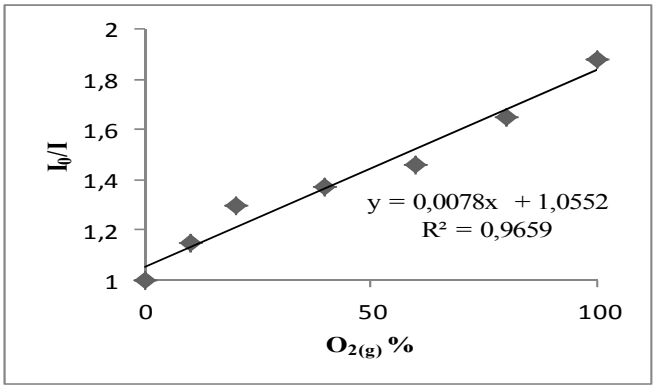

Figure 3.8 Stern–Volmer plot for sol-6a.

Table 3.12 Fluorescence intensity of sol-6a

% O_2	**I_{em}**	**I_o/I**
0	162	1
10	140	1.16
20	125	1.3
Air	125	1.3
40	118	1.37
60	111	1.46
80	98	1.65
100	86	1.88

Table 3.13Composition of the sol-6a

Coctail Name	**Acidified Water (µl)**	**Triton-x 100 (µl)**	**RTIL-I (µl)**	**RTIL-II (µl)**	**RTIL-III (µl)**	**dye solution (µl)**	**Gelation time (min)**	**Coctail pH**	**Drying Temperature (^{0}C)**	**I_0/I**
Sol-6a	193[a]	60	120	-	-	50	19	2	25	1.88

[a] 193 refers to 169 ul water 24 µl concentrated HCl

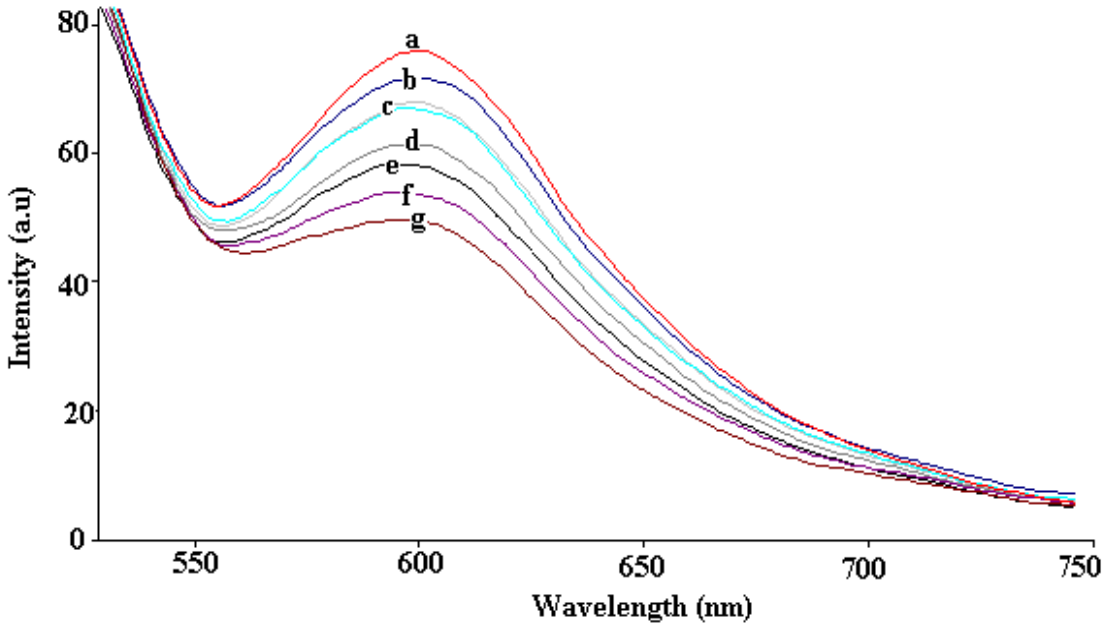

Figure 3.9 Response of sol-7 to $O_{2(g)}$ (a) 0% (b) 10%, (c) 20% O_2 , air(d) 40% O_2 (e) 60% O_2 (f) 80% O_2 (g) 100% O_2 (relative signal change is 33%).

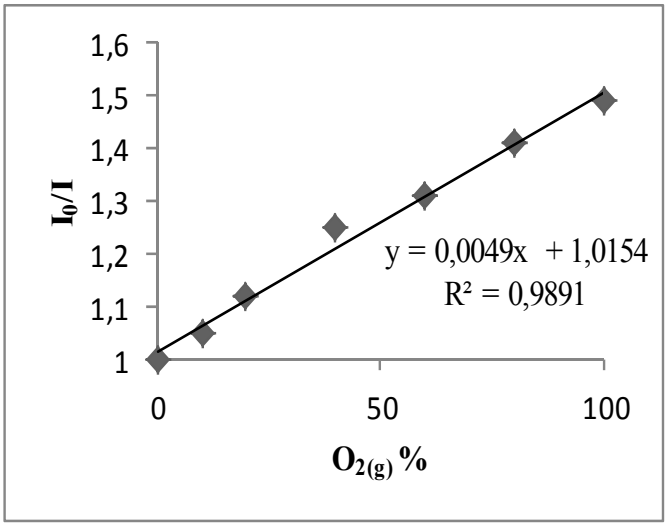

Figure 3.10 Stern–Volmer plot for sol-7.

Table 3.14 Fluorescence intensity of sol-7

% O_2	**I_{em}**	**I_o/I**
0	76	1
10	72	1,05
20	68	1,12
Air	68	1,12
40	61	1,25
60	58	1.31
80	54	1.41
100	51	1.49

Table 3.15 Composition of the sol-7

Coctail Name	**Acidified Water (µl)**	**Triton-x 100 (µl)**	**RTIL-I (µl)**	**RTIL-II (µl)**	**RTIL-III (µl)**	**dye solution (µl)**	**Gelation time (min)**	**Coctail pH**	**Drying Temperature (^{0}C)**	**I_0/I**
Sol-7	193[a]	60	120	-	-	25	10	2	25	1.49

[a] 193 refers to 169 ul water 24 µl concentrated HCl

3.3.3 O_2 sensing studies with cocktails of mol ratio ofwater/TEOS = 2 (R = 2)and mol ratio of water/TEOS = 4 (R = 4)

Type of catalyze is an important parameter for the preparation of sol–gel matrices which influences the gas permeability of the prepared sol–gel glass. The acid catalyzed sol–gel matrix has the disadvantage of low gas permeability while the base catalyzedmatrix can be obtained after a long process because of the very slowly proceeding hydrolysis and condensation reactions(Garcia, Fernandez & Diaz-garcia, 2004; Schubert&Husing, 2000). In this study, the process was acid catalyzed with different concentrations of mineral acid of HCl (concentrated HCl and 0.1M HCl)

and the molar ratios of TEOS, ethanol and water were either1:1:4 (R=4) or 1:1:2 (R=2). In the case of base catalysed sol gel matrix, usually the I_0/I values are higher, however the gelation times were increased to day long durations. The ionic liquid modified acid catalyzed sol–gel matrix combines both the advantages of acid catalyzed and base catalyzed sol–gel matrix. The ionic liquid modified sol–gel matrix increases the matrix pH and the oxygen response with moderate gelation times which are observed maximum 180 minutes in ionic liquid containing sol gel monolits in which R=4.The precise stage inthe process at which films are made is important because the viscocityof the solution increases by the time passes during the agingperiod and the rate of this increase depend on the cocktail composition(McDonagh &MacCraith, 2002).The films were casted by manual dip-coating technique on the glass slides after 10, 20, 30, 60 and 180 minutes and the best results were obtained for the films casted after 30 minutes of gelation process and (see Table 1).So, 30min. was selected as an optimum waiting time prior to casting for the glass slides prepared from the sol-9 compositions.The aging timewas different for some other cocktails depending onthe cocktail composition (see Table 3.1).In concantrated acidic coctail (R=4), maximum response of $Ru(bipy)_3^{2+}$ is observed in sol-6a. Thus the films were casted by manual dip-coating technique on the glass slides after 10, 30, 60 and 180 minutes to obtain best gelation time. Oxygen responses of the sol-gel monoliths under different geletion times in R=4 and concantrated acidic coctail are shown in Figure 3.13-3.20 and the I_0/I values were found to be 1.13, 1.52, 1.4 and 1.16 for sol 6b, sol 6c, sol 6d and sol 6e respectively.Therelative signal changes were 12 %, 47 %, 34 %, 29 % and 14 % for sol 6b, 6a, 6c, 6d and 6e respectively. Figure 3.12 shows the best oxygen response of sol-gel monolits in concantrated acidic coctail.Sol-6a where the gelation time is 19 minutes has maximum response of $Ru(bipy)_3^{2+}$in concantrated acidic coctail.Figure 3.11 compares oxygen response of the sol-gel monoliths from R=4 and less acidic coctail (0.1 M HCl) under different geletion times and the I_0/I values were found to be 1.15, 1.25, 2.2 and 1.21 for sol 9a, sol 9b, sol 9d and sol 9f respectively.After half an hour the response of ($Ru(bipy)_3^{2+}$) to gaseous oxygen was decrased and drying temperature of the sol-gel slides is not important for the oxygen sensing.The concerning aging times werebetween 10–60 min (R=4, 0.1 M HCl) and the films

were left to dry for 18 h at roomtemperature at 70 °C prior to the gas phase measurements. In the absence of ionic liquidat pH=4the I_0/I values were found to be 1.34, 1.09 and 1.39at room temperature for sol 8a, sol 8c and sol 8e and the response of the dye were 25 %, 8%, and 28 % respectively. The I_0/I values generally decreased when temperature increased from roomtemperature to 70 °C, and were found to be 1.12, 1.17 and 1.13 for gelation timesof 10, 20 and 30 minutes respectively. The response of dye were 11 %, 14%, and 12 % for sol 8b, sol 8d and sol 8f respectively (Figure 3.21-3.32, Table 3.24-3.35).

In the ionic liquid modified sol–gel matrix; the matrix pH increases from 4 to 5. The films were casted by manual dip-coating technique on the glass slides after 10, 20, 30 and 60 minutes at roomtemperature or 70 ^{0}C. The I_0/I values were found to be 1.15, 1.25, 2.2 and 1.21at room temperature for sol 9a, sol 9b, sol 9d and sol 9f respectively. Drying temperature was not observed as an important parameter generally. The oxygen response of the sol-gel monoliths at 70 ^{0}Cwere taken after 20, 30 and 60 minutes and the I_0/I values were found to be 1.64, 2.1 and 1,1 for sol 9c, sol 9e, and sol 9g respectively (Figure 3.34-3.51, Table 3.37-3.53).As it seems that the maximum response of $Ru(bipy)_3^{2+}$ is observed in sol 9d and adding ionic liquid to sol-gel coctails increased the relative signal changes from 28% to 55% (Figure 3.29 and Figure 3.39). The response of the sol-9d films for tested for three films and the Stern volmer plots with error bars below 5% standart deviation are seen in Figure 3.41.

The I_0/I values are higher, but the gelation times were increased to day long durations in ionic liquid containing base catalysed sol gel monolits in which R=2. The I_0/I values were found to be 1.08 and 1,04 for sol 10a, and sol 10b respectively in the absence of ionic liquid. Adding ionic liquid to sol-gel coctails increased the response of O_2 sensing slightly and the I_0/I values were found to be 1.11 and 1,22 for sol 11a, and sol 11b which were casted by manual dip-coating technique on the glass slides after 2900 and 2910 minutes at roomtemperature (Figure 3.52-3.59, Table 3.54-3.61).

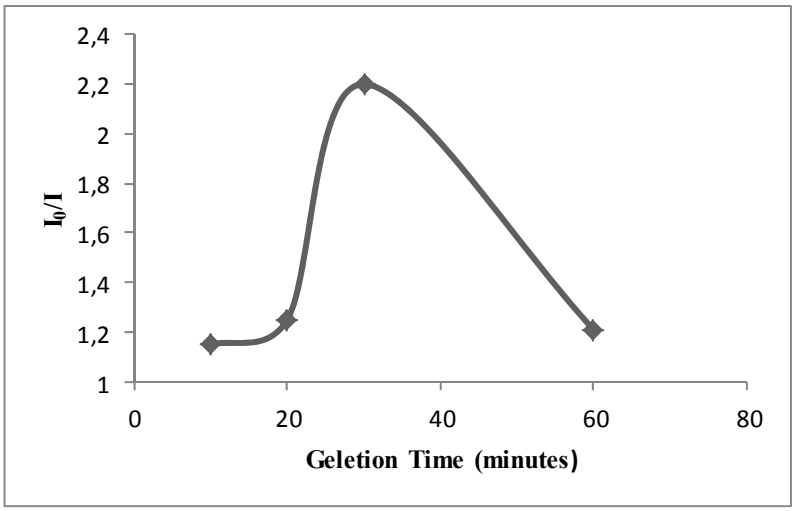

Figure 3.11 The effect ofgeletion time of the sol–gel monoliths prepared from sol-9 composition.

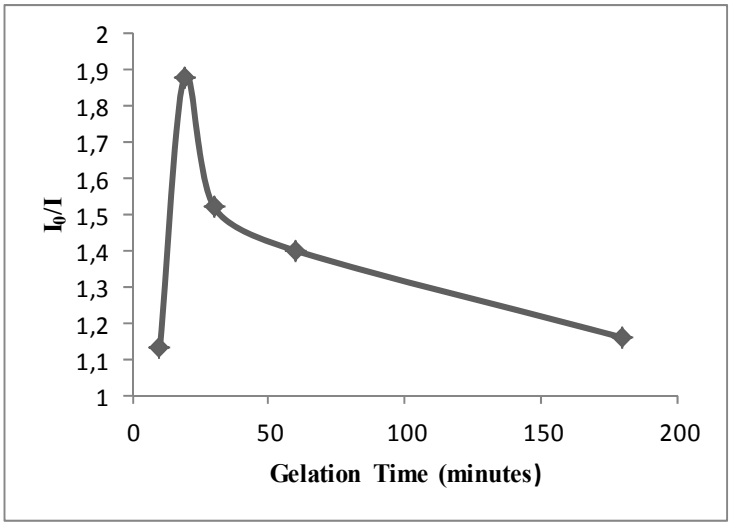

Figure 3.12 The effect ofgeletion time of the sol–gel monoliths prepared from sol-6 composition.

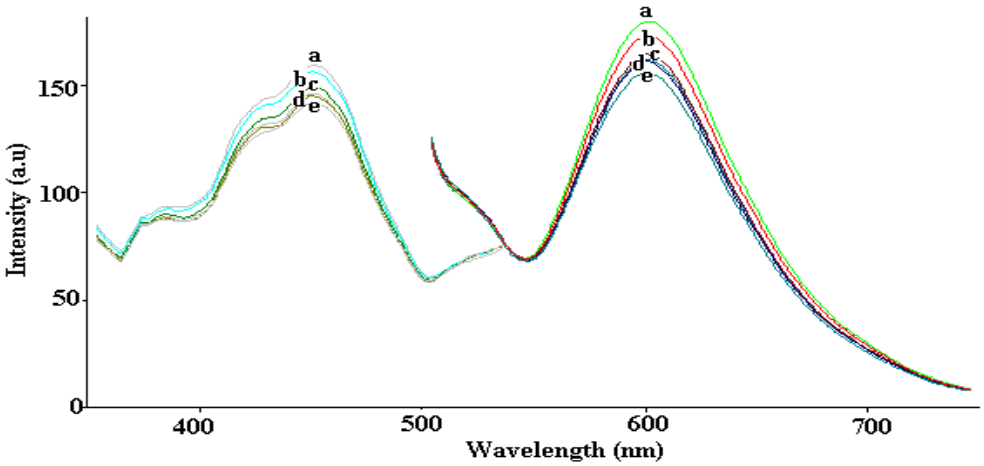

Figure 3.13 Response of sol-6b to $O_{2(g)}$ (a) 0% (b) 10%, (c) 20% O_2,air(d) 60% O_2 (e) 100% O_2(relative signal change is 12%).

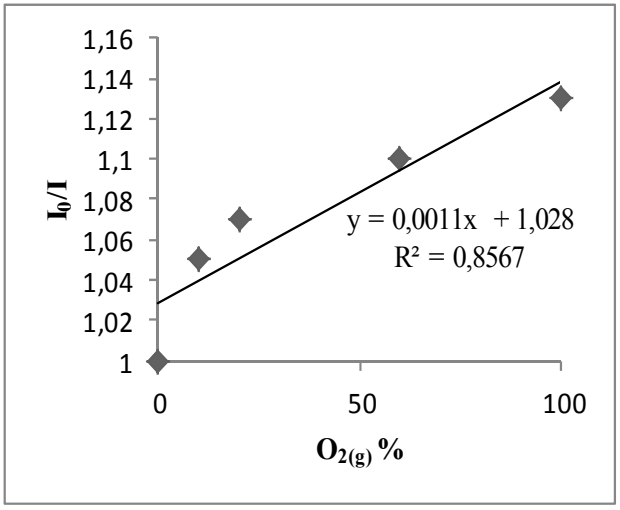

Figure 3.14 Stern–Volmer plot for sol-6b.

Table 3.16 Fluorescence intensity of sol-6b

% O_2	I_{ex}	I_{em}	I_o/I
0	164	183	1
10	159	175	1.05
20	155	171	1.07
Air	153	169	1.08
60	150	167	1.1
100	144	162	1.13

Table 3.17 Composition of the sol-6b

Coctail Name	Acidified Water (µl)	Triton-x 100 (µl)	RTIL-I (µl)	RTIL-II (µl)	RTIL-III (µl)	dye solution (µl)	Gelation time (min)	Coctail pH	Drying Temperature (^{0}C)	I_0/I
Sol-6b	193[a]	60	120	-	-	50	10	2	25	1.13

[a] 193 refers to 169 ul water 24 µl concentrated HCl

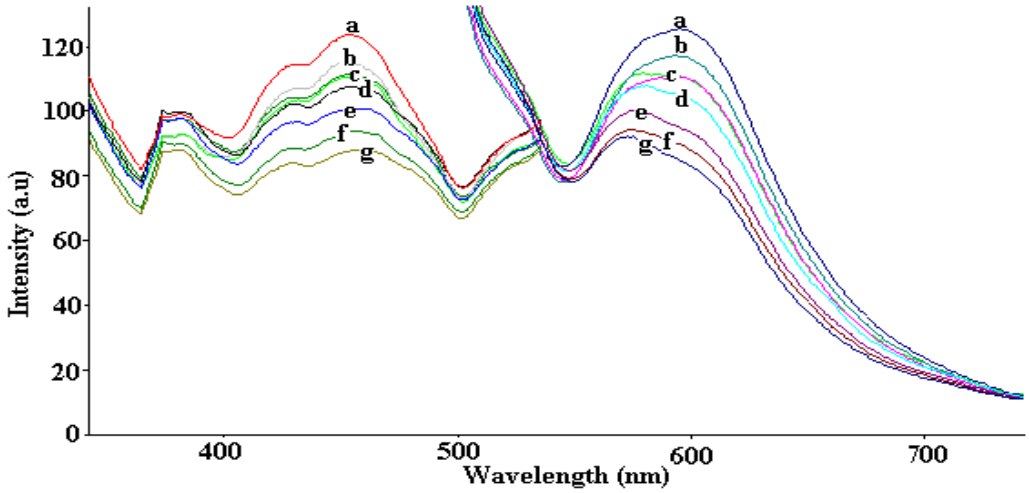

Figure 3.15 Response of sol-6c to $O_{2(g)}$ (a) 0% (b) 10%, (c) 20% O_2, air(d) 40% O_2 (e) 60% (f) 80% (g) 100% O_2 (relative signal change is 34%).

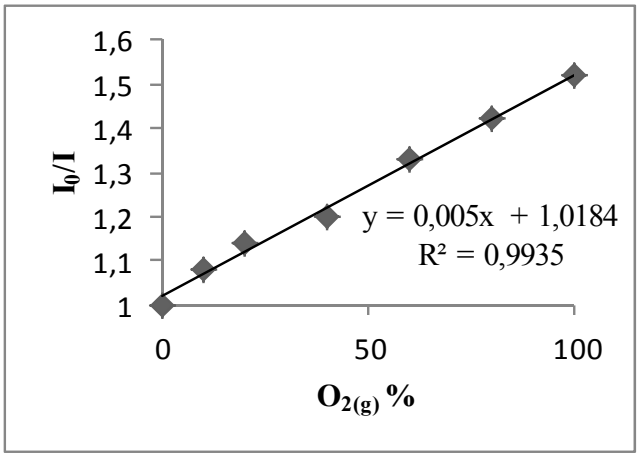

Figure 3.16 Stern–Volmer plot for sol-6c

Table 3.18 Fluorescence intensity of sol-6c

% O_2	I_{ex}	I_{em}	I_o/I
0	124	126	1
10	116	117	1.08
20	111	111	1.14
Air	110	110	1.15
40	106	105	1.2
60	100	95	1.33
80	93	89	1.42
100	86	83	1.52

Table 3.19 Composition of the sol-6c

Coctail Name	Acidified Water (µl)	Triton-x 100 (µl)	RTIL-I (µl)	RTIL-II (µl)	RTIL-III (µl)	dye solution (µl)	Gelation time (min)	Coctail pH	Drying Temperature (^{0}C)	I_0/I
Sol-6c	193[a]	60	120	-	-	50	30	2	25	1.52

[a] 193 refers to 169 ul water 24 µl concentrated HCl

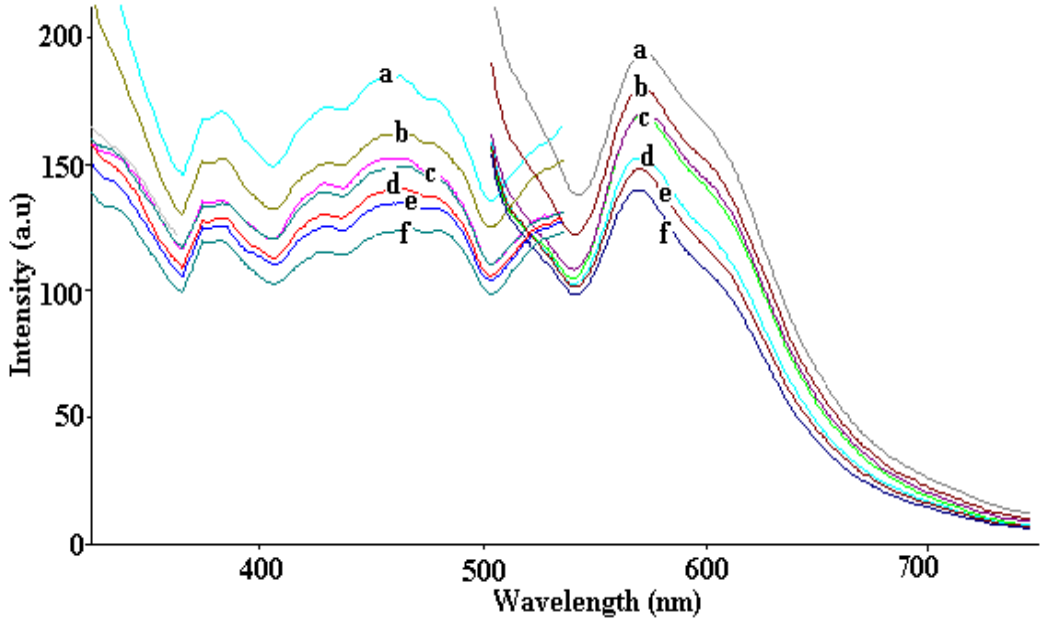

Figure 3.17 Response of sol-6d to $O_{2(g)}$ (a) 0% (b) 10%, (c) 20% O_2, air(d) 60% O_2 (e) 80% (f) 100% (relative signal change is 29%).

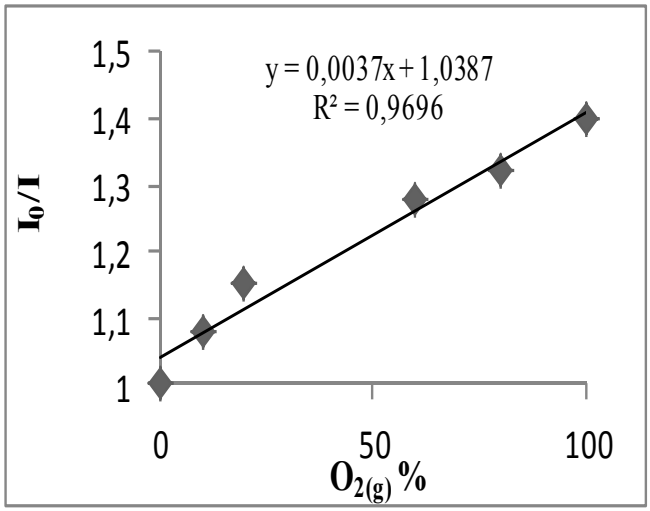

Figure 3.18 Stern–Volmer plot for sol-6d.

Table 3.20 Fluorescence intensity of sol-6d

% O_2	**I_{ex}**	**I_{em}**	**I_o/I**
0	185	194	1
10	162	179	1.08
20	151	169	1.15
Air	149	169	1.15
60	140	152	1.28
80	133	147	1.32
100	122	138	1.40

Table 3.21 Composition of sol-6d

Coctail Name	Acidified Water (µl)	Triton-x 100 (µl)	RTIL-I (µl)	RTIL-II (µl)	RTIL-III (µl)	dye solution (µl)	Gelation time (min)	Coctail pH	Drying Temperature (^{0}C)	I_0/I
Sol-6d	193[a]	60	120	-	-	50	60	2	25	1.40

[a] 193 refers to 169 ul water 24 µl concentrated HCl

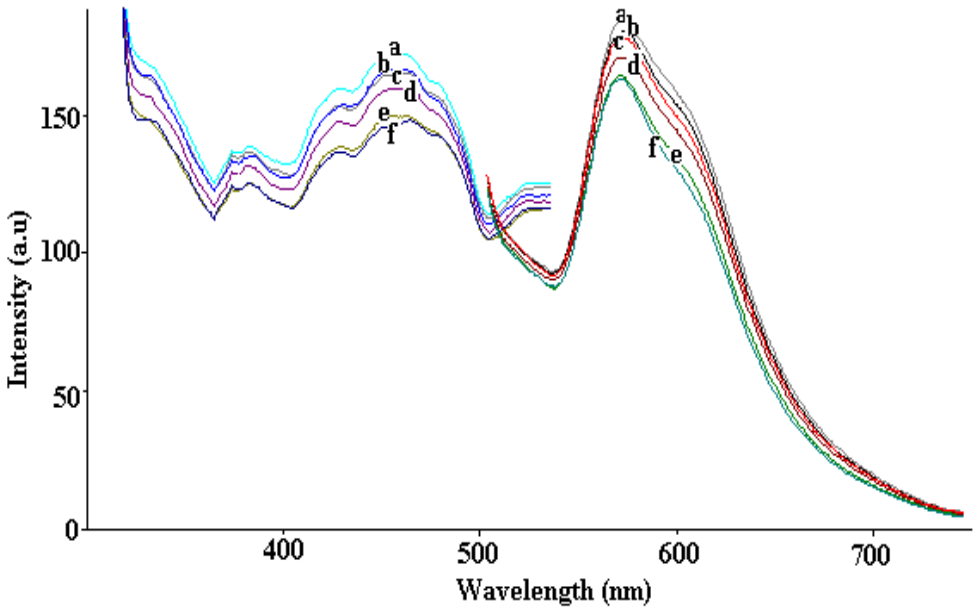

Figure 3.19 Response of sol-6e to $O_{2(g)}$ (a) 0% (b) 10%, (c) 20% O_2,air(d) 60% O_2 (e) 80% (f) 100% (relative signal change is 14%).

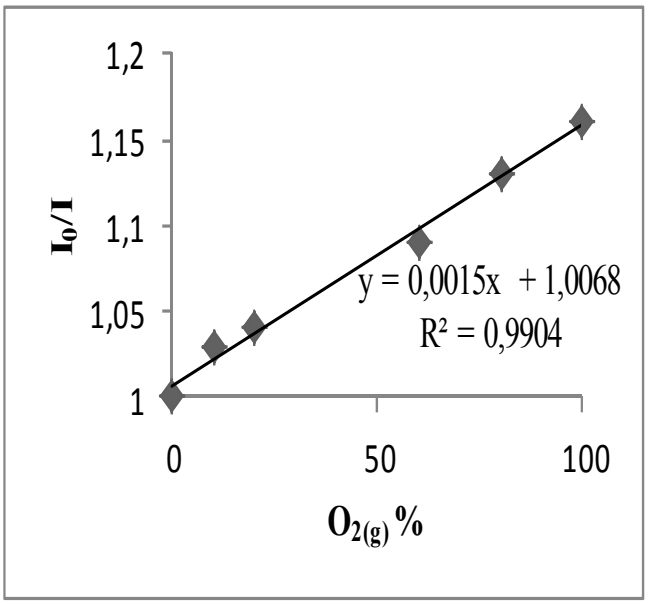

Figure 3.20 Stern–Volmer plot for sol-6e.

Table 3.22 Fluorescence intensity of sol-6e

% O_2	I_{ex}	I_{em}	I_o/I
0	173	185	1
10	167	180	1.03
20	164	178	1.04
Air	164	178	1.04
60	160	170	1.09
80	150	163	1.13
100	147	159	1.16

Table 3.23 Composition of the sol-6e

Coctail Name	Acidified Water (µl)	Triton-x 100 (µl)	RTIL-I (µl)	RTIL-II (µl)	RTIL-III (µl)	dye solution (µl)	Gelation time (min)	Coctail pH	Drying Temperature (^{0}C)	I_0/I
Sol-6e	193[a]	60	120	-	-	50	180	2	25	1.16

[a] 193 refers to 169 ul water 24 µl concentrated HCl

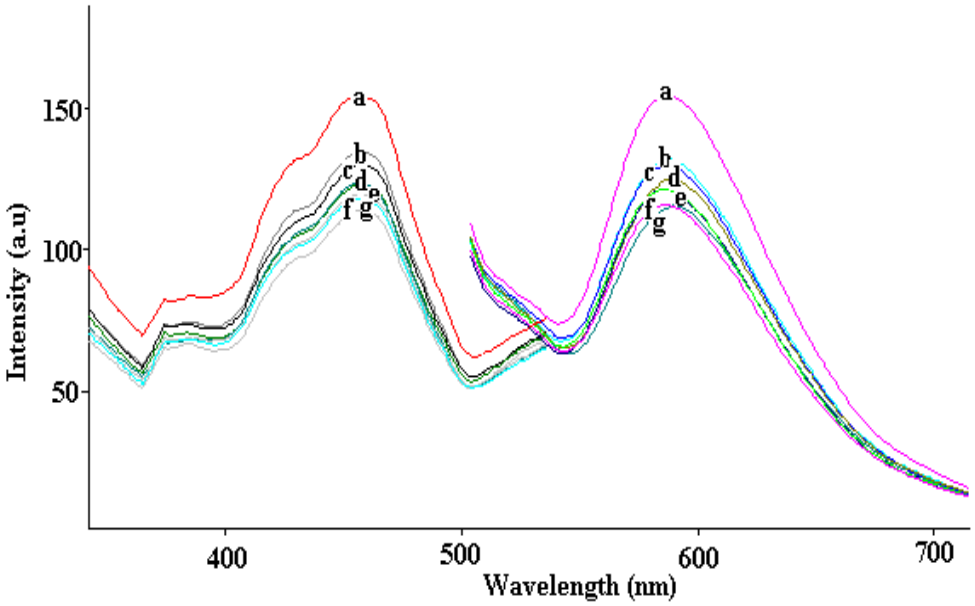

Figure 3.21 Response of sol-8a to $O_{2(g)}$ (a) 0% (b) 5% (c) 10% (d) 20% O_2, air(e) 40% (f) 60% (g)100% (relative signal change is 25%).

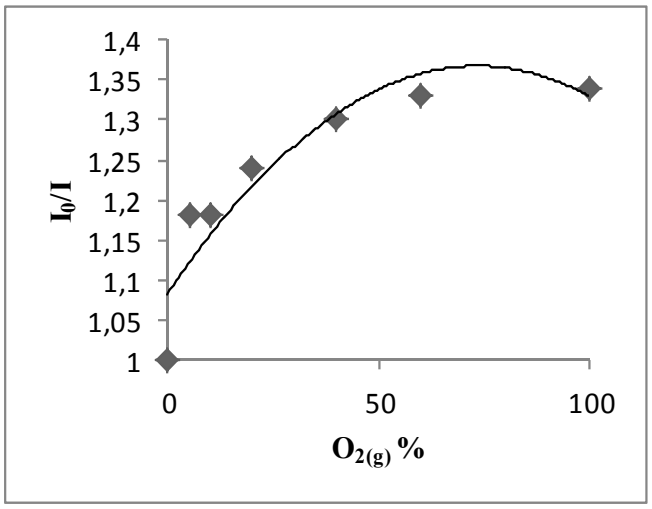

Figure 3.22 Stern–Volmer plot for sol-8a.

Table 3.24 Fluorescence intensity of sol-8a

% O_2	**I_{ex}**	**I_{em}**	**I_o/I**
0	156	154	1
5	135	131	1.18
10	130	130	1.18
20	123	124	1.24
Air	121	119	1.29
40	120	118	1.30
60	118	116	1.33
100	116	115	1.34

Table 3.25 Composition of the sol-8a

Coctail Name	**Acidified Water (µl)**	**Triton-x 100 (µl)**	**RTIL-I (µl)**	**RTIL-II (µl)**	**RTIL-III (µl)**	**dye solution (µl)**	**Gelation time (min)**	**Coctail pH**	**Drying Temperature (^{0}C)**	**I_0/I**
Sol-8a	193[b]	60	-	-	-	50	10	4	25	1.34

[b] 193 refers to 169 ul water 24 µl 0.1M HCl

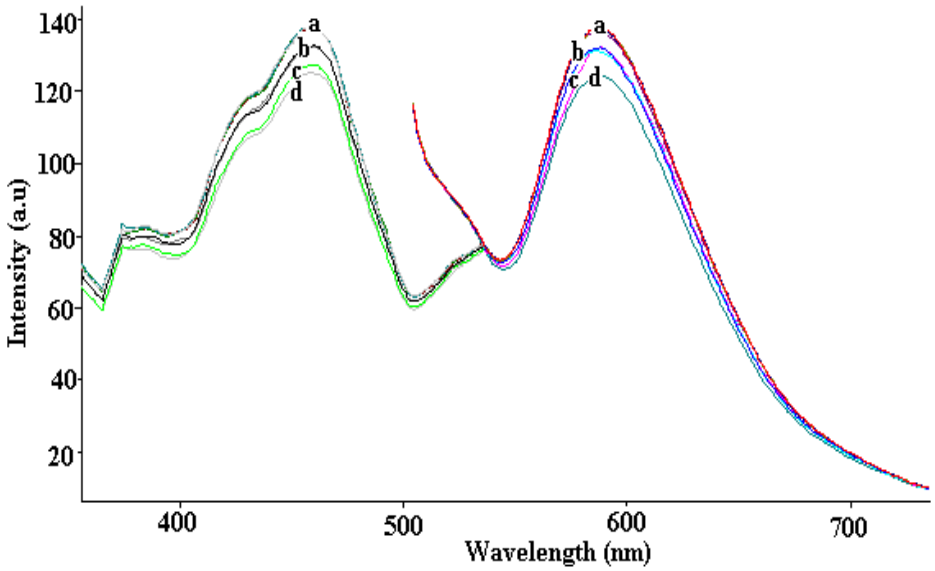

Figure 3.23 Response of sol-8b to $O_{2(g)}$ (a) 0% , 5%, %10 O_2 (b) 20%, başlangıç, 40% O_2 (c) 60% O_2 (d) 100% O_2 (relative signal change is 11%).

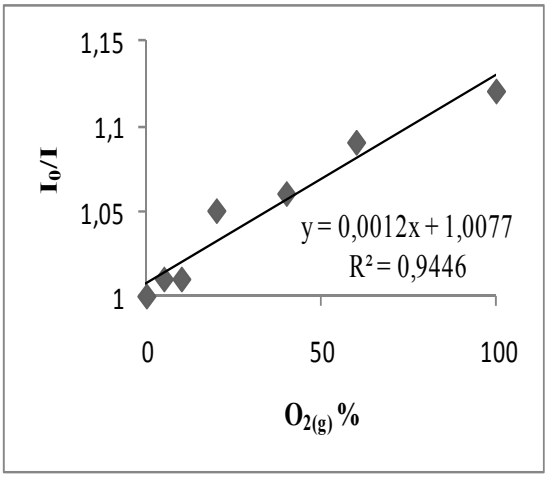

Figure 3.24 Stern–Volmer plot for sol-8b.

Table 3.26 Fluorescence intensity of sol-8b

% O_2	I_{ex}	I_{em}	I_o/I
0	138	138	1
5	137	136	1.01
10	136	136	1.01
20	133	131	1.05
Air	133	131	1.05
40	131	130	1.06
60	127	127	1.09
100	124	123	1.12

Table 3.27 Composition of the sol-8b

Coctail Name	Acidified Water (µl)	Triton-x 100 (µl)	RTIL-I (µl)	RTIL-II (µl)	RTIL-III (µl)	dye solution (µl)	Gelation time (min)	Coctail pH	Drying Temperature (^{0}C)	I_0/I
Sol-8b	193[b]	60	-	-	-	50	10	4	70	1.12

[b] 193 refers to 169 ul water 24 µl 0.1M HCl

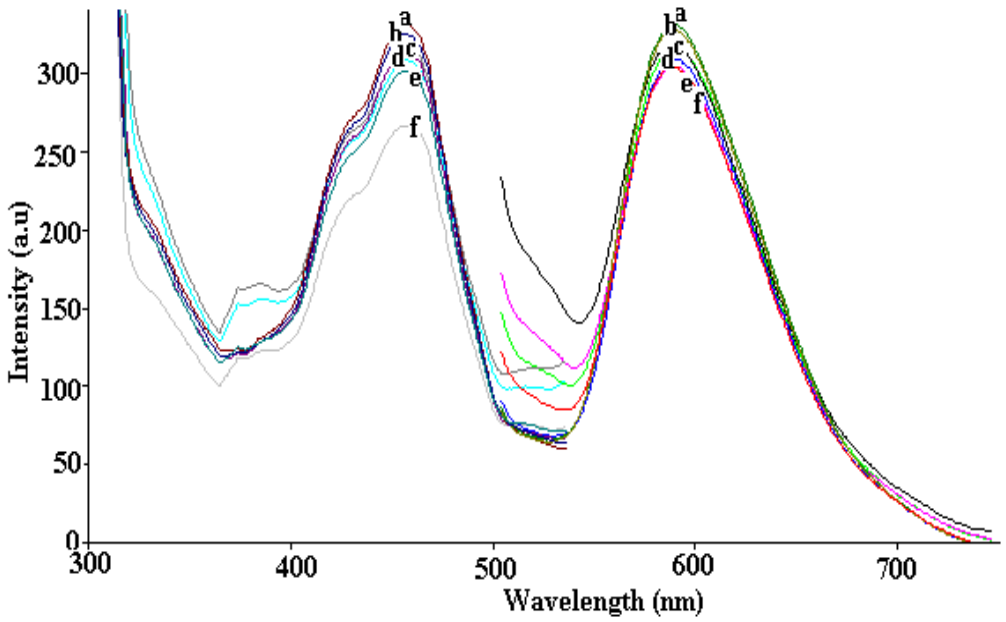

Figure 3.25 Response of sol-8c to $O_{2(g)}$ (a) 0, (b) 5%, (c) 10%, 20%, air (d) 40%, (e) 60%, (f) 100% O_2 (relative signal change is 8%).

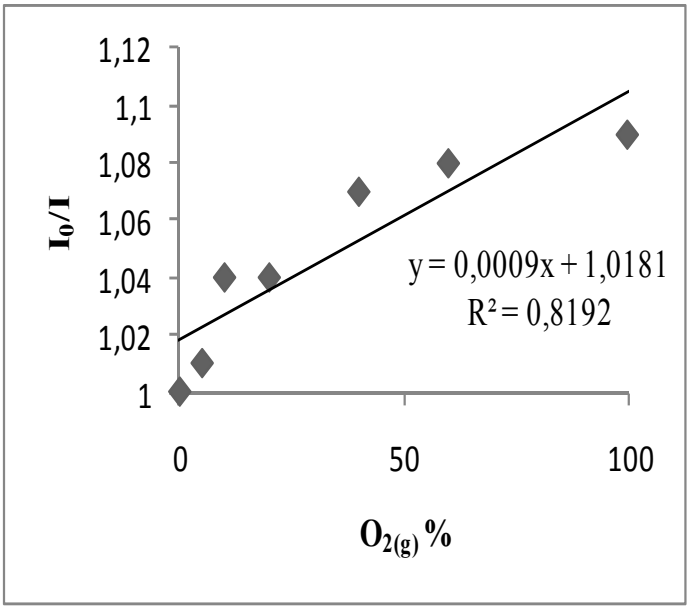

Figure 3.26 Stern–Volmer plot for sol-8c.

Table 3.28 Fluorescence intensity of sol-8c

% O_2	**I_{ex}**	**I_{em}**	**I_o/I**
0	331	331	1
5	324	327	1.01
10	314	318	1.04
20	311	317	1.04
Air	311	317	1.04
40	308	308	1.07
60	302	304	1.08
100	266	303	1.09

Table 3.29 Composition of the sol-8c

Coctail Name	**Acidified Water (µl)**	**Triton-x 100 (µl)**	**RTIL-I (µl)**	**RTIL-II (µl)**	**RTIL-III (µl)**	**dye solution (µl)**	**Gelation time (min)**	**Coctail pH**	**Drying Temperature (^{0}C)**	**I_0/I**
Sol-8c	193[b]	60	-	-	-	50	20	4	25	1.09

[b] 193 refers to 169 ul water 24 µl 0.1M HCl

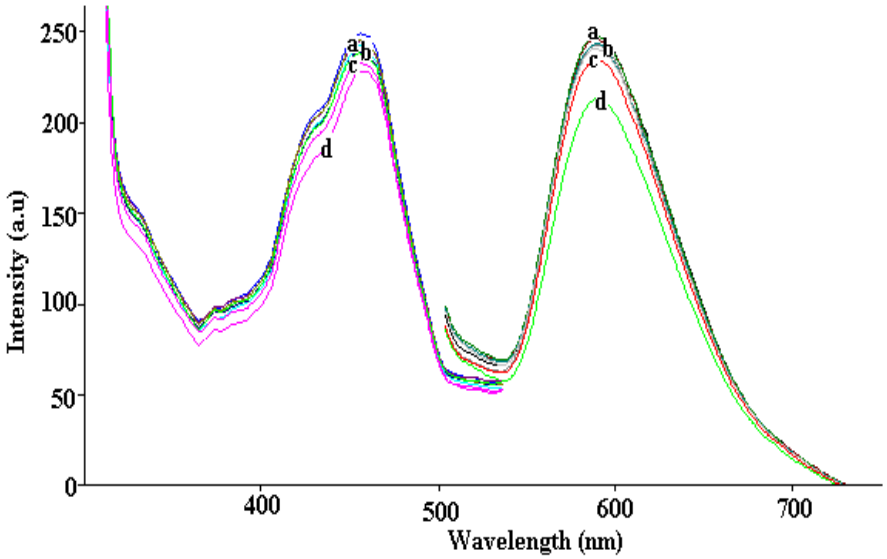

Figure 3.27 Response of sol-8d to $O_{2(g)}$ (a) 0% , 5%, %10 O_2 (b) 20%, air, 40% O_2 (c) 60% O_2 (d) 100% O_2 (relative signal change is 14%).

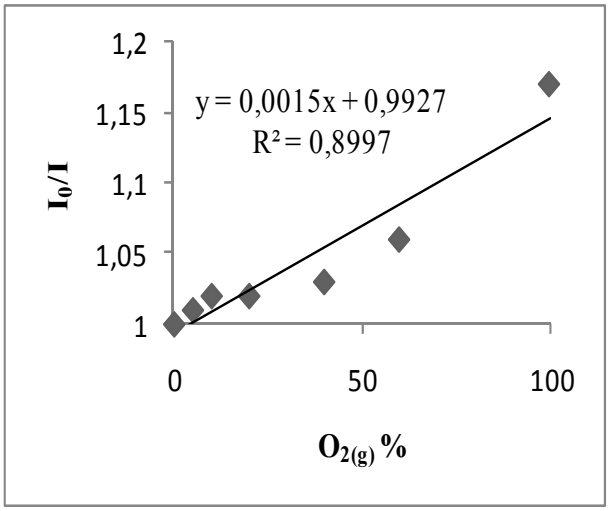

Figure 3.28 Stern–Volmer plot for sol-8d.

Table 3.30 Fluorescence intensity of sol-8d

% O_2	**I_{ex}**	**I_{em}**	**I_o/I**
0	247	247	1
5	245	245	1.01
10	244	243	1.02
20	242	241	1.02
Air	242	241	1.02
40	238	240	1.03
60	237	232	1.06
100	232	212	1.17

Table 3.31 Composition of the sol-8d

Coctail Name	**Acidified Water (µl)**	**Triton-x 100 (µl)**	**RTIL-I (µl)**	**RTIL-II (µl)**	**RTIL-III (µl)**	**dye solution (µl)**	**Gelation time (min)**	**Coctail pH**	**Drying Temperature (^{0}C)**	**I_0/I**
Sol-8d	193[b]	60	-	-	-	50	20	4	70	1.17

[b] 193 refers to 169 ul water 24 µl 0.1M HCl

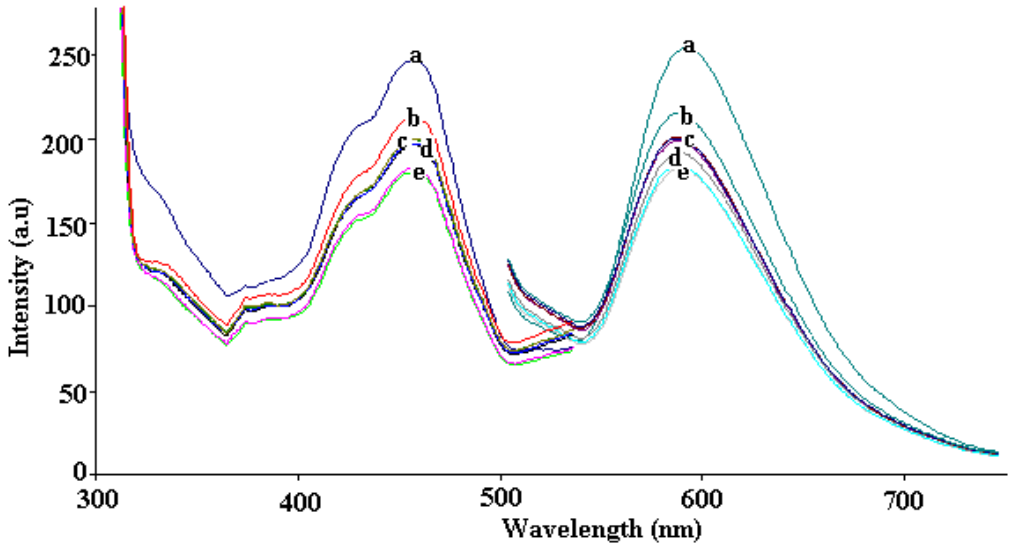

Figure 3.29 Response of sol-8e to $O_{2(g)}$ (a) 0% (b) 5% (c) %10 O_2 20%, air, (d) 40% O_2 (e) 60%, 100% O_2 (relative signal change is 28%).

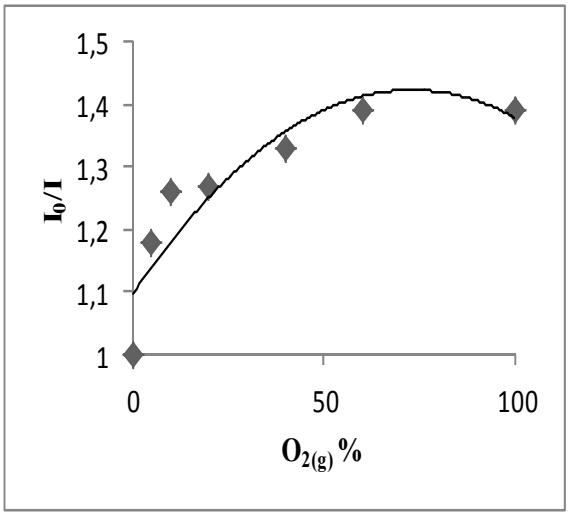

Figure 3.30 Stern–Volmer plot for sol-8e.

Table 3.32Fluorescence intensity of sol-8e.

% O_2	I_{ex}	I_{em}	I_o/I
0	246	253	1
5	215	215	1.18
10	201	201	1.26
20	200	200	1.27
Air	196	196	1.3
40	195	190	1.33
60	182	182	1.39
100	181	181	1.39

Table 3.33 Composition of the sol-8e

Coctail Name	Acidified Water (µl)	Triton-x 100 (µl)	RTIL-I (µl)	RTIL-II (µl)	RTIL-III (µl)	dye solution (µl)	Gelation time (min)	Coctail pH	Drying Temperature (^{0}C)	I_0/I
Sol-8e	193[b]	60	-	-	-	50	30	4	25	1.39

[b] 193 refers to 169 ul water 24 µl 0.1M HCl

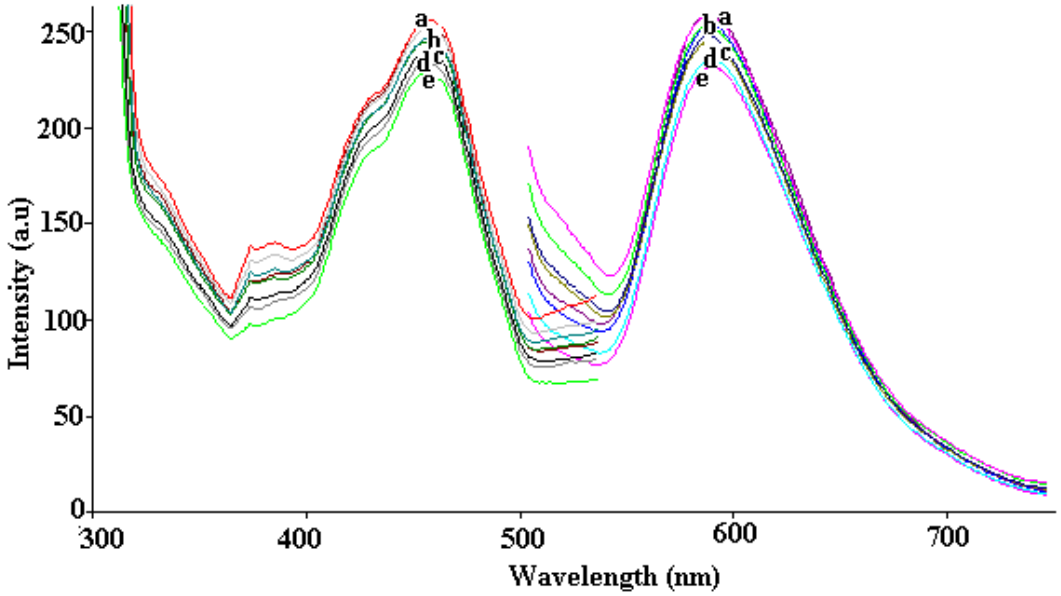

Figure 3.31 Response of sol-8f to $O_{2(g)}$ (a) 0%, 5%, %10 O_2 (b) 20%, air, (c) 40% (d)60%, (e) 100% O_2 (relative signal change is 12%).

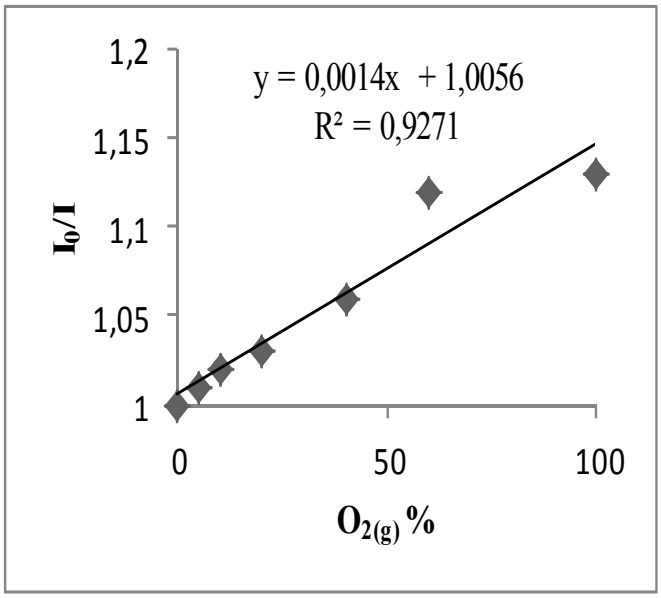

Figure 3.32 Stern–Volmer plot for sol-8f.

Table 3.34 Fluorescence intensity of sol-8f

% O_2	I_{ex}	I_{em}	I_o/I
0	255	259	1
5	252	256	1.01
10	251	254	1.02
20	245	252	1.03
Air	244	246	1.05
40	240	245	1.06
60	232	231	1.12
100	227	229	1.13

Table 3.35 Composition of the sol-8f

Coctail Name	Acidified Water (µl)	Triton-x 100 (µl)	RTIL-I (µl)	RTIL-II (µl)	RTIL-III (µl)	dye solution (µl)	Gelation time (min)	Coctail pH	Drying Temperature (^{0}C)	I_0/I
Sol-8f	193[b]	60	-	-	-	50	30	4	70	1.13

[b] 193 refers to 169 ul water 24 µl 0.1M HCl

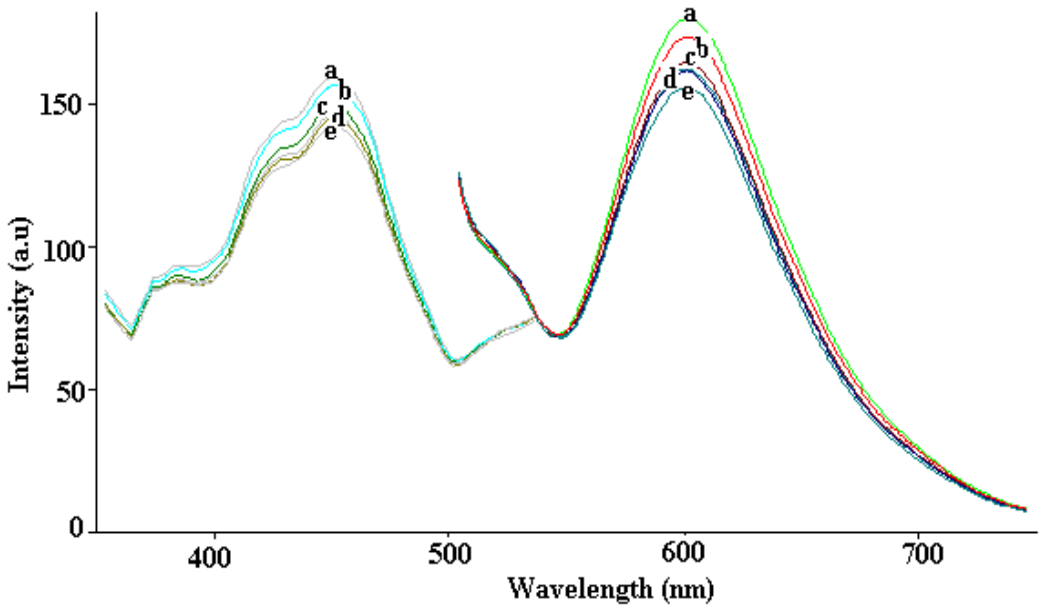

Figure 3.33 Response of sol-9a to $O_{2(g)}$ (a) 0%, (b) %10 O_2 (c) 20%, (d) air, 60% , (e) 100% O_2 (relative signal change is 13%)

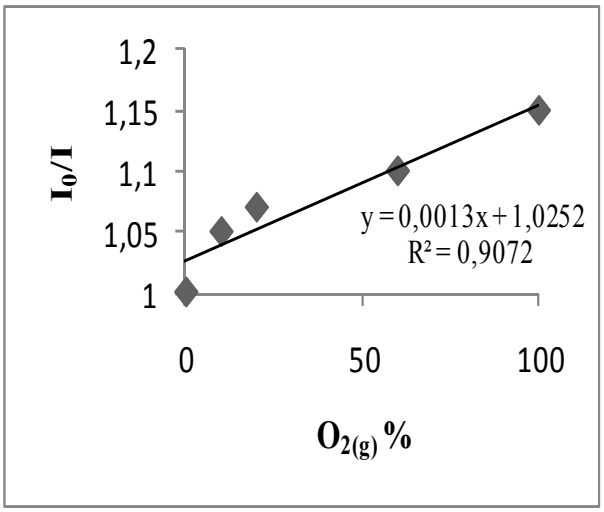

Figure 3.34 Stern–Volmer plot for sol-9a

Table 3.36Fluorescence intensity of sol-9a

% O_2	**I_{ex}**	**I_{em}**	**I_o/I**
0	163	180	1
10	157	172	1.05
20	155	168	1.07
Air	151	165	1.09
60	150	163	1.10
100	141	157	1.15

Table 3.37Composition of the sol-9a

Coctail Name	**Acidified Water (µl)**	**Triton-x 100 (µl)**	**RTIL-I (µl)**	**RTIL-II (µl)**	**RTIL-III (µl)**	**dye solution (µl)**	**Gelation time (min)**	**Coctail pH**	**Drying Temperature (^{0}C)**	**I_0/I**
Sol-9a	193[b]	60	120	-	-	50	10	5	25	1.15

[b] 193 refers to 169 ul water 24 µl 0.1M HCl

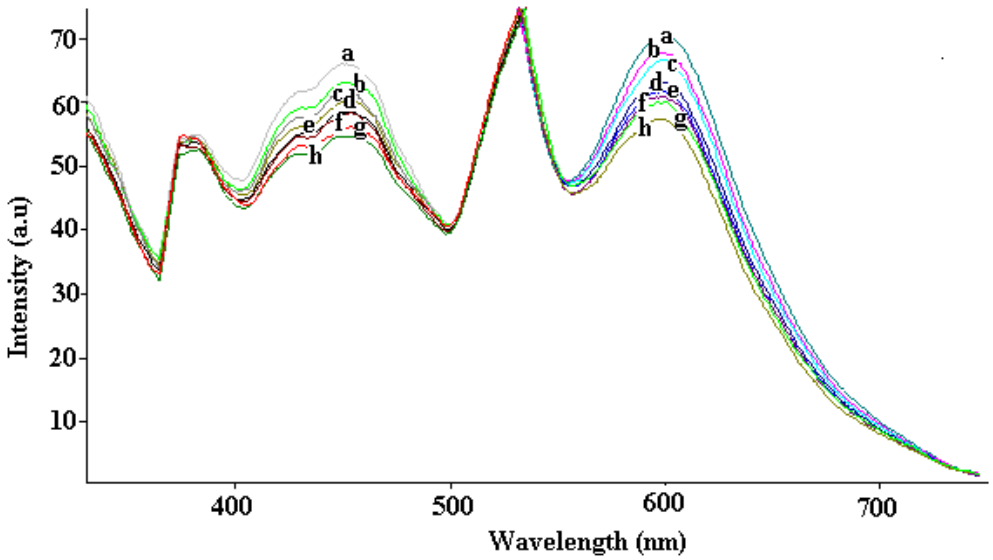

Figure 3.35 Response of sol-9b to $O_{2(g)}$ (a) 0%, (b) 5%, (c) 10%, (d) 20%, (e)başlangıç, (f)40%, (g) 60%O_2 (h) 100%O_2 (relative signal change is 20%)

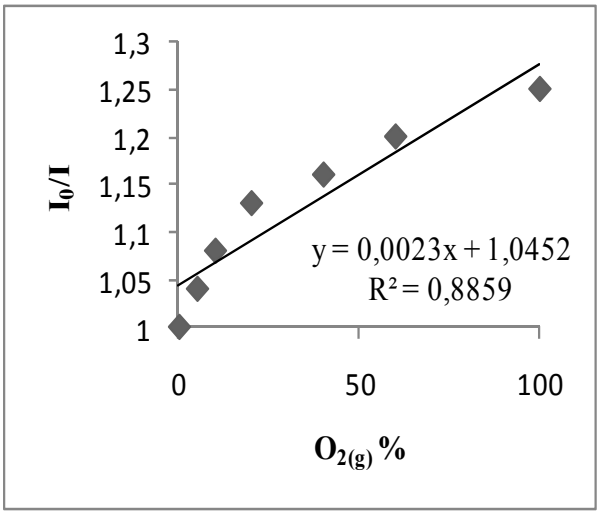

Figure 3.36 Stern–Volmer plot for sol-9b

Table 3.38 Fluorescence intensity of sol-9b

% O_2	**I_{ex}**	**I_{em}**	**I_o/I**
0	66	71	1
5	63	68	1.04
10	62	66	1.08
20	60	63	1.13
Air	59	62	1.15
40	58	61	1.16
60	56	59	1.20
100	55	57	1.25

Table 3.39 Composition of the sol-9b

Coctail Name	**Acidified Water (µl)**	**Triton-x 100 (µl)**	**RTIL-I (µl)**	**RTIL-II (µl)**	**RTIL-III (µl)**	**dye solution (µl)**	**Gelation time (min)**	**Coctail pH**	**Drying Temperature (^{0}C)**	**I_0/I**
Sol-9b	193[b]	60	120	-	-	50	20	5	25	1.25

[b] 193 refers to 169 ul water 24 µl 0.1M HCl

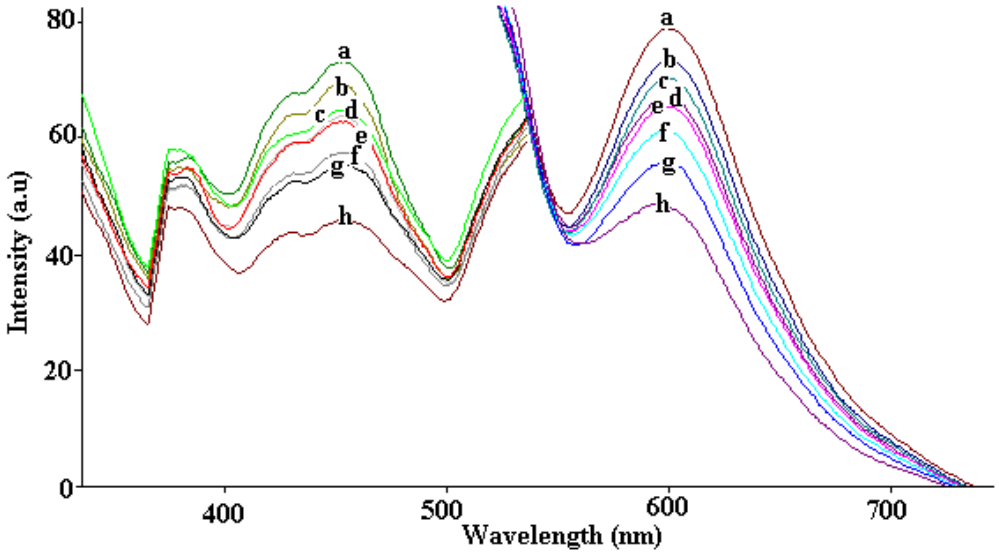

Figure 3.37 Response of sol-9c to $O_{2(g)}$ (a) 0%, (b) 5%, (c) 10%, (d) 20%, (e)air, (f)40%, (g)60%O_2 (h) 100%O_2 (relative signal change is 39%).

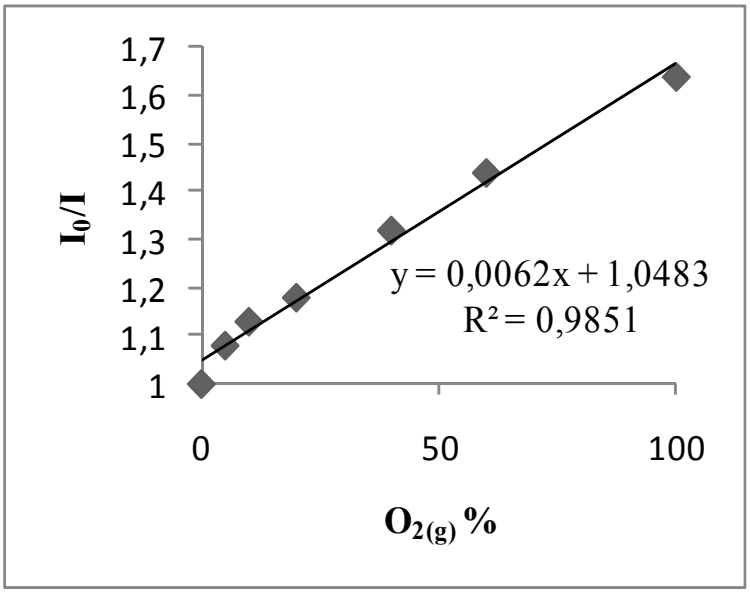

Figure 3.38 Stern–Volmer plot for sol-9c.

Table 3.40 Fluorescence intensity of sol-9c

% O_2	**I_{ex}**	**I_{em}**	**I_o/I**
0	73	79	1
5	69	73	1.08
10	65	70	1.13
20	63	67	1.18
Air	62	65	1.22
40	58	60	1.32
60	55	55	1.44
100	45	48	1.64

Table 3.41 Composition of the sol-9c

Coctail Name	**Acidified Water (µl)**	**Triton-x 100 (µl)**	**RTIL-I (µl)**	**RTIL-II (µl)**	**RTIL-III (µl)**	**dye solution (µl)**	**Gelation time (min)**	**Coctail pH**	**Drying Temperature (^{0}C)**	**I_0/I**
Sol-9c	193[b]	60	120	-	-	50	20	5	70	1.64

[b] 193 refers to 169 ul water 24 µl 0.1M HCl

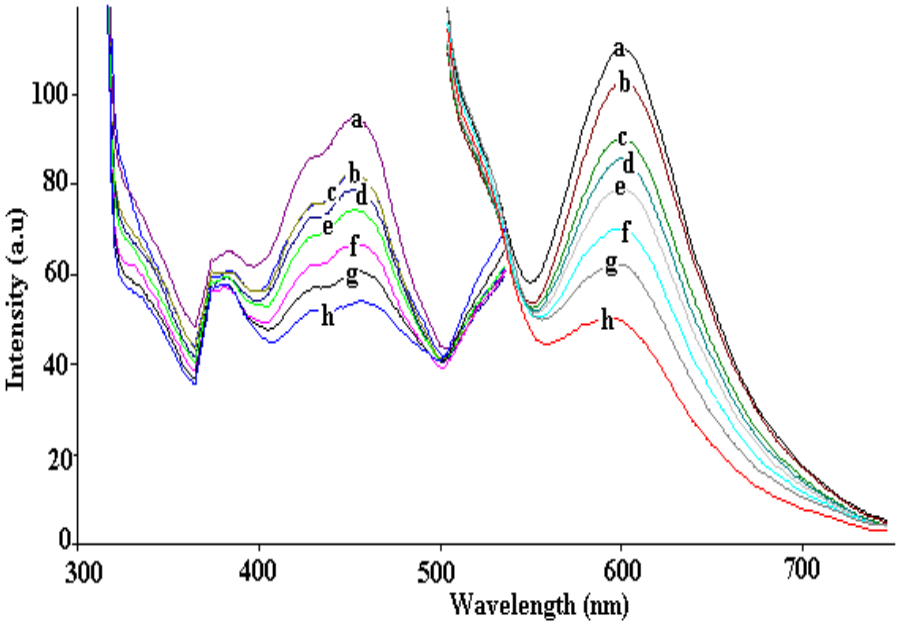

Figure 3.39 Response of sol-9d1 to $O_{2(g)}$ (a) 0%, (b) 5%, (c) 10%, (d) 20%, (e)air, (f)40%, (g)60%O_2 (h) 100%O_2 (relative signal change is 55%).

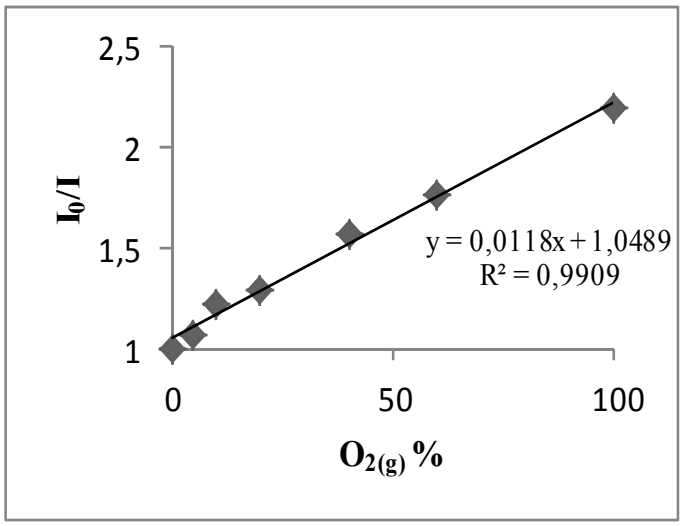

Figure 3.40 Stern–Volmer plot for sol-9d1.

Table 3.42 Fluorescence intensity of sol-9d1

% O_2	I_{ex}	I_{em}	I_o/I
0	95	110	1
5	82	103	1.07
10	81	90	1.22
20	78	85	1.29
Air	73	79	1.39
40	66	70	1.57
60	60	62	1.77
100	54	50	2.20

Table 3.43 Composition of the sol-9d1

Coctail Name	Acidified Water (µl)	Triton-x 100 (µl)	RTIL-I (µl)	RTIL-II (µl)	RTIL-III (µl)	dye solution (µl)	Gelation time (min)	Coctail pH	Drying Temperature (^{0}C)	I_0/I
Sol-9d	193[b]	60	120	-	-	50	30	5	25	2.20

[b] 193 refers to 169 ul water 24 µl 0.1M HCl.

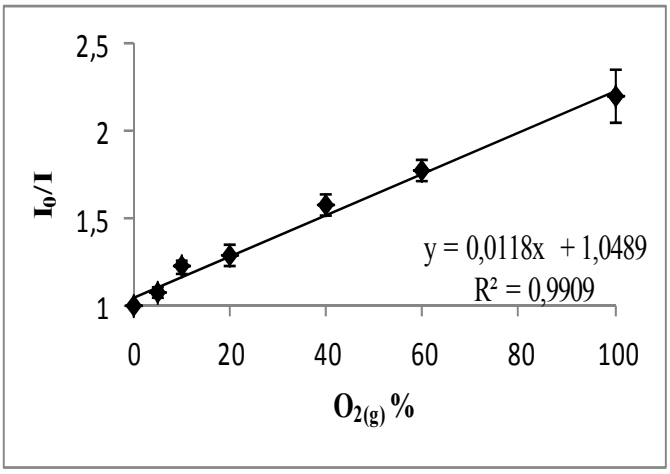

Figure 3.41 Stern–Volmer plot for sol-9d

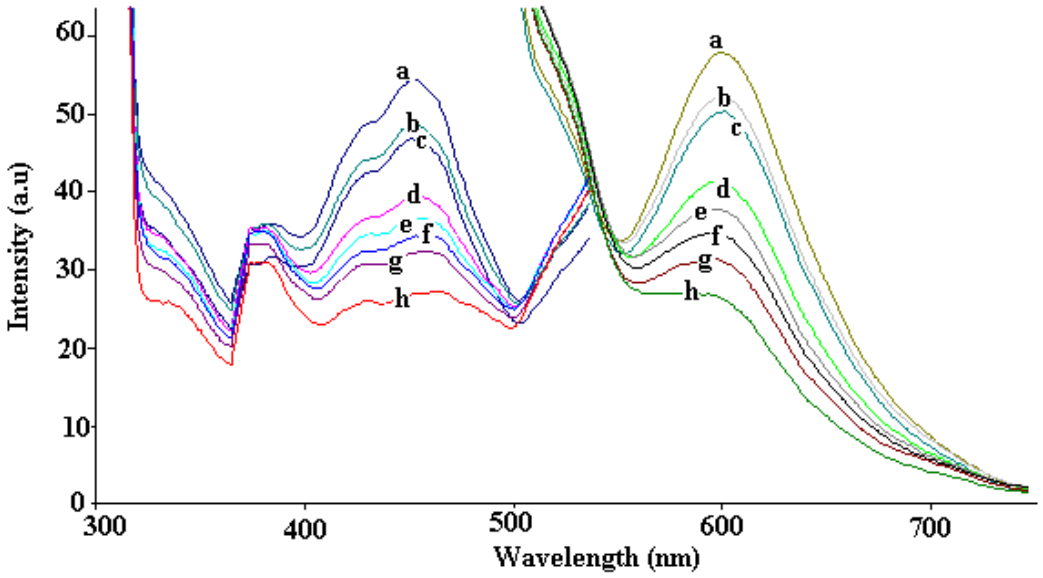

Figure3.42 Response of sol-9d2 to $O_{2(g)}$ (a) 0%, (b) 5%, (c) 10%, (d) 20%, (e)air, (f)40%, (g)60%O_2 (h) 100%O_2 (relative signal change is 52%).

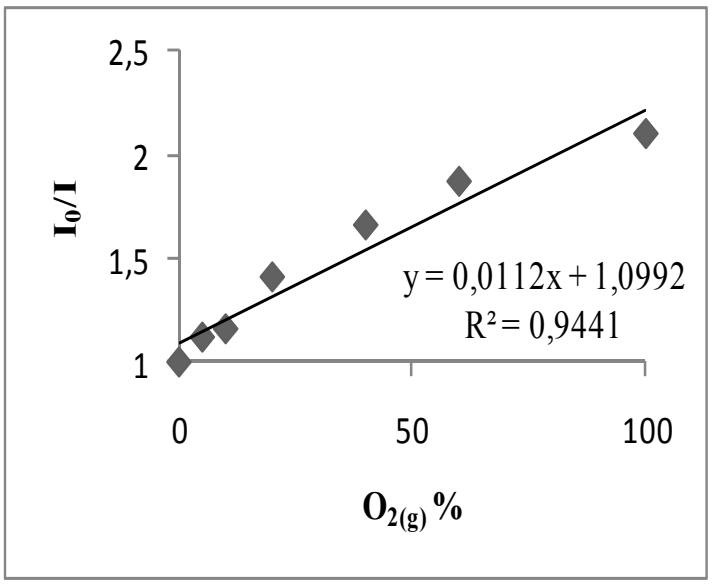

Figure3.43 Stern–Volmer plot for sol-9d2.

Table 3.44 Fluorescence intensity of sol-9d2

% O_2	**I_{ex}**	**I_{em}**	**I_o/I**
0	55	58	1
5	48	52	1.12
10	46	50	1.16
20	38	41	1.41
Air	36	38	1.52
40	32	35	1.66
60	30	31	1.87
100	26	28	2.1

Table 3.45 Composition of the sol-9d2

Coctail Name	**Acidified Water (µl)**	**Triton-x 100 (µl)**	**RTIL-I (µl)**	**RTIL-II (µl)**	**RTIL-III (µl)**	**dye solution (µl)**	**Gelation time (min)**	**Coctail pH**	**Drying Temperature (^{0}C)**	**I_0/I**
Sol-9d2	193[b]	60	120	-	-	50	30	5	25	2.10

[b] 193 refers to 169 ul water 24 µl 0.1M HCl

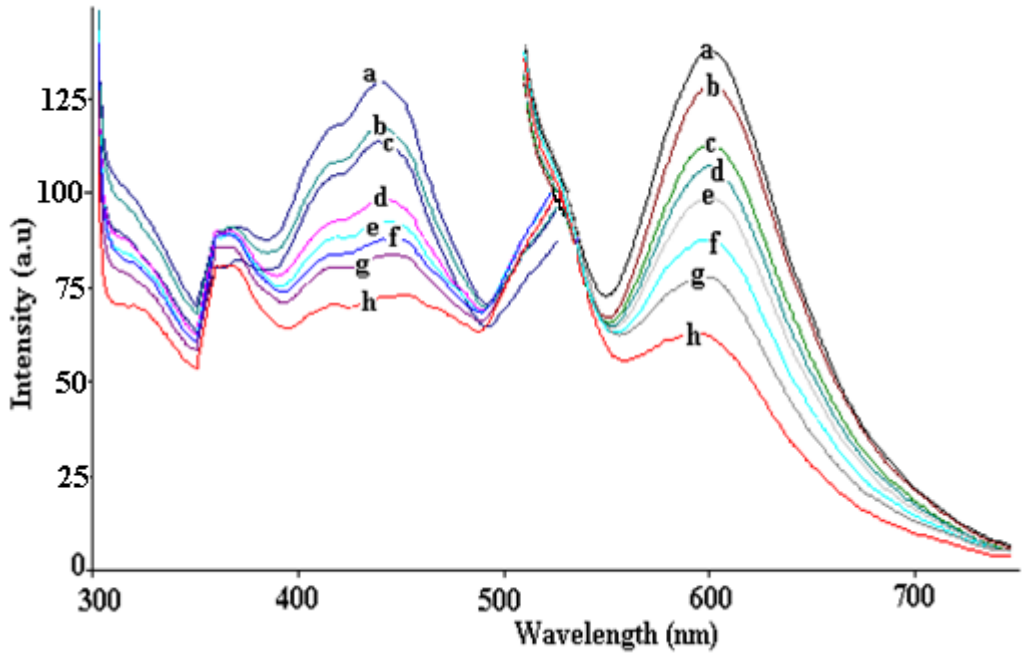

Figure 3.44 Response of sol-9d3 to $O_{2(g)}$ (a) 0%, (b) 5%, (c) 10%, (d) 20%, (e)air, (f)40%, (g)60%O_2 (h) 100%O_2 (relative signal change is 47 %).

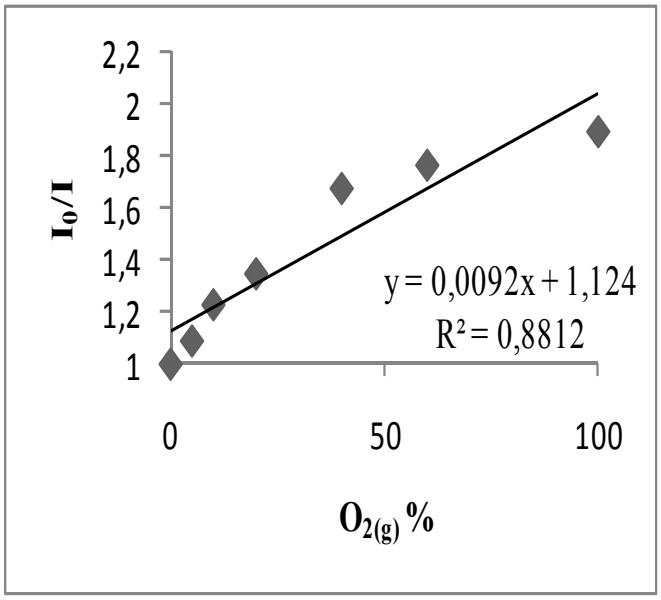

Figure 3.45 Stern–Volmer plot for sol-9d3.

Table 3.46 Fluorescence intensity of sol-9d3

% O_2	**I_{ex}**	**I_{em}**	**I_o/I**
0	136	138	1
5	125	127	1.09
10	123	112	1.23
20	98	102	1.35
Air	95	97	1.42
40	91	82	1.68
60	87	78	1.77
100	77	73	1.90

Table 3.47 Composition of the sol-9d3

Coctail Name	**Acidified Water (µl)**	**Triton-x 100 (µl)**	**RTIL-I (µl)**	**RTIL-II (µl)**	**RTIL-III (µl)**	**dye solution (µl)**	**Gelation time (min)**	**Coctail pH**	**Drying Temperature (^{0}C)**	**I_0/I**
Sol-9d3	193[b]	60	120	-	-	50	30	5	25	1.90

[b] 193 refers to 169 ul water 24 µl 0.1M HCl

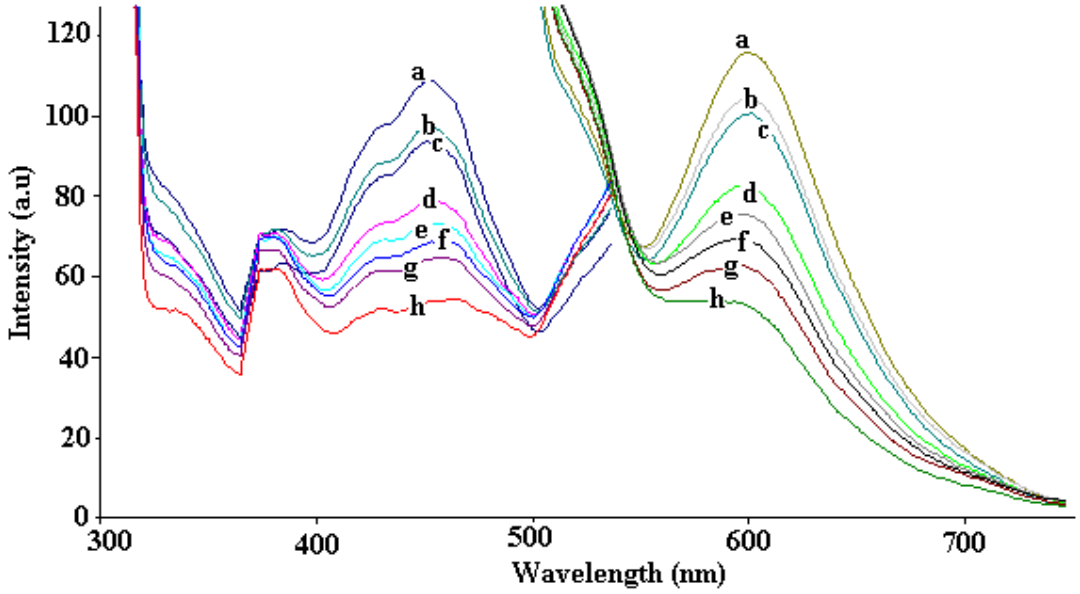

Figure 3.46 Response of sol-9e to $O_{2(g)}$ (a) 0%, (b) 5%, (c) 10%, (d) 20%, (e)air, (f)40%, (g)60%O_2 (h) 100%O_2 (relative signal change is 54%).

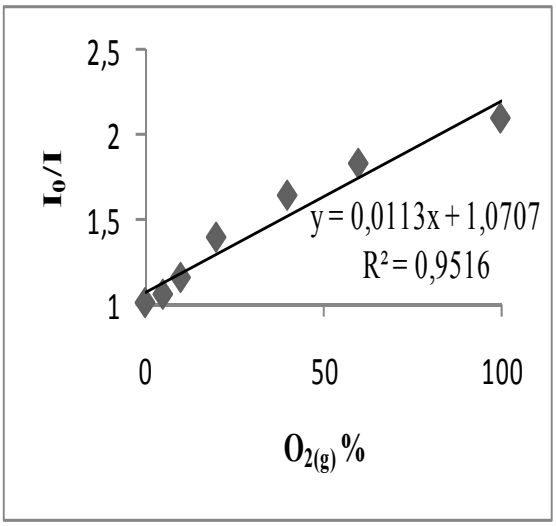

Figure 3.47 Stern–Volmer plot for sol-9e

Table 3.48 Fluorescence intensity of sol-9e

% O_2	**I_{ex}**	**I_{em}**	**I_o/I**
0	109	115	1
5	97	104	1.05
10	93	100	1.15
20	79	83	1.39
Air	73	75	1.53
40	68	70	1.64
60	64	63	1.83
100	54	53	2.10

Table 3.49 Composition of the sol-9e

Coctail Name	**Acidified Water (µl)**	**Triton-x 100 (µl)**	**RTIL-I (µl)**	**RTIL-II (µl)**	**RTIL-III (µl)**	**dye solution (µl)**	**Gelation time (min)**	**Coctail pH**	**Drying Temperature (^{0}C)**	**I_0/I**
Sol-9e	193[b]	60	120	-	-	50	30	5	70	2.10

[b] 193 refers to 169 ul water 24 µl 0.1M HCl

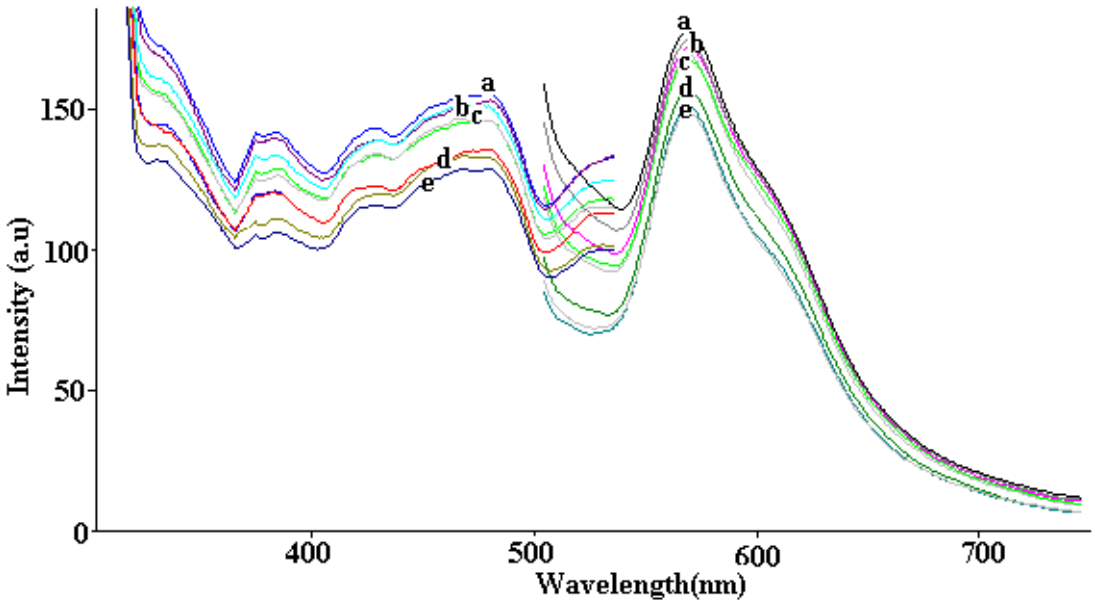

Figure 3.48 Response of sol-9f to $O_{2(g)}$ (a) 0%, (b) 5%, 10% (c) 20%, air, (d)40%, 60%O_2 (e) 100%O_2 (relative signal change is 17%).

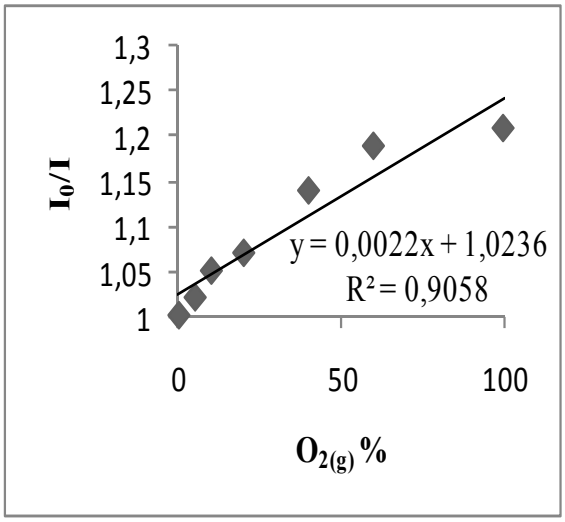

Figure 3.49 Stern–Volmer plot for sol-9f.

Table 3.50 Fluorescence intensity of sol-9f

% O_2	**I_{ex}**	**I_{em}**	**I_o/I**
0	156	178	1
5	151	174	1.02
10	149	170	1.05
20	146	167	1.07
Air	143	164	1.08
40	136	156	1.14
60	132	150	1.19
100	126	147	1.21

Table 3.51 Composition of the sol-9f

Coctail Name	**Acidified Water (µl)**	**Triton-x 100 (µl)**	**RTIL-I (µl)**	**RTIL-II (µl)**	**RTIL-III (µl)**	**dye solution (µl)**	**Gelation time (min)**	**Coctail pH**	**Drying Temperature (^{0}C)**	**I_0/I**
Sol-9f	193[b]	60	120	-	-	50	60	5	25	1.21

[b] 193 refers to 169 ul water 24 µl 0.1M HCl

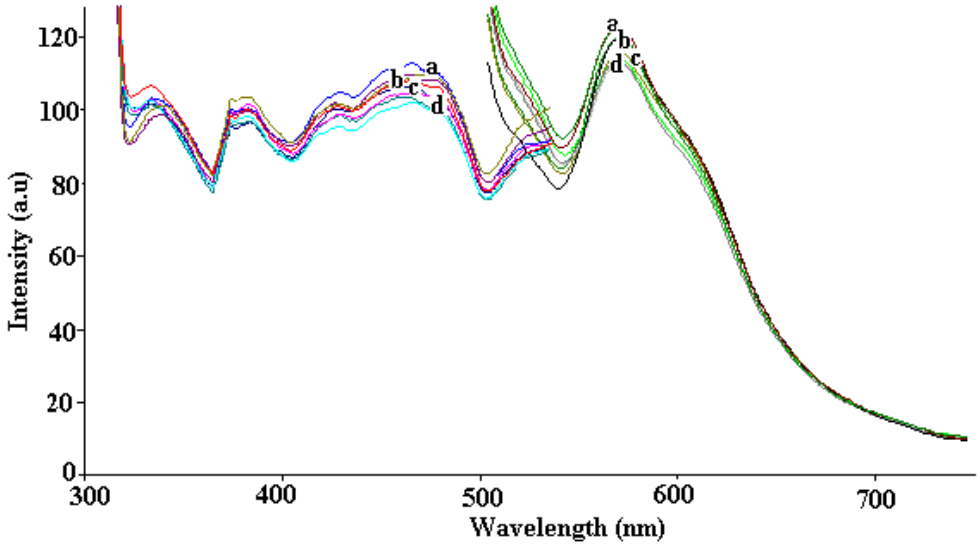

Figure 3.50 Response of sol-9g to $O_{2(g)}$ (a) 0%, 5%, 10% (b) 20%, air, (c)40%, (d) 60%, 100%O_2 (relative signal change is 10%).

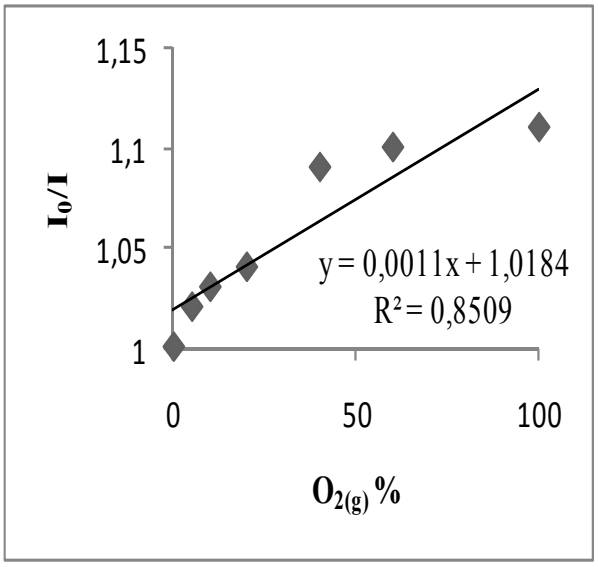

Figure3.51 Stern–Volmer plot for sol-9g.

Table 3.52 Fluorescence intensity of sol-9g

% O_2	**I_{ex}**	**I_{em}**	**I_o/I**
0	113	123	1
5	109	121	1.02
10	108	120	1.03
20	107	118	1.04
Air	105	115	1.07
40	104	113	1.09
60	102	112	1.11
100	100	111	1.10

Table 3.53 Composition of the sol-9g

Coctail Name	**Acidified Water (µl)**	**Triton-x 100 (µl)**	**RTIL-I (µl)**	**RTIL-II (µl)**	**RTIL-III (µl)**	**dye solution (µl)**	**Gelation time (min)**	**Coctail pH**	**Drying Temperature (^{0}C)**	**I_0/I**
Sol-9g	193[b]	60	120	-	-	50	60	5	70	1.10

[b] 193 refers to 169 ul water 24 µl 0.1M HCl

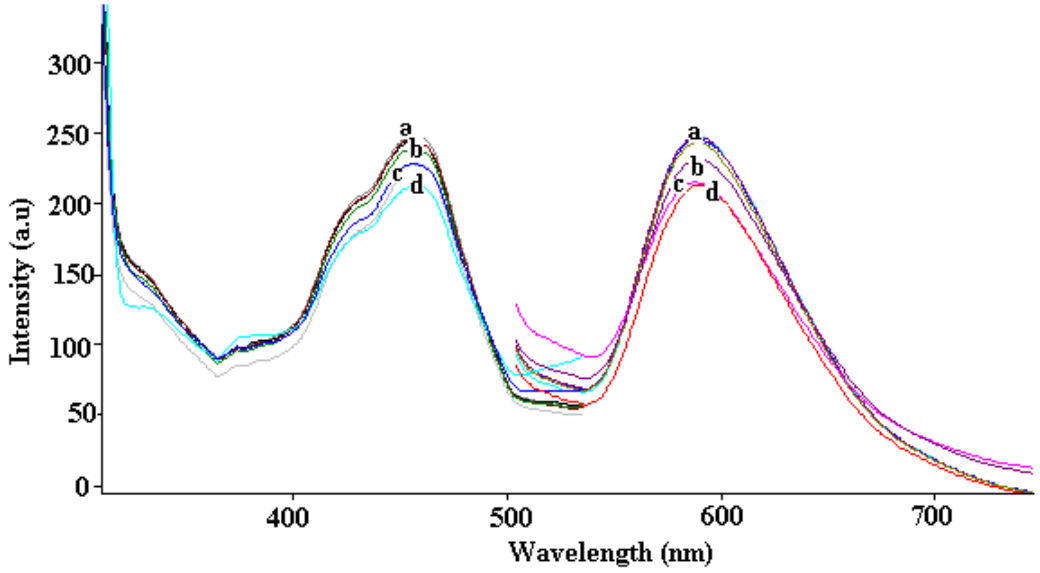

Figure3.52 Response of sol-10a to $O_{2(g)}$ (a) 0%, 5%, 10%, 20%, air, (b)40%, (c) 60% (d)100%O_2 (relative signal change is 7%).

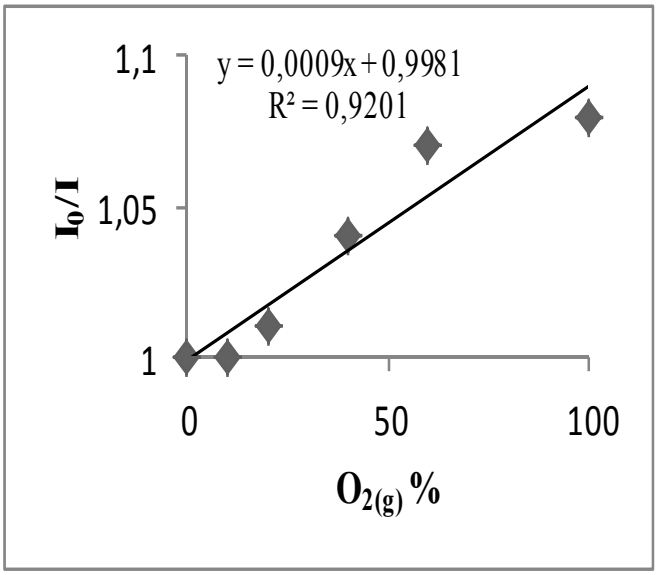

Figure3.53 Stern–Volmer plot for sol-10a.

Table 3.54 Fluorescence intensity of sol-10a

% O_2	**I_{ex}**	**I_{em}**	**I_o/I**
0	249	248	1
10	248	248	1
20	248	247	1.01
Air	247	246	1.01
40	235	238	1.04
60	234	231	1.07
100	224	230	1.08

Table 3.55 Composition of the sol-10a

Coctail Name	**Acidified Water (µl)**	**Triton-x 100 (µl)**	**RTIL-I (µl)**	**RTIL-II (µl)**	**RTIL-III (µl)**	**dye solution (µl)**	**Gelation time (min)**	**Coctail pH**	**Drying Temperature (^{0}C)**	**I_0/I**
Sol-10a	96.5[c]	60	-	-	-	50	48h +20 min	6	25	1.08

[c] 96.5 refers to 84.5 ul water 12 µl 0.1M HCl

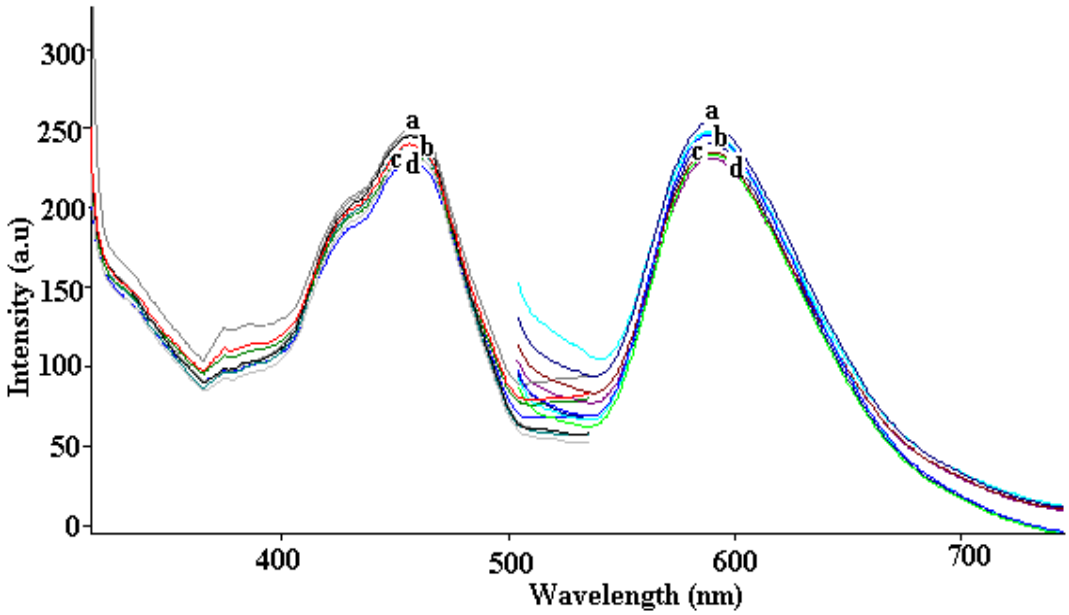

Figure 3.54 Response of sol-10b to $O_{2(g)}$ (a) 0%, (b)10%, 20%, air, (c)40%, (d) 60%, 100%O_2 (relative signal change is 4%).

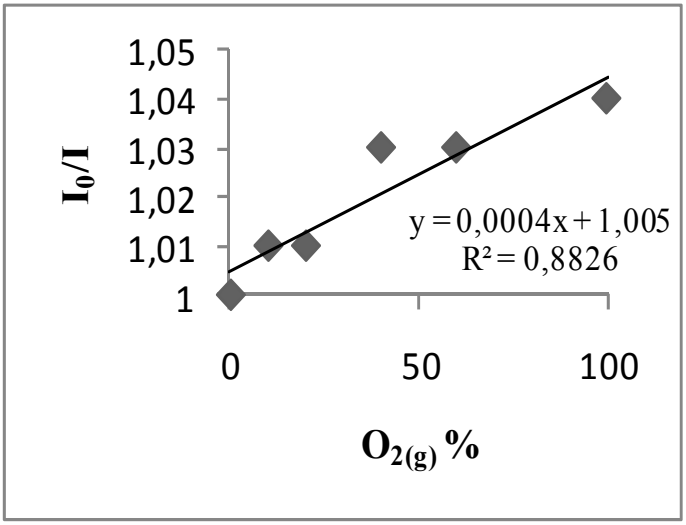

Figure 3.55 Stern–Volmer plot for sol-10b.

Table 3.56 Fluorescence intensity of sol-10b

% O_2	I_{ex}	I_{em}	I_o/I
0	248	252	1
10	247	250	1.01
20	245	250	1.01
Air	245	248	1.02
40	241	245	1.03
60	240	244	1.03
100	236	243	1.04

Table 3.57 Composition of the sol-10b

Coctail Name	Acidified Water (µl)	Triton-x 100 (µl)	RTIL-I (µl)	RTIL-II (µl)	RTIL-III (µl)	dye solution (µl)	Gelation time (min)	Coctail pH	Drying Temperature (^{0}C)	I_0/I
Sol10b	96.5[c]	60	-	-	-	50	48h +30min	6	25	1.04

[c] 96.5 refers to 84.5 ul water 12 µl 0.1M HCl

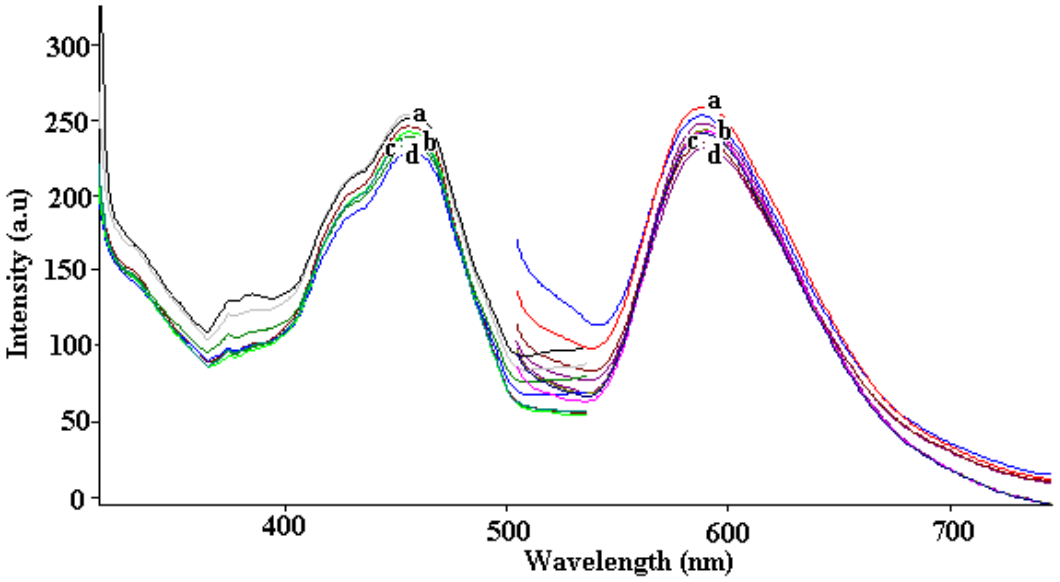

Figure 3.56 Response of sol-11a to $O_{2(g)}$ (a) 0%, (b)10%, 20% (c)air, 40%, (d) 60%, 100%O_2 (relative signal change is 10%).

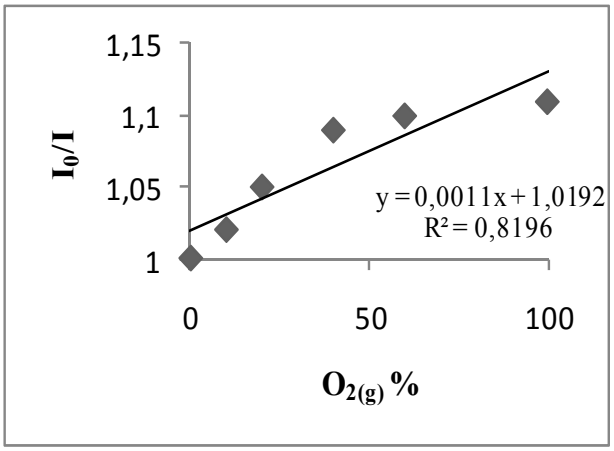

Figure 3.57 Stern–Volmer plot for sol-11a.

Table 3.58 Fluorescence intensity of sol-11a

% O_2	**I_{ex}**	**I_{em}**	**I_o/I**
0	251	252	1
10	250	246	1.02
20	247	239	1.05
Air	246	233	1.08
40	241	232	1.09
60	236	229	1.1
100	231	227	1.11

Table 3.59 Composition of the sol-11a

Coctail Name	**Acidified Water (µl)**	**Triton-x 100 (µl)**	**RTIL-I (µl)**	**RTIL-II (µl)**	**RTIL-III (µl)**	**dye solution (µl)**	**Gelation time (min)**	**Coctail pH**	**Drying Temperature (^{0}C)**	**I_0/I**
Sol-11a	96.5[c]	60	120	-	-	50	48h +20min	7	25	1.11

[c]96.5 refers to 84.5 ul water 12 µl 0.1M HCl

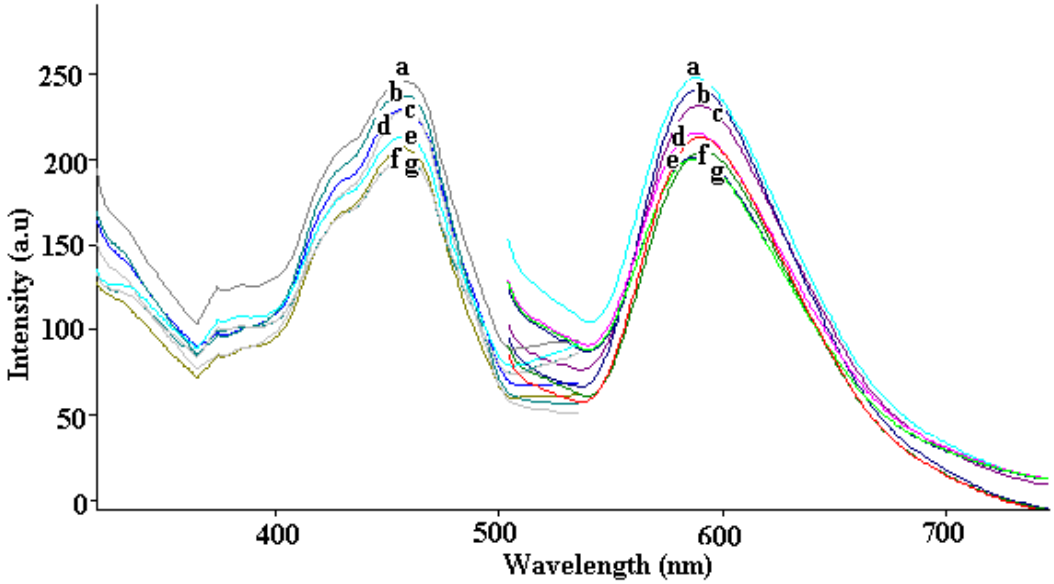

Figure 3.58 Response of sol-11b to $O_{2(g)}$ (a) 0%, (b)10%, (c) 20% (d)air, (e) 40%, (f) 60%, (g) 100%O_2 (relative signal change is 18%).

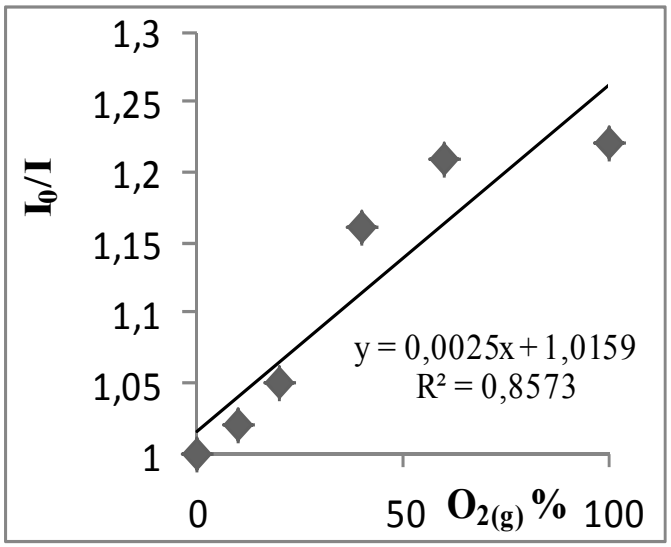

Figure 3.59 Stern–Volmer plot for sol-11b.

Table 3.60 Fluorescence intensity of sol-11b

% O_2	I_{ex}	I_{em}	I_o/I
0	249	248	1
10	237	243	1.02
20	225	232	1.05
Air	224	216	1.15
40	210	214	1.16
60	205	204	1.21
100	198	202	1.22

Table 3.61 Composition of the sol-11b

Coctail Name	Acidified Water (µl)	Triton-x 100 (µl)	RTIL-I (µl)	RTIL-II (µl)	RTIL-III (µl)	dye solution (µl)	Gelation time (min)	Coctail pH	Drying Temperature (^{0}C)	I_0/I
Sol-11b	96.5[c]	60	120	-	-	50	48h +30min	7	25	1.22

[c] 96.5 refers to 84.5 ul water 12 µl 0.1M HCl

3.3.4 Absorption, emission and excitation spectra

The absorption, excitation, and corrected emission spectra of ruthenium complex were recorded for different compositions prepared from the concerning cocktails (see Table 3.1, Figure 3.60 and 3.61).When dissolved in water, $Ru(bipy)_3^{2+}$ exhibits a metal–ligand charge transfer (MLCT) band at 447 nm (Cook et al., 1984). Similarly, in different sol–gel compositions, absorption spectra of $Ru(bipy)_3^{2+}$ exhibited an intense band between 410 and 470 nm which can be assigned to the metal–ligand charge transfer from t_{2g} band of Ru to л* level of ligand and a smaller band at 380

nm originated from metal centered (MC) d–d transition.It iswell established that solvent can play a key role in influencing the absorption and emission spectra of ruthenium polypyridyl complexes (Hush & Reimers, 1998).

By the addition of different ionic liquids into the sol–gel composition, the MLCT bands were not affected (see Figure 3.60, Table 3.62). The excitation, and corrected emission spectra of ruthenium complexes were recorded for different films prepared from the coctails in presence and in absence of ionic liquid which exhibited the best O_2 response (Figure 3.61, Table 3.63). The maximum emission wavelength of sol-9d doped $Ru(bipy)_3^{2+}$ exhibited a blue shift of 9 nm (from 600 to 591 nm) with respect to emission maximum recorded in aqueous solution. This result exactly matches with the literature information. Maruszewski et al. reported maximum emission wavelengths of 608 and 587nm in aqueous solution and bulk sol–gel silicates, respectively (Maruszewski, Jasiorski, Salamon & Strek, 1999). Innocenzi et al. (Innocenzi, Kozuka & Yoko, 1997) have also reported similar blue shifts in emission maximum for the sol–gel entrapped ruthenium complexes.The addition of 120 μL [BMIM][PF_6] into the sol–gel matrix caused a blue shift of 9 nm in the emission maximum with respect to water and a red shift of 4 nm with respect to [BMIM][PF6]free sol–gel. The addition of ionic liquid only slightly changed the Stokes shift value from 147 to 134 nm. High Stokes shifts values are desirable for optical sensor design technologies in order to prevent interference and both values are high enough for this purpose.

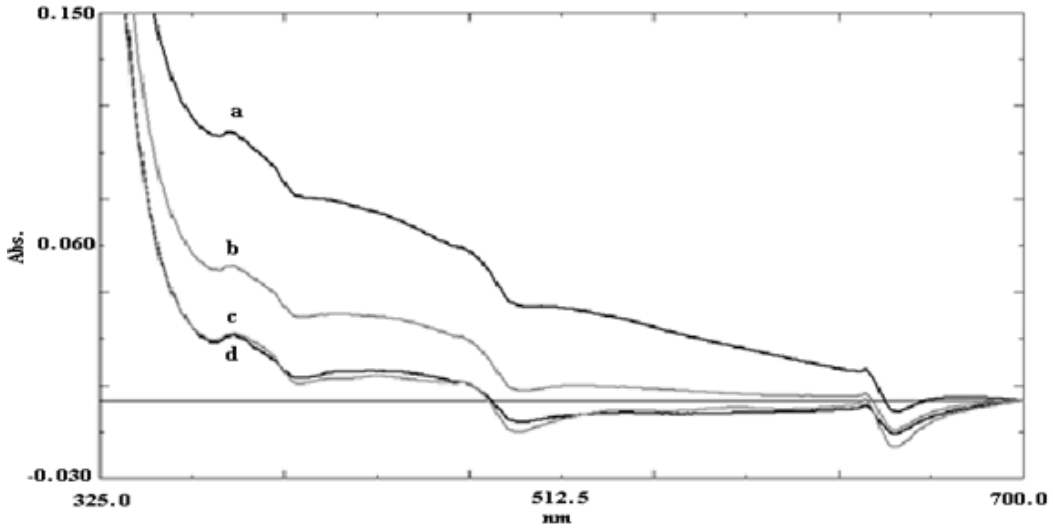

Figure 3.60 Absorption spectra of $Ru(bipy)_3^{2+}$ (a) in sol-2, (b) in sol-3 , (c) in sol-4 and (d) in sol-1.

Table 3.62 Absorption data of $Ru(bipy)_3^{2+}$ dye in different matrices

	λ_{max1}, (nm)	A_1	λ_{max2}, (nm)	A_2	λ_{max3}, (nm)	A_3
Sol 1	636	-0.002	473	0.007	379	0.025
Sol 2	636	0.02	472	0.059	379	0.103
Sol 3	636	0.003	472	0.025	379	0.052
Sol 4	636	0	472	0.008	379	0.026

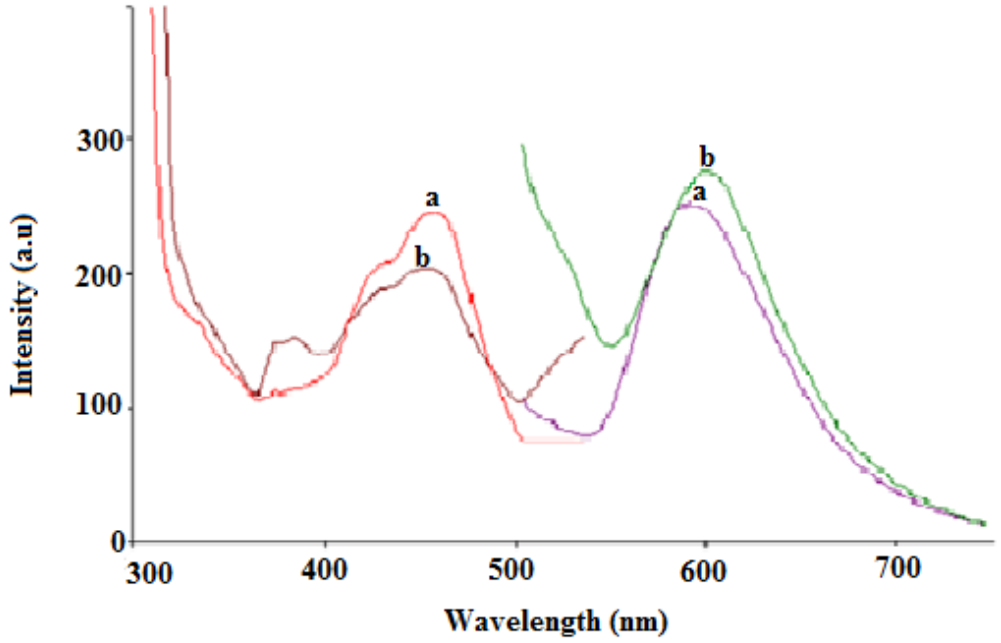

Figure 3.61 Excitation and emission spectra of the $Ru(bipy)_3^{2+}$ dye (a) in sol-8e, (b) in sol-9d.

Table 3.63 Emission and exitation spectra related data of$Ru(bipy)_3^{2+}$ in sol8-e and sol-9d.

	$\lambda_{max(em)}$, nm	I_{em}, a.u	$\lambda_{max(ex)}$, nm	I_{ex}, a.u
Sol-8e	600	277	453	206
Sol-9d	591	254	457	246

3.3.5 Response and regeneration

Response and regeneration performances were tested for sol- 8e and sol-9d which represent TEOS:water molar ratio is 4. Both of the coctails contain the same amount of chemicals in addition sol-9d contain 120 µL [BMIM][PF_6].Figure 3.62illustrates the response characteristics of sol-8e and the response time was found to be 12 s.The response times for oxygen sensing of sol-9d (R = 4) after exposure to 100 and 0% O_2 were quite fast and found to be 1s. Sol 8e could not be completely regenerated while the regeneration time of sol-9d was found to be only 9s (Figure 3.63). Thus the

presence of in [BMIM][PF_6] coctail decreased the significantly both the response and regenaration times.

The sensor performances were tested for sol- 8e and sol-9d after two monts and Figure 3.64illustrates the response characteristics of sol-8e and response time found to be 14 s. Response characteristics of sol-9d was shown in Figure 3.65 and found to be 4s and regeneration times of sol-9d was found to be 18s.

.

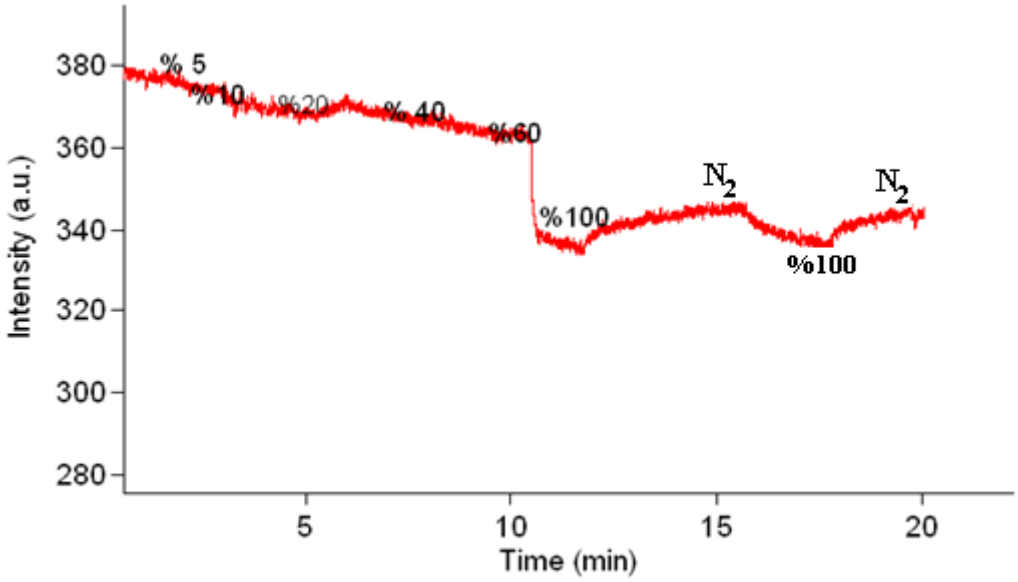

Figure 3.62 Response kinetics of sol-8e

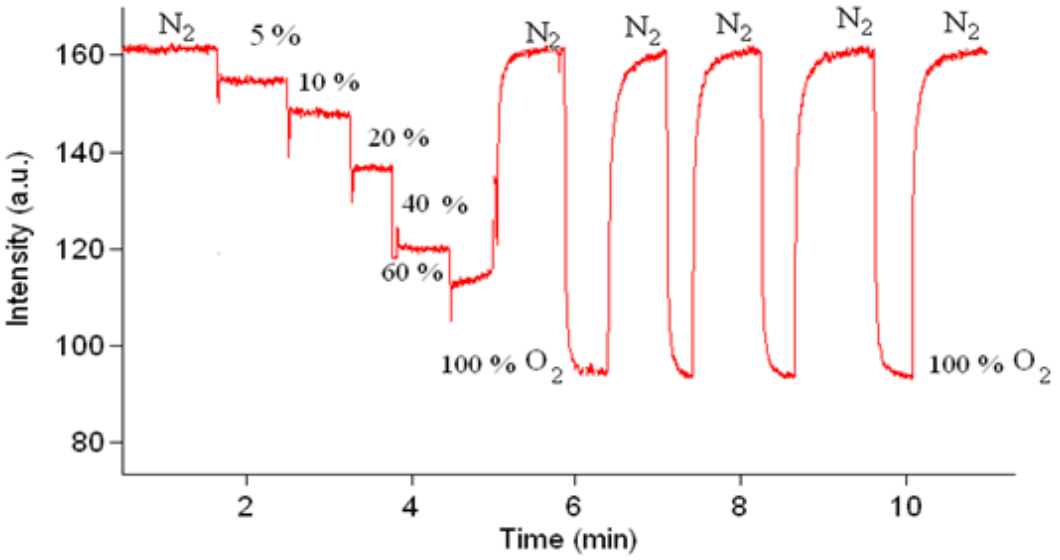

Figure 3.63 Response kinetics of sol-9d

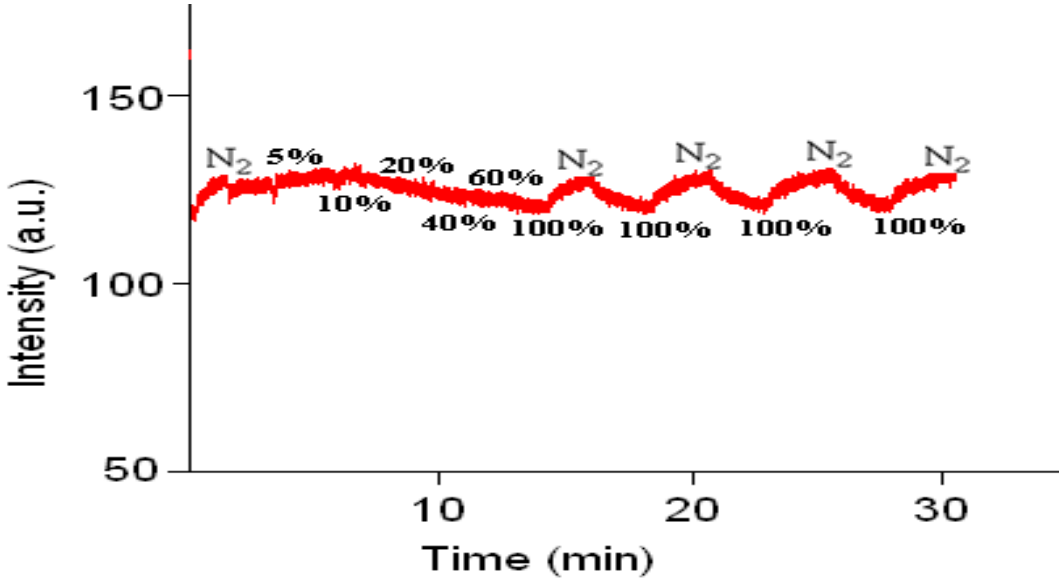

Figure3.64 Response kinetics of sol-8e

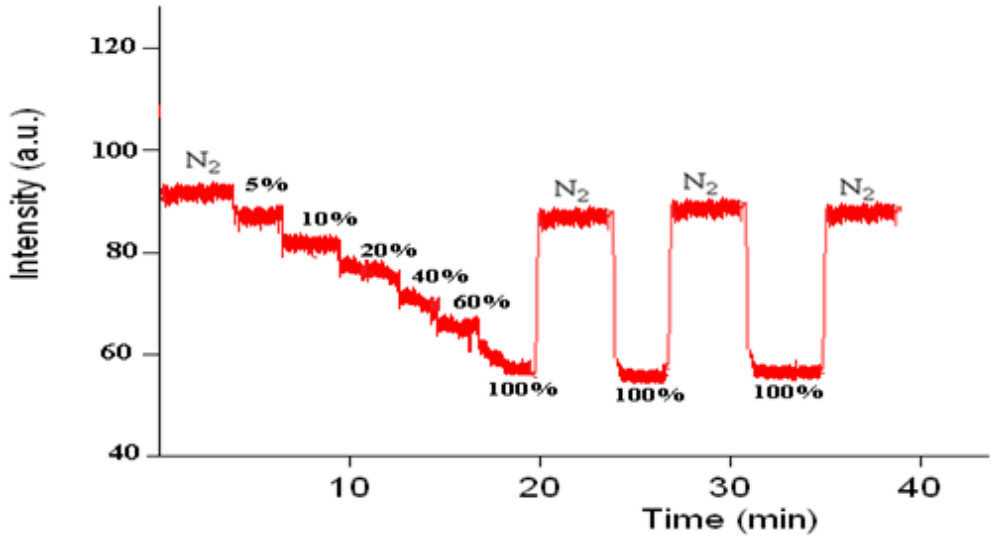

Figure 3.65 Response kinetics of sol-9d

3.3.6 Dissolved oxygen sensing

As the maximum oxygen response of $Ru(bipy)_3^{2+}$ is observed in sol 9d, the dissolved oxygen response sol-9d was evaluated for that coctail composition. The I_0/I value was found to be 1.41 at room temperature. The response of the sol-9d film for dissolved oxygen and the Stern volmer plot are given in Figure 3.66 and 3.67.The I_0/I versus oxygen pressure (atm.) and oxygen concentration (mM) are given in Figure 3.68 and Table 3.64. To obtain the oxygen concentration in the solvents from the external oxygen pressure, the Henry constants were taken from the literature (Chebbo, Catte & Richard, 1993; Tokugawa, 1975; Franco & Olmsted, 1990).

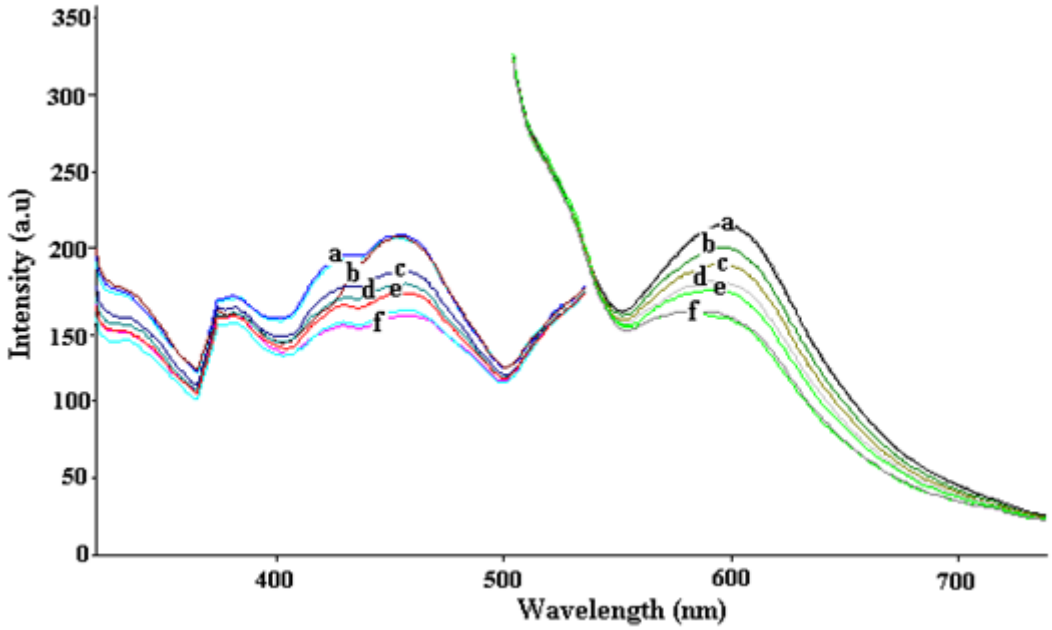

Figure 3.66 Response of sol-9d to dissolved $O_{2(g)}$ (a) 0% , 5% O_2(b) %10 O_2 (c) 20%O_2(d) air (e) 40% O_2 (f)60%, 100% O_2 (relative signal change is 29%).

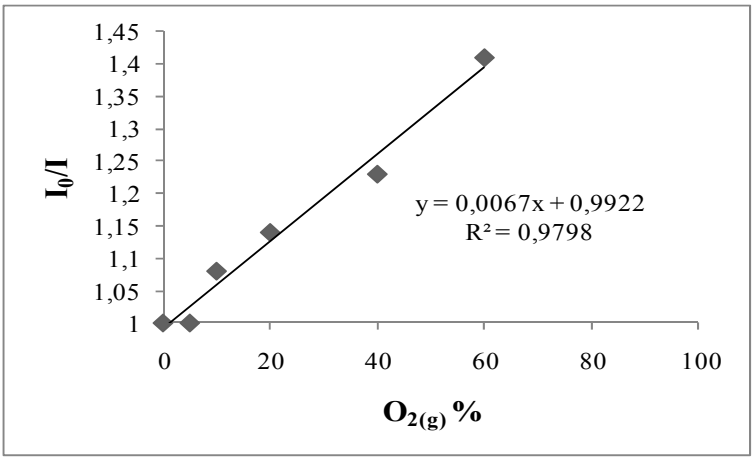

Figure 3.67 Stern Volmer plot for sol 9d to dissolved $O_{2(g)}$.

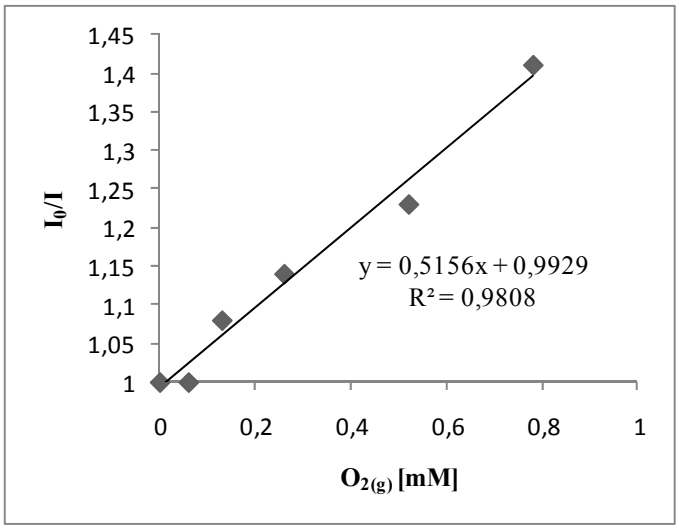

Figure 3.68 Stern Volmer plot for sol 9d to dissolved $O_{2(g)}$.

Table 3.64 Fluorescence intensity of sol-9d

% O_2	**$O_{2(g)}$ [mM]**	**I_{ex}**	**I_{em}**	**I_o/I**
0	0	205	225	1
5	0.06	205	225	1
10	0.13	204	209	1.08
20	0.26	186	197	1.14
Air	0.27	176	185	1.22
40	0.52	175	183	1.23
60	0.78	157	160	1.41
100	1.3	157	160	1.41

Table 3.65 Composition of the sol-9d

Coctail Name	Acidified Water (µl)	Triton-x 100 (µl)	RTIL-I (µl)	RTIL-II (µl)	RTIL-III (µl)	dye solution (µl)	Gelation time (min)	Coctail pH	Drying Temperature (^{0}C)	I_0/I
Sol-9d	193[b]	60	120	-	-	50	30	5	25	1.41

[b] 193 refers to 169 ul water 24 µl 0.1M HCl.

3.4 Conclusion

The oxygen sensitive dye of tris (2, 2'-bipyridyl) ruthenium (II) chloride was characterised in conventional and three different ionic liquids modified sol-gel matrices.

Three different ionic liquids, 1-butyl-3-methylimidazolium tetrafluoroborate ($[BMIM^+][BF_4^-]$), 1-butyl-3-methylimidazolium thiocyanate ([BMIM][SCN]) and 1-butyl-3-methylimidazolium hexafluorophosphate ([BMIM][PF_6]) were employed for the modification of acid- catalyzed tetraethyl orthosilicate (TEOS) based sol-gel matrix. Photophysical characteristics and emission based response of ($Ru(bipy)_3^{2+}$) to gaseous oxygen was investigated in these ionic liquid containing sol–gel matrix by spectrofluorimetric method.

The response of the dye in absence of ionic liquid and in ($[BMIM^+][BF_4^-]$), ([BMIM][SCN]), ([BMIM][PF_6]) containg coctails were 22 %, 3%, 18 % and 55 %, respectively.An enhanced O_2sensitivity, linear response and crack-free monoliths were obtained by the addition of [BMIM][PF_6]into the sol–gel composites. The sensor presented here exhibits a fast and reversible response to gaseous oxygen. It has been found that the adition of [BMIM][PF_6]has increased the O_2sensitivity and created a more smooth, crackles surface structure.

The response and regeneration times of 1 and 9 s. were obtained after exposure to 100 and 0% pO_2, respectively and two months later response and regeneration times found to be 4 and 18 s.

CHAPTER FOUR

PHOTOCHARACTERIZATION OF DYES AND INVESTIGATION OF THE UTILITY AS AN OPTICAL SENSOR IN PVC MATRIX

4.1 Introduction

Carbazoles are well known as a conjugated, good hole-transporting, electron-donor, planar compound and ease to introduce solubilizing groups to rigid ring structure. Carbazole derived compounds have technological interest due to their photoconducting and second-order non-linear optical properties, being suitable candidates for photorefractiveand electroluminescence applications (Ganguly et al., 1995; Tamura, Padias & Hall, 1992).

In this study, the previously synthesized oxazolones were taken from our organic chemistry group and photocharacterized by fluorescence spectroscopy in PVC matrix. The utility of the dyes as metal sensing agents in polymer matrix of PVC was also investigated.

4.2 Cocktail preparation protocols

The optode membranes werepreparedtocontain 120 mg of PVC, 240 mg of plasticizer, 1 mg of dyes (4-[4-(9H-carbazol-9-yl)benzylidene]-2-(4-nitrophenyl)-1,3-oxazol-5(4H)-one (3) concentration was 6.1 $\times 10^{-3}$mol dye/kg polymer, 4-[(9-methyl-9H-carbazol-3-yl)methylene]-2-(4-nitrophenyl)-1,3-oxazol-5(4H)-one (5a) was 7.0 $\times 10^{-3}$mol dye/kg polymer and 4-[(9-hexyl-9H-carbazol-3-yl)methylene]-2-(4-nitrophenyl)-1,3-oxazol-5(4H)-one (5b)was 5.9×10^{-3}mol dye/kg polymer in the coctail),equivalentamount of potassiumtetrakis (4-chlorophenyl) borateand 1.5 ml

of THF. The prepared cocktailscontained 33% PVC and 66% plasticizer by weight which is quite common.

The resulting cocktails were spread into a 125 μm polyester support (Mylar TM type) in order to obtain the sensing films. Each sensing film was cut to 1.2 cm width and fixed diagonally into the sample cuvette and the excitation and fluorescence emission spectra were recorded.

4.3 Results and discussion

4.3.1 UV Spectrum of Dyes

The absorption spectra of the dyes were recorded in PVC and are shown in Figure 4.1 and maximum absorption wavelengths of the dyes in PVC are given in Table 4.1.

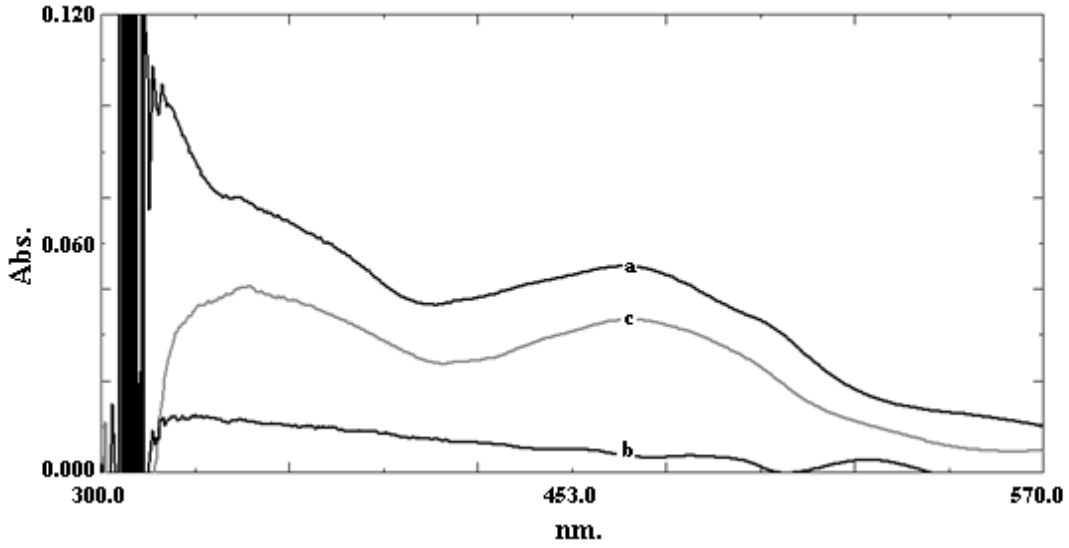

Figure 4.1 Absorption spectra of dyes in PVC (a) 5a, (b) 3 (c) 5b.

Table 4.1 Absorptiondata of dyes in PVC.

DYE	λ_{max}	ε (L/cm.mol)
3	472	5534
5b	451	38296
5a	450	67572

4.3.2 Emission and ExcitationSpectra of Dyes in PVC

The gathered excitation-emission spectra of the dyes in PVC matrix are shown in Figure4.2 and emissionandexitationspectrarelated data of dyes in PVC matrix are given in Table 4.2.The spectra of the dyes exhibited broad emission bands ranging from 480 to 700 nm. The maximum emission wavelengths range in the higher visible region of the electromagnetic spectrum from 540 to 565 nm in PVC. The excitation wavelength of the dyes 3, 5a and 5b were 490, 460, 490 nm, respectively. High excitation and emission wavelengths and Stoke's shift values are important for fluorescence and optical sensor studies. This result may be related to the enhanced conjugation in immobilized polymer phase by hindrance of rotational and vibrational motions. In all the employed solvents, the Stoke's shift values, $\Delta\lambda$ (the difference between absorption and emission maximum), calculated from the spectral data were moderately high and was found to spread in the wavelength range of 47-100 nm. The high Stoke's shift value allows the emitted fluorescence photons to be easily distinguished from the excitation photons and is of importance in optical sensor measurements with fiber optics.

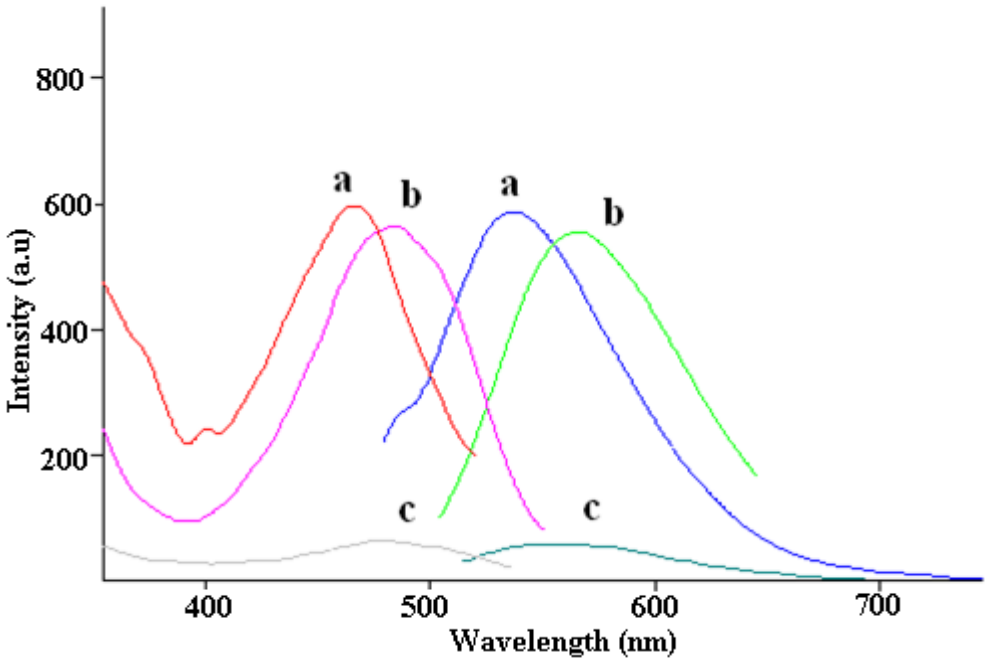

Figure 4.2 Excitationandemissionspectra of dyes in PVC matrix (a) 5a (7.0×10^{-3}mol dye/kg polymer), (b) 3 (6.1×10^{-3}moldye/kg polymer) and (c) 5b (5.9×10^{-3}mol dye/kg polymer).

Table 4.2 Emissionandexitationspectrarelated data of dyes in PVC matrix.

Dye	Media	λ_{ex} (nm)	I_{ex}, (a.u)	λ_{em} (nm)	I_{em}, (a.u)	Stoke'sshift	Quantum Yield
3	PVC	490	562	565	560	82	0.12
5a	PVC	460	598	540	597	72	0.40
5b	PVC	490	52	560	51	73	0.54

4.3.3 Quantum Yield of Dyes

The fluorescence quantum yields of dyes in PVC matrice were calculated by William's Method. The Williams method and the calculation of quantum yield values were explained in detail in Chapter 2.

For this purpose, the emission spectra of five different concentrations of reference standard (Floresein) were recorded by exciting at 460 and 490 nm(Figure 4.3 and

Figure 4.4). By similar way, the emission spectra of the five different concentrations of dyes were recorded (Figure 4.5-4.7).

The integrated fluorescence intensities were plotted *vs* absorbance for the reference standard, and dyes. The ratio of gradients of the plots is important and proportional to the quantum yield. The linearized plots of the dyes in THF can be described by equations and the relevant correlation coefficients of [*y*=213886x, R^2= 0.9961] , [y=257906x, R^2=0.9953] and [y=55741x, R^2=0.9917], for dye 5a, 5b and 3 respectively. For quantum yield standard; floresein, the equations are [y=468398x, R_2=0.9986] at 460 nm and [y=422025x, R_2=0.9976] at 490 nm and the data are also shown in Table 4.2.

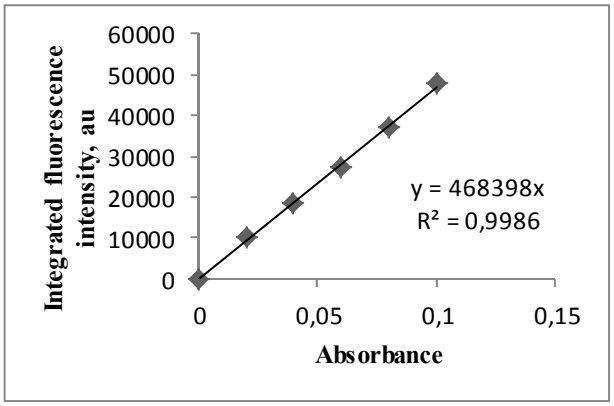

Figure 4.3 The integrated fluorescence intensities vs absorbance values of floresein in 0.1M NaOH (Emission at 460 nm).

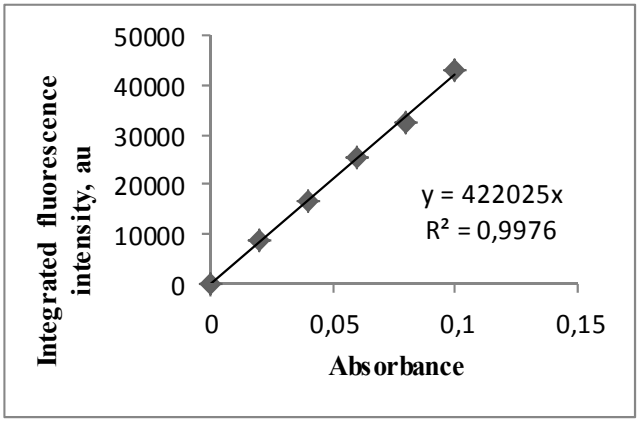

Figure 4.4 The integrated fluorescence intensities vs absorbance values of floresein in 0.1M NaOH (Emission at 490 nm).

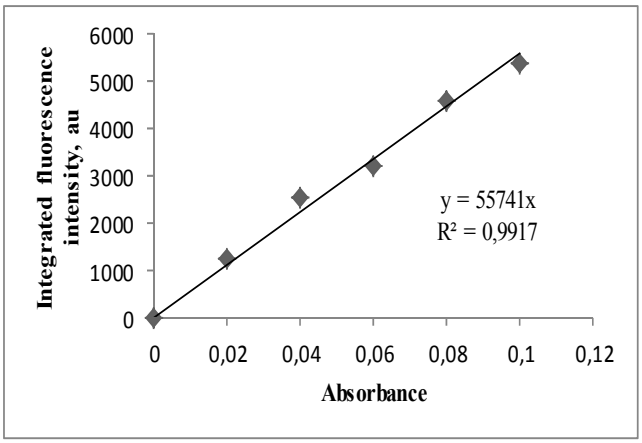

Figure 4.5 The integrated fluorescence intensities *vs* absorbance values of dye (3) in THF. (Emission at 490 nm).

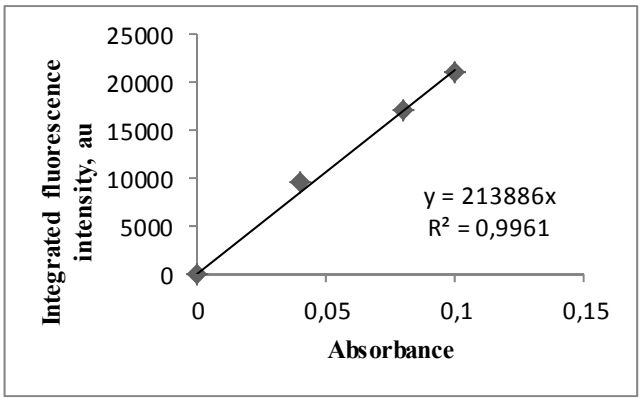

Figure 4.6 The integrated fluorescence intensities *vs* absorbance values of dye (5a) in THF. (Emission at 460 nm).

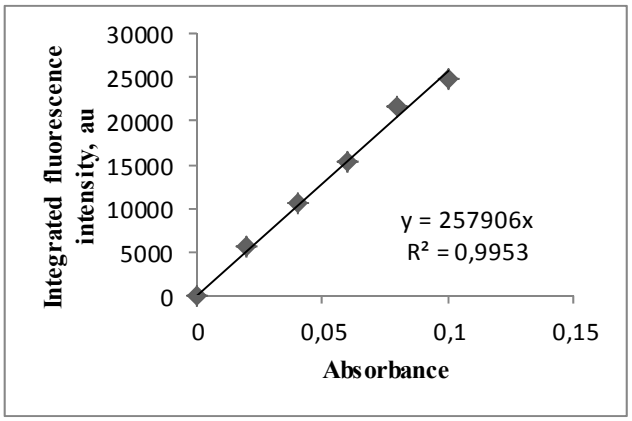

Figure 4.7 The integrated fluorescence intensities *vs* absorbance values of dye (5b) in THF. (Emission at 490 nm).

4.3.4 Effect of the pH

The effect of the pH on the emission and excitation spectra of the dye 3 doped PVC films were studied over the pH range of 3.0–11.0. The pH dependence of the 5a and 5b dye-doped membranes were investigated in acidic (pH=2.0), slightly acidic (pH 6.0), and basic buffer solutions (pH= 10.0). The 5a and 5b doped films strongly resisted to pH changes and no change was observed in the fluorescence intensity with changes in pH. The 3 dye doped films was slightly effected from pH and the maximum fluorescence intensity was observed at pH 5.0. The resistance of the dye doped films to pH is of significance to eliminate the interfering effect of pH in future metal sensing studies. The emission and excitation based relative signal changes of dyes were shown in Figure 4.8-4.12.

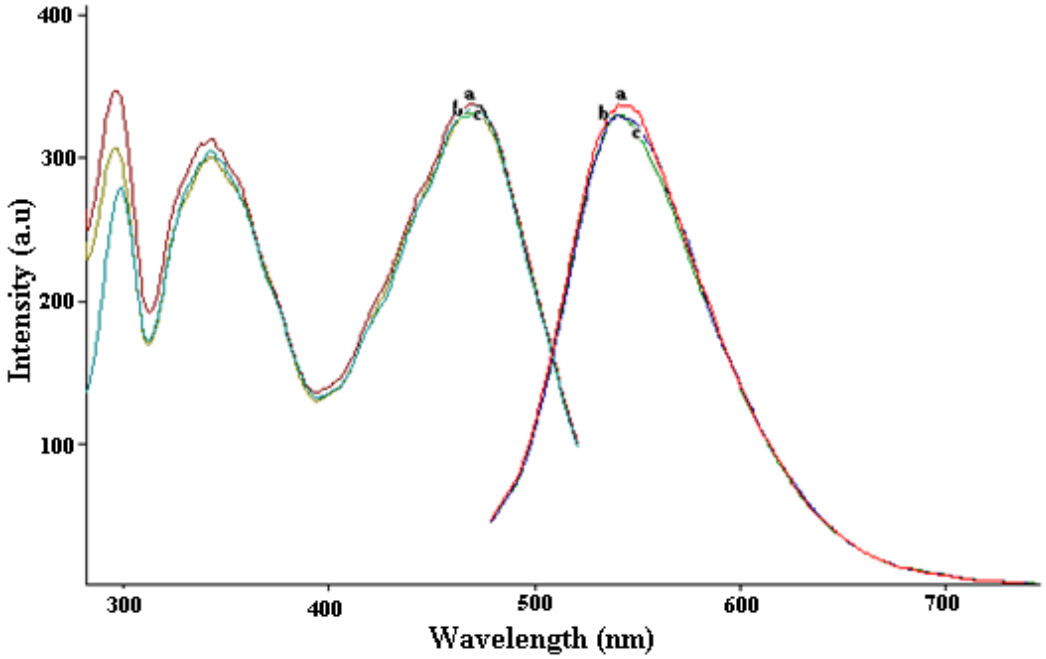

Figure 4.8 Excitation and emission spectra of (5a) in PVC matrix(7.0×10^{-3}mol dye/kg polymer) (a) pH=10.0, (b) pH=6.0 and (c) pH=2.0.

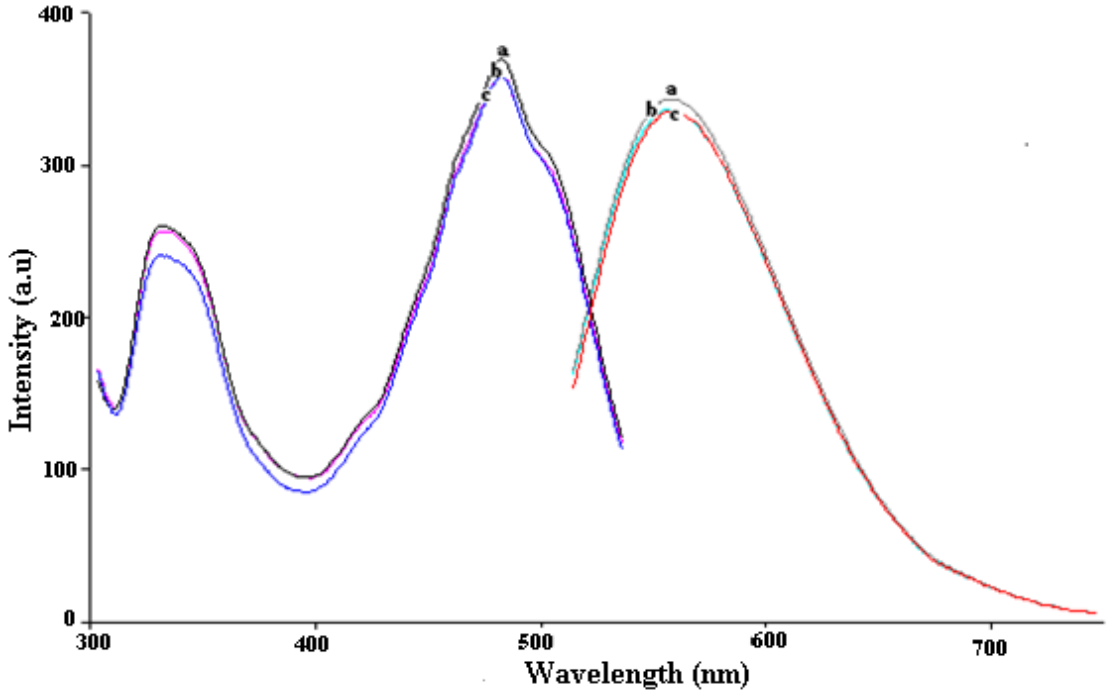

Figure 4.9 Excitationandemissionspectra of (5b) in PVC matrix(5.9×10^{-3}mol dye/kg polymer)(a) pH=10.0, (b) pH=6.0 and (c) pH=2.0.

pH response of (3) in basic and acidic buffer are shown in Figure 4.10 and Figure 4.11 and pH response results are shown in Figure 4.12.

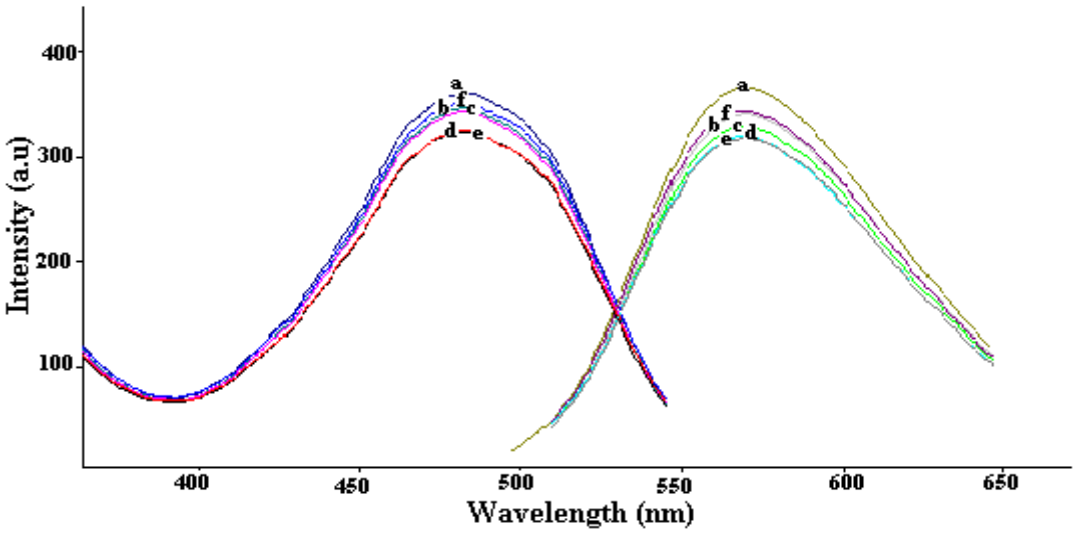

Figure 4.10 Excitation and emission spectra of (3) in PVC matrix (6.1×10^{-3}mol dye/kg polymer) (a) pH=6.0, (b) pH=7.0, (c) pH=8.0, (d) pH=9.0, (e) pH=10.0, (f) pH=11.0.

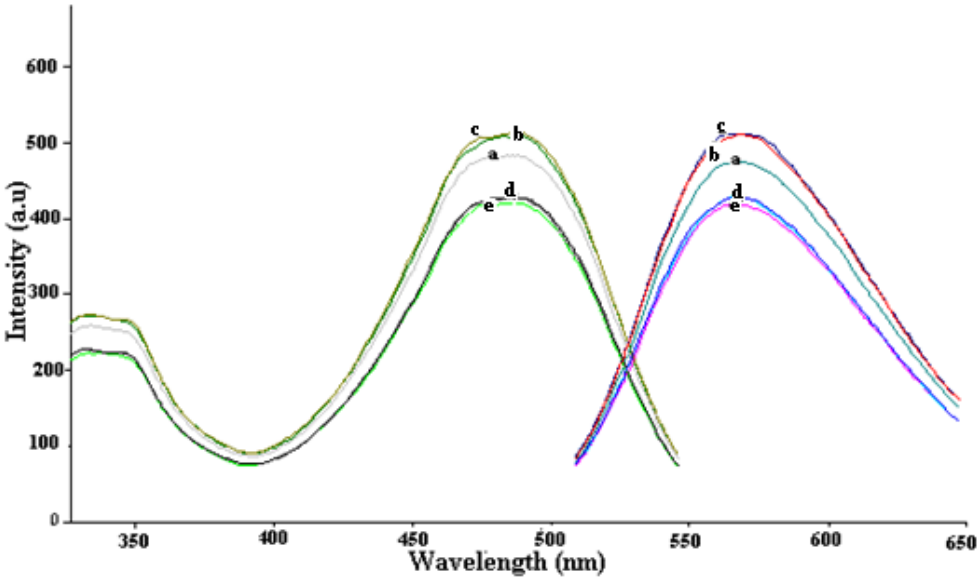

Figure 4.11 Excitation and emission spectra of (3) in PVC matrix (6.1×10^{-3}mol dye/kg polymer) (a) pH=3.0, (b) pH=4.0, (c) pH=5.0, (d) pH=6.0, (e) pH=7.0.

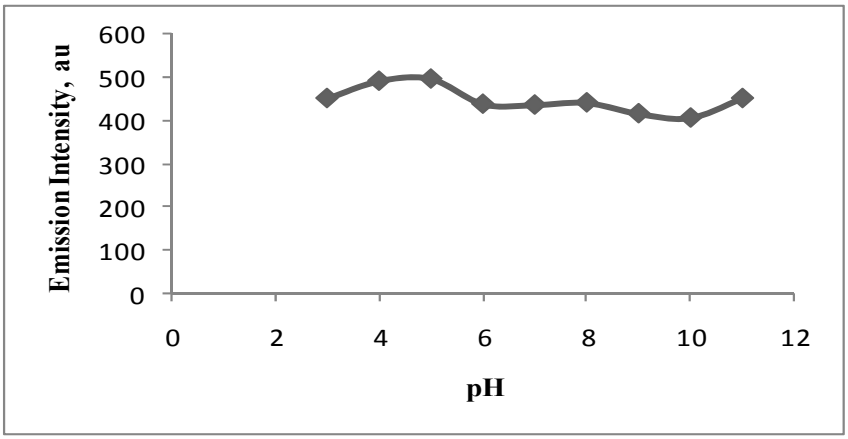

Figure 4.12 pH response of (3) in PVC matrix (6.1×10^{-3}mol dye/kg polymer) .

4.3.5 Response of Dyes to Different Metal Ions

The effect of metal ions to the fluorescence intensity of the dyes were investigated by introducing the thin films in 10^{-3} M pH 5.0 buffered solutions of Al^{3+}, Na^{+}, Sb^{3+}, Fe^{2+}, Fe^{3+},As^{3+}, Mo^{2+}, Li^{+}, Zn^{2+}, K^{+}, Ni^{2+}, Pb^{2+}, Cu^{2+}, Ca^{2+}, Hg_2^{2+}, Hg^{2+}, Al^{3+}, Cr^{3+}, Mn^{2+},Mg^{2+}, Sn^{2+}, Cd^{2+}, Co^{2+} and Ni^{2+} ions in separate solutions. Among the three dyes only dye 3-doped membrane exhibited remarkable fluorescence intensity quenching upon the metal ions while the responses of the other ions were negligible. The selective Zn^{2+} ion response of dye,3 at pH 5.0 can be seen at Figure 4.13.

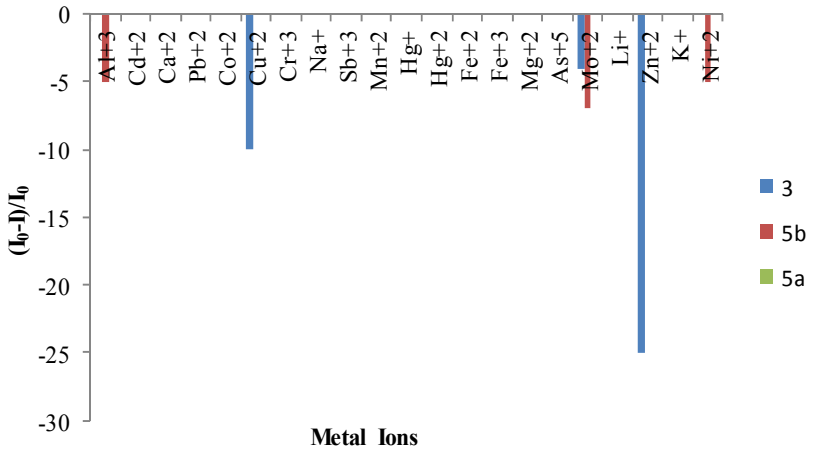

Figure 4.13 Metal response of dyes at pH=5 acetic acid/acetat buffer

4.3.6 Response of Dye 3 to Zinc Ions

Emission based response of dye, 3 to Zn^{2+} was tested in the pre-determined optimum conditions: molar ratio of dye over PTCPB was 1:2; dye concentration was $1.3x10^{-2}$ M in coctail solution and at optimum pH of 5.0. Figure 4.14shows the decreasing fluorescence intensity based response of the dye 3 doped PVC films to Zn^{2+} ions. Figure 4.15shows the normalized calibration plot of metal concentration versus relative signal intensity ($(I-I_0)/I_0$), where I was the measured fluorescence intensity at any Zn^{2+} concentration and I_0 was the intensity in absence of Zn^{2+}. The dye exhibited a linear emission based response to Zn^{2+} in the concentration range of 10^{-10}–10^{-6} mol/L. The equation of the plot was $(I_0-I)/I_0$=-0,1902log[Zn^{2+}] + 2,1951, r=0,9731. The films could detect the nanomolar concentrations of zinc ions and the limit of quantification which was found experimentally was 10^{-10} M.

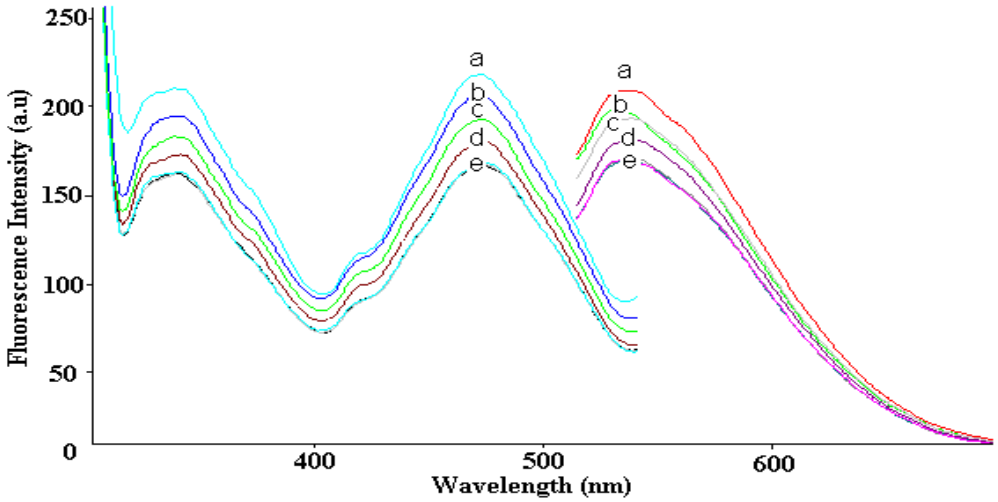

Figure 4.14 Response of the dye 3 doped PVC films to Zn^{2+} ions.

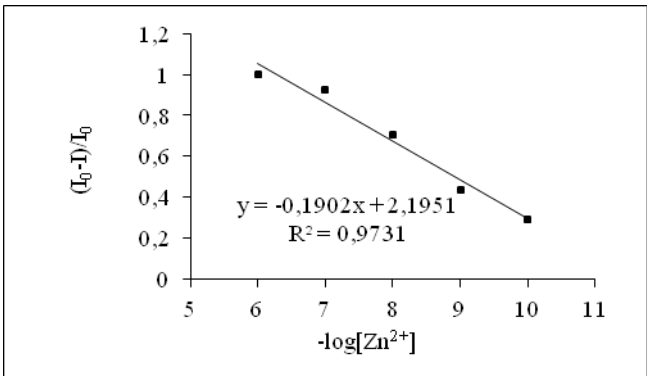

Figure 4.15 Emission based calibration plot of dye 3 for Zn^{2+}

4.4 Conclusion

All of the dyes have promising spectral properties such as visible region excitation (460-490 nm) and emission wavelength (540-565 nm), high molar absorbtivities (5530-67570 L /cm.mol) and high photostabilities in PVC matrix. All of the dyes were evaluated in case of their proton and metal sensitivity in their immobilized forms in PVC thin films and the dye 3 was found selectively sensitive to Zn^{2+} ions. The total response of the dye to zinc ions is not satisfactory, however the response in nanomolar concentrations level, selectivity of the dye and high linear working range (10^{-10}-10^{-6}). The quantum yield of Dye 3 was also calculated and is 0.12which is quite high for optical sensor designs.

CHAPTER FIVE

CONCLUSIONS

In the first part of this thesis, the oxygen sensitive dye of tris (2, 2'-bipyridyl) ruthenium (II) chloride was characterised with spectrophotometric and spectrofluorimetric method in conventional and modified sol-gel matrices.Three different ionic liquids, 1-butyl-3-methylimidazolium tetrafluoroborate ([$BMIM^+$][BF_4^-]), 1-butyl-3-methylimidazolium thiocyanate ([BMIM][SCN]**)** and 1-butyl-3-methylimidazolium hexafluorophosphate ([BMIM][PF_6]) were employed for the modification of acid- catalyzed tetraethyl orthosilicate (TEOS) based sol-gel matrix. Photophysical characteristics and emission based response of ($Ru(bipy)_3^{2+}$) to gaseous and dissolved oxygen was investigated.

The response of the dye in absence of ionic liquid and in ([$BMIM^+$][BF_4^-]), ([BMIM][SCN]**),** ([BMIM][PF_6]) containg coctails were 22 %, 3%, 18 % and 55 %, respectively.An enhanced O_2sensitivity, linear response and crack-free monoliths were obtained by the addition of [BMIM][PF_6] into the sol–gel composites. The sensor presented here exhibits a fast and reversible response to gaseous oxygen. It has been found that the adition of [BMIM][PF_6]has increased the O_2sensitivity and created a more smooth, crackles surface structure.

The response time of the ionic liquid free membranes were found as 12 s.The response and regeneration times for the [BMIM][PF6] modified sol-gel films were found as 1 and 9 s. after exposure to 100 and 0% pO_2, respectively. These values are quite shorter than the ionic liquid free ones. The total response of the films didn't change after two months later.

In the second part of this thesis, all of the dyes have promising spectral properties such as visible region excitation (460-490 nm) and emission wavelength (540-565 nm), high molar absorbtivities (5530-67570 L /cm.mol) and high photostabilities in PVC matrix. All of the dyes were evaluated in case of their proton and metal sensitivity in their immobilized forms in PVC thin films and the dye 3 was found selectively sensitive to Zn^{2+} ions. The total response of the dye to zinc ions is not satisfactory, however the response in nanomolar concentrations level, selectivity of the dye and high linear working range (10^{-10}-10^{-6}). The quantum yield of Dye 3 was also calculated and is 0.12which is quite high for optical sensor designs.

REFERENCES

Aelion, R., Loebel, A. &Eirich, F. J. (1950). Hydrolysis of ethyl silicate. Am. Chem. Soc., 72, 5705-5712.

Andrew, K.N. &, Worsfold, P.J. (1994). Comparison of multivariate calibrationtechniques for the quantification of model process streams using diode-array.Analyst, 119, 1541-1569.

Assink, R. A. &Kay, B. D. J. (1988). Sol-gel kinetics I. Functional group kinetics.Non-Crystalline Solids, 99 (2-3), 359-370.

Baker, S. N., Baker, G. A., &Bright, F. V. (2002). Temperature-dependent microscopic solvent properties of dry and wet 1-butyl-3-methylimidazolium hexafluorophosphate: correlation with ET(30) and Kamlet-Taft polarity scales. Green Chem., 4, 165–169.

Brinker, C. J. &Scherer, G.W. (1990). *Sol-Gel Science: The Physics and Chemistryof Sol-Gel Processing.* Academic Press: New York.

Cao, N. W., Shakin, C. M. &Sun, W. D. (1992). Quasiparticle properties of thequarks of the Nambu–Jona-Lasinio model**.** *Phys. Rev. C, 46,* 2535 – 2546.

Chebbo M, Catte M, Richard C (1993). Measurement and prediction of oxygen solubility water-alcohol media. *Recent ProgGenie Procedes, 7*(27), 379–384.

Choi, M.M.F. &Xiao, D. (1999). Linear calibration function of luminescence quenching-based optical sensor for trace oxygen analysis. *Analyst, 124*, 695-698.

Cook, M.J., Lewis, A.P., McAuliffe, G.S., Skarda, V., Thomson, A.J., Glasper, J.L., Robbins, D.J., 1984. J. Chem. Soc., Perkin Trans., *2*, 1293.

Dhami, S., Mello A. J., Rumbles, G., Bishop, S. M., Phillips, D. &Beeby, A. (1995). Phthalocyanine fluorescence at high concentration: dimers or reabsorption effect? *Photochem. Photobiol.*, *61*, 341.

Electromagnetic spectrum. (n.d.).Retrieved April 10, 2011, from http://en.wikipedia.org/wiki/Electromagnetic_spectrum.

Engelhardt, V. Q., Altenburg, W., Hoebbel**,** D. &Wieker, W. (1977). Si-NMR spectroscopy of silicate solutions. IV. investigations on the condensation of monosilicic acid*. Anorg. Allg. Chem.*, *428* (1), 43-52.

Ensafi, A. A & Bakhshi, M. (2003). New stable optical film sensor based on immobilization of 2-amino-1-cyclopentene-1-dithiocarboxylic acid on acetyl cellulose membrane for Ni(II) determination . *Sensors and Actuators B: Chemical, 96,* 435-440.

Franco C, Olmsted J (1990) Photochemical determination of the solubility of oxygen in various media. *Talanta, 37,* 905–909.

Galster, H. (1991). *pH Measurements: Fundamentals, Methods, Applications,Instrumentatio.* Weinhein,VCH: Germany.

Ganguly T, Bergeron JY, Farmer L, Gravel D, Durocher G. J. Lumin. (1994). Time-resolved luminescence technique as a probe for phase-transitions in some polysiloxane liquid-crystals bearing the chromophore 2,7-dimethoxy-N-methyl carbazole (dmnmc) as a pendant group. *Journal of Luminescence*,*59,* 247-255.

García, E. A, Fernández, R. G. & Díaz-garcía, M. E. (2004). Tris(bipyridine)ruthenium(II) doped sol–gel materials for oxygen recognition in organic solvents . *Microporous and Mesoporous Materials, 77* (2-3), 235-239.

Göpel, W. & Schierbaum, K.D. (1995). SnO_2 sensors: Current status and futureprospects. *Sensors and Actuators B, 26,* 1–12.

Göpel, W., Reinhardt, G. & Rösch, M. (2000). Trends in the development of solidstate amperometric and potentiometric high temperature sensors. *Solid StateIonics*, 136-137 (2): *519-531.*

Gündoğdu, L., Güneş, M. B. (2009). *N'-[(4-nitrofenil)metiden]piridin-4-karbohidrazid boyası ile spektroflorimetrik metodla seçimli alüminyum tayini*. College Thesis İzmir, Dokuz Eylül University.

Hisamoto, H., Nakagawa, E., Nagatsuka, K., Abe, Y., Sato, S., Siswanta, D., Suzuki,K. (1995). Silver Ion Selective Optodes Based on Novel Thia Ether Compounds. *Anal. Chem.,67,* 1315-1317.

How does nitrocellulose lacquer and common dyes used in guitars fade?.(n.d.). Retrieved April 12, 2011 from http://www.mylespaul.com/forums/historics-reissues/84987-fading-guitars.html.

Hulanicki, A., Geab, S. & Ingman, F. (1991). Chemical sensors definitions and classification. *Pure and Applied Chemistry, 63* (9)*,* 1247-1250.

Hush, N. S. & Reimers, J. R. (1998). Solvent effects on metal to ligand charge transfer excitations . *Coordination Chemistry Reviews, 177* (1), 37-60.

Iler, R. K. (1979). *The Chemistry of Silica*. Wiley: New York.

Innocenzi, P., Kozuka, H. & Yoko, T. (1997). Fluorescence Properties of the $Ru(bpy)_3^{2+}$ Complex Incorporated in Sol−Gel-Derived Silica Coating Films. *Journal of Physics Chemistry B, 101* (13), 2285-2291.

Khania, H, Rofoueia, M. H., Arabb, P., Guptac, V. K. & Vafaeia, Z. (2010)Multi-walled carbon nanotubes-ionic liquid-carbon paste electrode as a superselectivity sensor: Application to potentiometric monitoring of mercury ion(II). *Journal of Hazardous Materials, 18 ,* 402–409.

Kitai, A., (2008). *Limunescent Materials and Aplication*.England: Wiley.

Lakowicz, J. R. (1993). *Principles of Fluorescence Spectrocopy.* Plenum Press:NewYork and London.

Lobnic, A. (1998). *Optical characterization of sol-gels and their application tochemical sensors.* Ph.D Thesis. Graz.

Maruszewski, K., Jasiorski, M., Salamon, M. & Strek, W. (1999). Physicochemical properties of $Ru(bpy)_3^{2+}$ entrapped in silicate bulks and fiber thin films prepared by the sol–gel method . *Chemical Physics Letters,* 314 *(1-2)*, 83-90.

Materials and Polymers in Optical Sensing (n.d.).Retrieved April 13, 2011, from http://www.personal.uni-jena.de/~c1moge/Mohr/ASCOS2002.pdf.

Matos, I., Fernandes, S., Guerreiro, L. Barata S., Ramos A. M., Vital J. & Fonseca I. M. (2006). The effect of surfactants on the porosity of carbon xerogels. *Microporous and Mesoporous Materials, 92* (1-3), 38-46.

Mcdonagh, C., Maccraith, B. D. (2002). Enhanced Fluorescence Sensing Using Sol-Gel Materials . *Journal of Fluorescence,* 12 (3-4), 333-342.

Mcdonagh, C., Maccraith, D. & Mcevoy, A. K. (1998). Tailoring of Sol-Gel Films for Optical Sensing of Oxygen in Gas and Aqueous Phase. *Anal. Chem, 70,* 45-50.

Mcevoy, A. K., Macdonagh, C., Maccraith, B. D., 1997. *Optimisation of Sol-Gel-Derived Silica Films for Optical Oxygen Sensing.* Journal of Sol-Gel Science and Techonology, *8*, 1121-1125.

Mukundan, R., Brosha, E. L., Brown, D.R. &Garzon, F.H. (1999). Ceria-Electrolyte-Based Mixed Potential Sensors for the Detection of Hydrocarbons and Carbon Monoxide, Electrochemical and Solid State Letters, *2*(8), 412-414.

Oehme, I. &Wolfbeis, O.S. (1997). Fundamental Review: Optical Sensors for Determination of Heavy Metal Ions. *Mikrochim. Acta*, *126,* 177-192.

Oter, O. (2007). *Investigation of Sensor Characteristics of Some Chromoionophore Structures in Polymer and Sol-Gel Matrices*. Ph.D Thesis. Izmir, Dokuz Eylül University.

Oter, O., Ertekin, K., Derinkuyu, S., 2009. Photophysical and optical oxygen sensing properties of tris(bipyridine)ruthenium(II) in ionic liquid modified sol–gel matrix.*Materials Chemistry and Physics.,113,* 322-328.

Owen, T. (2000). *Fundamentals of modern UV-visible spectroscopy.* Germany: Agilent Technologies.

Parker, C. A. (1968). *Photoluminescence of Solutions.* Elsevier:Amsterdam.

Pohl, E. R. &Osterholtz, F. D. (1985). *Molecular Characterization of Composite Interfaces*; eds. Ishida, H. &Kumar, G., Plenum: New York, p. 157.

Rantwijk, F., Lau, R. M., &Sheldon, R. A. (2003). Biocatalytic transformations in ionic liquids. *Trends Biotechnol., 21*, 131–138.

Sacksteder, L., Demas, J. N., DeGraff, B. A., 1993. Design of oxygen sensors based on quenching of luminescent metal complexes: Effect of ligand size on heterogeneity. *Anal. Chem.*, *65* (23), 3480–3483.

Schmidt, W. (1994). *Optische Spektroskopie*. VCH: Weinheim.

Schubert, U. & Husing, N. (2000). *Synthesis of inorganic materials*. : Wiley-VCH.

Shimizu, Y. &Egashira, M. (1999). Basic aspects and challenge of semiconductorgas sensors. *MRS Bull.*, *24* (6),18–24.

Sol-Gel Methods. (n.d.).Retrieved April 13, 2011, from http://cheminfo.chemi.muni.cz/materials/InorgMater/sol_gel.pdf.

Sol-gel. (n.d.).Retrieved April 13, 2011, from http://en.wikipedia.org/wiki/Sol-gel.

Soukup-Hein, R. J., Warnke, M. M., Armstrong, D. W., 2009. Ionic Liquids in Analytical Chemistry. *Annu. Rev. Anal. Chem., 2,* 145-168.

Stetter, J. R., Penrose, W. R. & Yao, S. (2003). Sensors, Chemical Sensors, Electrochemical Sensors, and ECS. *Journel of The Electrochemical Society*, *150* (2), 11-16.

Tamura K, Padias AB, Hall HK, Peyghambarian N. (1992). New polymeric material containing the tricyanovinylcarbazole group for photorefractive applications*Applied Physics Letters*,*60*, 1803-1805.

Tokugawa J (1975) Solubilities of oxygen, nitrogen, and carbondioxide in aqueous alcohol solutions. *J Chem Eng Data, 20*(1), 41–46.

Ultraviolet theory.(n.d.).Retrieved April 10, 2011, from http://www.molecularinfo.com/MTM/UV.pdfm.

Ultraviolet–visible spectroscopy. (n.d.).Retrieved April 10, 2011, from http://en.wikipedia.org/wiki/Ultraviolet%E2%80%93visible_spectroscopy.

UV-VIS Spectroscopy. (n.d.).Retrieved April 12, 2011, from http://upetd.up.ac.za/thesis/available/etd02202007173756/unrestricted/04chapter4 pdf.

UV-Visible Spectroscopy. (n.d.).Retrieved April 12, 2011, from http://www2.chemistry.msu.edu/faculty/reusch/VirtTxtJml/Spectrpy/UV-Vis/uvspec.htm#uv1.

Vanyur, R., Biczok, L. & Miskolczy, Z. (2007). Micelle formation of 1-alkyl-3-methylimidazolium bromide ionic liquids in aqueous solution. *Colloids and Surfaces A: Physicochemical and Engineering Aspects*, *299* (1-3), 256-261.

Wasserscheid, P., Welton, T., *Ionic Liquids in Synthesis*, Weinheim:Wiley-VCH Verlag GmbH & Co. KGaA, 2003.

Wavelength. (n.d.).Retrieved April 10, 2011, from http://en.wikipedia.org/wiki/Wavelength.

Welton, T. (2004). Ionic liquids in catalysis . *Coordination Chemistry Reviews, 248 (21-24)*, 2459-2477.

Williams, A. T. R., Winfield S. A. &Miller, J. N. (1983). Relative fluorescencequantum yields using a computer controlled luminescence spectrometer. *Analyst*,*108*, 1067.

Wolfbeis, O. S. &Schaffar, B. P. H. (1987). An Ion-selective Optrode for Potassium.*Anal. Chim. Acta., 198*, 1-12.

Wolfbeis, O. S. (Ed.) (1991). *Fiber Optic Chemical Sensors and Biosensors*. *CRCPress: London.*

Xu, W.Y., McDonough, R.C., Langsdorf, B., Demas, J.N. &DeGraff, B.A. (1994). Oxygen Sensors based on luminescence quenching: Interaction of metal complexes with the polymersupports. *Anal. Chem, 66*, 4133-4141.

Yamazoe, N. &Miura, N. (1996). Prospect and Problems of Solid Electrolyte-Based Oxygenic Gas Sensors. *Journal of Solid State Ionics*, *86-88 (Part II)*: 987-993.

Yamazoe, N. (2005). Toward innovations of gas sensor technology. *Sensors and Actuators B, 108,* 2-14.